Doctoral theses at NTNU, 2021:267

Alicja Molska

Hypoxic-ischemic brain injury: Melatonin treatment with lipid-based nanoparticles.

Doctoral thesis

NTNU
Norwegian University of Science and Technology
Thesis for the Degree of
Philosophiae Doctor
Faculty of Medicine and Health Sciences
Department of Circulation and Medical Imaging

NTNU
Norwegian University of
Science and Technology

Alicja Molska

Hypoxic-ischemic brain injury: Melatonin treatment with lipid-based nanoparticles.

Thesis for the Degree of Philosophiae Doctor

Trondheim, September 2021

Norwegian University of Science and Technology
Faculty of Medicine and Health Sciences
Department of Circulation and Medical Imaging

NTNU
Norwegian University of
Science and Technology

NTNU
Norwegian University of Science and Technology

Thesis for the Degree of Philosophiae Doctor

Faculty of Medicine and Health Sciences
Department of Circulation and Medical Imaging

© Alicja Molska

ISBN 978-82-326-5471-0 (printed ver.)
ISBN 978-82-326-6641-6 (electronic ver.)
ISSN 1503-8181 (printed ver.)
ISSN 2703-8084 (online ver.)

Doctoral theses at NTNU, 2021:267

Printed by NTNU Grafisk senter

I dedicate this thesis to my daughter, Anastasia.

SUMMARY

Hypoxic-ischemic brain injury - Melatonin treatment with lipid-based nanoparticles

Inadequate levels of oxygen and restriction of blood supply around birth, known as perinatal hypoxia-ischemia (HI) may lead to brain injury through a progressive injury cascade. HI brain injury is one of the main causes of neonatal mortality and is also associated with an increased risk of neurodevelopmental disabilities, such as cerebral palsy. The standard treatment of these infants consists of supportive care and therapeutic hypothermia started within six hours after the event. However, the cooling treatment is only partially effective with almost 50% of treated newborns having side effects. Hence, there is an urgent need to develop more efficient, safe, and simple neuroprotective treatment.

Melatonin, a neurohormone secreted primarily from the pineal gland, is a potential neuroprotective agent after a neonatal HI event, presumably due to its antioxidative properties. Many rodent and large animal studies have shown that melatonin prevents neuronal and astroglial apoptosis following HI injury in the perinatal period. These findings suggest that melatonin could provide clinical neuroprotection in human neonates. Although oral melatonin administration is feasible in humans, bioavailability is low due to high first-pass metabolism. Moreover, melatonin is only slightly soluble in water, light sensitive, and unstable in solution. In animal experiments, this issue has been circumvented by using organic solvents, like DMSO or ethanol, to make injectable formulations. However, such solvents may have neurotoxic effects in neonates.

The overall aim of this thesis was to develop a melatonin formulation without organic solvents and to study its effect on hypoxic-ischemic brain injury.

Due to the lipophilic character of melatonin, lipid-based nanoparticles, such as liposomes and nanoemulsions, represent a promising solubilizing platform for melatonin. Melatonin loaded in liposomes and nanoemulsions were developed and characterized *in vitro* and *in vivo* showing that liposomal melatonin is superior to nanoemulsions and to conventional melatonin formulation using organic solvents. In the pharmacokinetic study, melatonin loaded in liposomes, MCT-nanoemulsions, and DMSO-formulation were administrated to adult rats; nanoparticles produced a higher melatonin concentration in the brain than DMSO-melatonin, while all three formulations showed a similar concentration of melatonin in blood. Then, the optimal nanoformulation, liposomes loaded with melatonin, was used in the

treatment study. There, we examined the effect of a high-dose parenteral liposomal melatonin compared to the conventional melatonin formulation in DMSO on an established HI brain injury model in neonatal rats. The results of this study indicated that liposomal melatonin is moderately neuroprotective after HI. However, we observed reduced weight gain in melatonin-treated animals, which could be caused by reduced feeding as a result of the sedative effect of melatonin. More importantly, reduced weight gain may mask the neuroprotective effect of the drug and is associated with more severe brain injury representing a complex relationship between weight gain and the outcome of the study. After statistically correcting the data for weight gain, liposomal melatonin was superior to melatonin dissolved in DMSO and to the control group (PBS). However, large variabilities were observed in all treatment groups of the *in vivo* model, making small differences in outcomes hard to detect. This identified a need for a more controlled and reproducible model of HI brain injury to study the effect of melatonin where factors including weight change would not have an influence on the results. Therefore, in a third study, we developed an *ex vivo* model of oxygen-glucose deprivation (OGD) in an NMR-compatible perfused system called a bioreactor. We optimized this model using adult rat brain slices and studied real time metabolic changes in the tissue. In this study, NMR data clearly distinguished three severity groups (mild, moderate, and severe) after 30, 60, and 120 min of OGD, respectively, compared with Control. ^{31}P NMR spectra obtained from Controls showed that PCr/Pi levels were stable over 5 h of bioreactor experiment. Control ^{1}H NMR spectra showed that Lac/NAA levels were stable with a tendency to gradually increase due to the recirculation of the aCSF in the perfusion system. This set-up produced satisfactory ^{1}H and ^{31}P spectral quality that enables observation of changes in metabolite levels before, during and after applied OGD. Together with high reproducibility and environmental control, it is an excellent model system to study the treatment effect of melatonin and other promising agents after HI event.

This research has shown that it is feasible to develop a non-toxic parenteral formulation with melatonin using liposomes. The results of the treatment study on neonatal rats indicate the need for further melatonin dosage optimization. In addition, we have established a highly reproducible and controlled *ex vivo* model for real time measurements of energy metabolism during and after HI in brain tissue. Future studies to characterize the impact of therapeutic agents such as melatonin and melatonin-augmented hypothermia on metabolic response and mitochondrial function can now be investigated using this bioreactor system with the OGD model.

GRAPHICAL SUMMARY

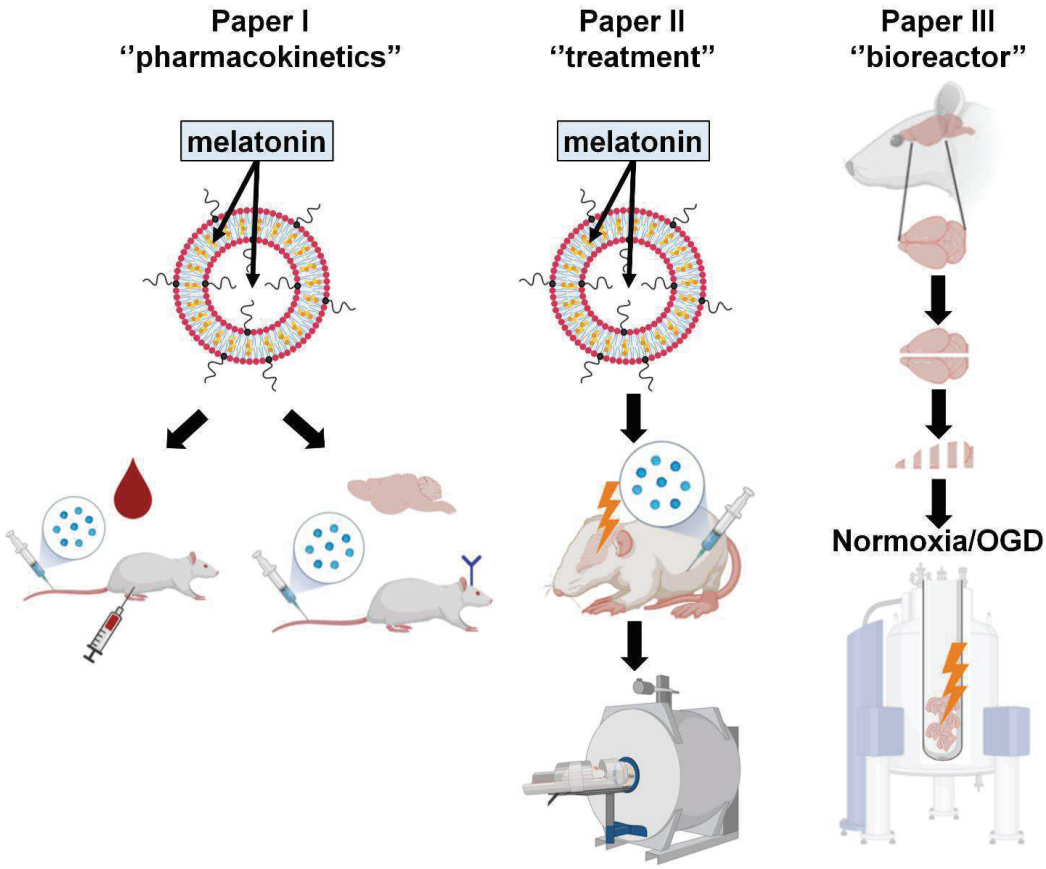

SAMMENDRAG (summary in Norwegian)

Hypoksisk-iskemisk hjerneskade – Melatoninbehandling med lipid-baserte nanopartikler.

Lave nivå av oksygen og begrenset blodforsyning rundt fødsel, også kjent som perinatal hypoksisk iskemi (HI), kan forårsake hjerneskade gjennom en progressiv kaskade (1). HI-indusert hjerneskade er en av de viktigste årsakene til neonatal dødelighet, og er assosiert med økt risiko for nevrologiske utviklingsforstyrrelser, som cerebral parese. Tilstanden er derfor et alvorlig helseproblem. Behandlingen består i dag av støttende behandling og terapeutisk hypotermi som startes innen seks timer etter at skaden har inntruffet. Behandlingen har imidlertid bare delvis effekt, og nesten 50% av nyfødte som får behandlingen har bivirkninger (4). Det er derfor behov for ny effektiv, trygg og enkel nevroprotektiv behandling for denne pasientgruppen.

Melatonin, et nevrohormon utskilt hovedsakelig fra epifysen, er et mulig nevroprotektivt legemiddel mot HI-indusert hjerneskade, antageligvis på grunn av dets antioksidative egenskaper (5). Flere studier blant dyr har vist at melatonin forhindrer død av nevroner og astroglia celler etter HI-indusert hjerneskade i den nyfødtperioden (6). Disse funnene understøtter melatonins potensielle rolle i forebygging av HI-indusert hjerneskade hos nyfødte mennesker. Selv om melatonin kan gis peroralt til mennesker, så har middelet lav biotilgjengelighet på grunn av høy førstepassasjemetabolisme (7). Melatonin er også lite løselig i vann, lyssensitivt, og ustabilt når det er oppløst (8). Dette har i dyrestudier blitt omgått gjennom bruk av organiske løsemidler, som DMSO eller etanol, for å lage formuleringer som kan injiseres. Slike løsemidler kan imidlertid ha nevrotoksiske virkninger, som nyfødte er særlig sårbare for (9).

Det overordnede målet ved denne avhandlingen var å utvikle en melatoninformulering uten organiske løsemidler, og undersøke dets effekt på HI-indusert hjerneskade.

På grunn av melatonins fettløselighet så er lipidbaserte nanopartikler, som liposomer og nanoemulsjoner, lovende løsemidler. I dette arbeidet har vi utviklet og karakterisert melatonin løst i liposomer og nanoemulsjoner, og vist at melatonin løst i liposom er bedre enn melatonin løst i nanoemulsjoner eller organiske løsemidler. Vi gjennomførte en farmakokinetisk studie, som viste at når 10 mg/kg melatonin som ble løst i liposomer, nanoemulsjoner og DMSO-formulering og deretter gitt til voksne rotter, så hadde melatonin

fra lipidbaserte nanopartikler høyere konsentrasjon i hjernen enn melatonin fra DMSO, og alle tre formuleringene viste lignende konsentrasjon i blodet. Den beste nanoformuleringen ble så brukt i en behandlingsstudie med nyfødte rotter. Vi undersøkte effekten av liposom-løst melatonin gitt intraperitonealt i en etablert dyremodell for HI-hjerneskade, og sammenlignet med melatonin løst i DMSO. Studien indikerte at liposomalt melatonin har en moderat nevroprotektiv effekt. Vi fant imidlertid redusert vektøkning hos melatoninbehandlede dyr, som kan ha blitt forårsaket av redusert matinntak på grunn av melatonins søvninduserende effekt. Redusert vektøkning kan også maskere virkningen av medisinen, da redusert vektøkning også er assosiert med mer alvorlig hjerneskade. Etter justering av resultatene for vektøkning var liposomalt melatonin bedre enn både melatonin løst i DMSO, og kontrollgruppen. Det ble imidlertid observert stor variasjon i alle behandlingsgruppene som gjorde det vanskelig å finne forskjeller i effekt. Det var derfor behov for en mer kontrollert og reproduserbar modell for HI-hjerneskade, for å kunne studere melatonins effekt isolert fra andre faktorer. I den tredje studien utviklet vi derfor et et nukleær-magnetisk resonans (NMR)-kompatibelt perfusjonssystem for å utføre oksygen-glukose deprivasjon (OGD) på hjernevev ex vivo, kalt en bioreaktor. Vi optimaliserte og brukte bioreaktoren for å studere snitt fra voksne rotter, og studerte metabolske endringer i vevet i sanntid. Resultatene viste klare forskjeller i metabolsk respons mellom 30, 60 og 120 minutters OGD, sammenlignet med kontroll. ^{31}P NMR-spekter av kontrollprøvene viste at nivåene av PCr/Pi var stabile over fem timer i bioreaktoreksperimentet. ^{1}H NMR spectra viste at nivåene av Lac/NAA var stabile, med en tendens til gradvis økning på grunn av resirkulasjon av aCSF i perfusjonssystemet. Dette oppsettet resulterte i tilfredsstillende spekterkvalitet for både ^{1}H og ^{31}P, og muliggjorde observasjon av metabolske forandringer før, under og etter OGD. Systemet gav også høy reproduserbarhet og kontroll over miljøet. Dette gjør dette bioreaktoren til et velegnet modellsystem for å undersøke effekten av melatonin og andre lovende legemidler etter HI-hjerneskade.

Denne forskningen har vist at det er mulig å utvikle ikke-toksiske parenterale formuleringer av melatonin ved bruk av liposomer. Behandlingsstudien på nyfødte rotter har vist at det er behov for ytterligere doseoptimalisering. I tillegg har vi etablert en reproduserbar og kontrollert ex vivo-modell for sanntidsmålinger av energimetabolisme under og etter HI-hjerneskade. Denne modellen kan brukes i fremtidige studier for å studere effekten av intervensjoner, som melatonin, og melatonin understøttet av hypotermi, på metabolsk respons og mitokondriell funksjon.

Kandidat: Alicja Molska

Institutt: Institutt for sirkulasjon og bildediagnostikk

Veiledere: Marius Widerøe, Sjoerd Hak, Olav Haraldseth, Catharina de Lange Davies

Finansieringskilde: Norges Teknisk-Naturvitenskaplige Universitet (NTNU)

Ovennevnte avhandling er funnet verdig til å forsvares offentlig for graden:
Philosophiae Doctor i medisinsk teknologi.
Disputas finner sted torsdag 2. September via Zoom.

ACKNOWLEGDMENTS

Presented work was performed at the MR Core Facility, Department of Circulation and Medical Imaging, and at the Department of Physics, Biophysics and Medical Technology section at NTNU.

From the first day I have started my journey at NTNU, I have only met people with an intention to help, teach, solve the problem, or share their experience with me and I am very grateful for that.

First, I would like to thank my main supervisor Marius Widerøe. Thank you for your guidance, sharing your knowledge about HI model but mostly for making me more independent. You have been a big help for me, especially in the end of the project and for that I am very appreciated.

Second, I would like to thank the co-supervisor of the project, Sjoerd Hak, one of the best teachers I have met. Sjoerd, I am amazed that you did not kill me during my first months as a PhD candidate and instead you have patiently taught me basics around nanoparticles, explained stuff again and again and again…. Besides being a great researcher, knowing your topic well, you also care about a person, and I can say it was an honor to have you in my team and call you a friend. THANK YOU, Master Yoda.

Third, I would like to thank Paweł Sikorski for giving me a chance to start Erasmus practice at Biophysics and for being my reference for this job. From hundreds of e-mails that I have sent to NTNU in 2015 looking for an Erasmus project to start, only Paweł has answered me saying ''ok but how does it work?''. Thank you for introducing me to the tissue bioengineering world, and for being present. In addition, I would like to thank David Bassett for presenting me his incredible work with CLEX technology.

I would like to express my special thanks to Catharina de Lange Davies, for allowing me using the labs at the Biophysics, as well as being a part of the biophysics group; thanks to Tone Frost Bathen for welcoming me in the MR Cancer group and helping me with the formalities around the manuscript. A huge thank you to Kristin Grendstad, highly experienced engineer and one of the nicest people at Biophysics.

Then, I would like to acknowledge Debbie Hill, who I had a pleasure to work with on a bioreactor project. Debbie, you are one of the best human beings walking on this planet and

it was simply an honor working with you. When I have found out about the bioreactor idea, I was scared at first, but hearing that you will be involved I went all in and I do not regret it.

Next person that I would like to thank is Trygve who is an NMR specialist at the MR Core. I am very grateful for your solution with the temperature measurement in the bioreactor and I will always remember that ''symmetry is the key''. The work at MR Core would not happen without Tina, a person that knows the answer to all questions, the one that knows everybody. On the top of that, she is one of the funniest girls at ISB.

This acknowledgment can't be written without mentioning two of my best friends from Biophysics: Marieke, and Alexandros. Guys, we have all started together and shared many courses, some painful ones as well. Marieke, you have always been there for me, and I know I can count on you. You are one of the smartest girls I know, and I am happy to call you, my friend. Alexandros, my ''third supervisor'', there are no words describing how thankful I am for your help with this project, especially first paper. You taught me a lot, and I am looking forward seeing your future work.

Special thanks to my colleagues, and co-authors of the papers: Sofie, Nina, Liv, Natasa from Biophysics; Marco, Elise, Therese, Torfinn (thanks for your help with the Norwegian summary), Line, Alex, Mohammed, Julia, Maria Karoline, Kaia, Feng, Shanti, Neil, Axel, and Hester from ISB, and Kåre from the Department of Biotechnology, NTNU.

I would also like to thank people behind the hard work with laboratory animals: Anne, Knut, and Venke-Lill; Ingunn from CMIC for accepting the challenge with brain slices; Arnfinn for developing the hand-made pieces for the bioreactor and engineers helping behind the scenes: Astrid from Biophysics and Torill from ISB.

Last, but not least, I would like to thank my friends and family. My mom who taught me how to aim high. Mamo, dziękuję Ci za wszystko! (Mom, thank you for everything!). My dad, my grandma Ula, and my sister Kasia.

A big thank you to Ilija; for the support, dealing with me at my worst, lifting me when I have doubted in myself and was exhausted. Thank you, my dearest Anastasia, for teaching me patience.

This work would not happen without the use of laboratory animals and I would like to acknowledge rats and mice involved in the experiments.

SYMBOLS AND ABBREVIATIONS

^{1}H NMR	Hydrogen-1 Nuclear Magnetic Resonance
^{31}P NMR	Phosphorus-31 Nuclear Magnetic Resonance
aCSF	artificial Cerebrospinal Fluid
ADC	Apparent Diffusion Coefficient
ADP	Adenosine Diphosphate
ATP	Adenosine Triphosphate
Co-A	Coenzyme A
DWI	Diffusion-Weighted Imaging
$FADH_2$	Flavin Adenine Dinucleotide Hydrate
FID	Free Induction Decay
HI	Hypoxia-Ischemia
HIE	Hypoxic-Ischemic Encephalopathy
IV	Intravenous injection
IM	Intramuscular injection
IP	Intraperitoneal injection
LP	Liposome
MPS	Mononuclear Phagocyte System
MRI	Magnetic Resonance Imaging
MRS	Magnetic Resonance Spectroscopy
NADH	Nicotinamide Adenine Dinucleotide Hydride
NE	Nanoemulsion
NO	Nitric Oxide
NP(s)	Nanoparticle(s)
OGD	Oxygen-Glucose Deprivation
P7	Postnatal day 7
PEG	Polyethylene Glycol
PK	Pharmacokinetics
PO	*Per Os*, oral administration
ROS	Reactive Oxygen Species
SC	Subcutaneous injection

LIST OF PAPERS INCLUDED IN THIS THESIS

Paper I

***In vitro* and *in vivo* evaluation of organic solvent-free injectable melatonin nanoformulations**

Alicja Molska, Axel Karl Gottfrid Nyman, Alexandros Marios Sofias, Kåre Andre Kristiansen, Sjoerd Hak, Marius Widerøe.

Eur J Pharm Biopharm 2020;152:248–56.

Paper II

Effects of liposomal melatonin on HI in the neonatal rat

Axel Karl Gottfrid Nyman, Alicja Molska, Alexandros Marios Sofias, Hester Rijkje Berger, Sjoerd Hak, Marius Widerøe.

In manuscript.

Paper III

Perfusion system for studying dynamic metabolomics in rat brain slices exposed to oxygen-glucose deprivation (OGD) using ^{1}H and ^{31}P NMR

Alicja Molska, Deborah Katherine Hill, Trygve Andreassen, Marius Widerøe.

Submitted.

Table of Contents

1. Introduction

1.1. Hypoxic-ischemic brain injury

Intrapartum-related complications including a significant drop in maternal blood pressure, placenta or umbilical cord pathologies are the cause of an inadequate oxygen delivery in the body called birth asphyxia (1). According to WHO birth asphyxia is a major cause of global mortality contributing to 24% of neonatal deaths worldwide (2). Moreover, if an episode of oxygen and blood deprivation, hypoxia-ischemia (HI), is severe enough to damage the brain it leads within 12 to 36 hours to neonatal hypoxic-ischemic encephalopathy (HIE) (**Fig 1.**) (3).

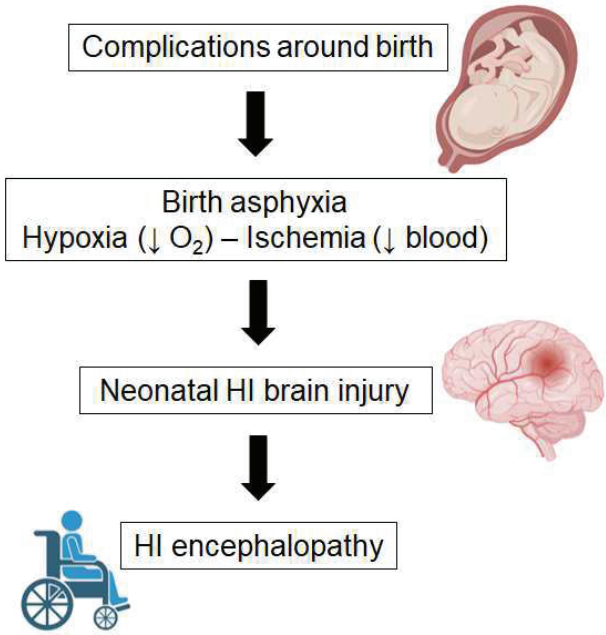

Figure 1. Progression of hypoxia-ischemia insult leading to hypoxic-ischemic encephalopathy in neonates.

HIE is a heterogeneous condtions in term neonatal infants with no specific biomarkers easily available for clinical use (4). However, if the birth was traumatic accompanied by low APGAR score, metabolic acidosis, hypotonia or organ failure, a diagnosis of HIE might be confirmed (5). Infant with HIE can demonstrate a variety of neurologic outcomes including acute symptoms such as seizures, alteration of consciousness, weak breathing or poor muscle tone as well as chronic conditions such as cerebral palsy, epilepsy, intellectual disability,

and behavioral disorders (6). Based on the presence of these clinical symptoms, a three-stage categorization of HIE by Sarnat and Sarnat (7) is in common use where the severity of brain injury is divided into mild, moderate and severe.

1.1.1. Pathophysiology of HI brain injury

At the cellular level, the reduction in cerebral blood flow and oxygen delivery initiates an evolving cascade of deleterious biochemical events causing neuronal death over hours to days from the initial insult. The pathophysiology of HI brain injury is very complex but can be divided into four major phases: primary energy failure associated with anaerobic metabolism; a latent phase, which is a consequence of reoxygenation and reperfusion; a secondary energy failure with inflammation and the fourth phase when the inflammation becomes chronic (8).

Under normal physiological conditions with an adequate level of oxygen a cell balance of the production and usage of high energetic molecules (ATP) occurs, and it is achieved by the consumption of glucose in aerobic respiration. In this three-step process that begins with glycolysis followed by the citric acid cycle, most of the ATP is generated in the last phase called oxidative phosphorylation (9).

Once the glucose has entered the cell, the glycolysis begins where various enzymes are used to break glucose down into two molecules of pyruvate releasing a small amount of energy (two ATP and two NADH molecules). The rate of glycolysis is regulated to supply the energy necessary for normal cellular function. When the rate of aerobic metabolism varies in parallel with functional activity of the cell, glycolytic production of pyruvate is adjusted to the rate of activity of the citric acid cycle (10). If oxygen is available, aerobic respiration goes forward with the pyruvate molecules transported into mitochondrial matrix. There, pyruvate will be converted into acetyl group picked by coenzyme A (Co-A) resulting in a compound called acetyl coenzyme A. Only in the presence of oxygen, acetyl Co-A enters the citric acid cycle which is an eight-step series of chemical reactions closed in a loop. The end products of this cycle are CO_2, ATP, and high-energy NADH and $FADH_2$ molecules that will connect to the last part of the aerobic respiration to produce more ATP molecules. The last stage of the aerobic respiration, oxidative phosphorylation, takes place in the inner mitochondrial membrane. Electrons from NADH and $FADH_2$ are passed to protein complexes (I – IV) in the electron transport chain while losing energy. Some of that energy is used to pump hydrogen ions from the matrix into the intermembrane space in the

mitochondria. In the last protein complex (IV), the electrons are accepted by oxygen, which combines with two hydrogen ions to form water. The end products of the electron transport chain are then water and 30 - 34 molecules of ATP. If there were no oxygen present, the electrons could not be removed, and the entire electron transport chain would stop (11).

During HI, depletion of blood flow and oxygen precludes citric acid cycle and oxidative phosphorylation in mitochondria. In the absence of oxygen supply, the tissue can obtain energy only by spending energy-rich phosphate reserves (PCr, ATP, and ADP). The energy metabolism switches to the anaerobic respiration where glucose is metabolized to lactic acid and provides the brain with a limited amount of energy (only two ATP molecules instead of 36 in aerobic respiration) to maintain ion homoeostasis and other essential processes (12). The consequence of the too little energy being produced is the failure of the energy-dependent Na^+/K^+ pump in the outer cell membrane. With a severe insult, this results in an influx and intracellular accumulation of Na^+, and Ca^+ causing an osmotic gradient that brings increased water into the cell. The consequence is then rapid cell swelling leading to cytotoxic edema and membrane disintegration called necrotic cell death (13). With a less severe insult, the reduction in the cell membrane potential results in a membrane depolarization following high intracellular Ca^{2+}. Moreover, it leads to a release of excitatory neurotransmitters, especially glutamate, from axon terminals into the synaptic cleft. The glutamate then activates specific cell surface receptors resulting in an influx of Na^+ and Ca^{2+} into postsynaptic neurons. This triggers a cascade of spreading depolarization and release of glutamate among neurons called excitotoxicity inducing a series of events leading to a secondary energy failure and a delayed cell death (14).

The high intracellular Ca^{2+} also induces the production of nitric oxide (NO), a free radical that diffuses to neighboring cells susceptible to nitric oxide toxicity (15). NO induces the production of radical oxygen species (ROS) in the mitochondria that leads to impaired mitochondrial function. The oxidative stress can be further increased in the reperfusion stage due to the high blood oxygen concentration boosting the production of ROS. Mitochondrial failure leads to further energy depletion and intracellular accumulation of lactate. The translocation of apoptotic triggering proteins such as cytochrome c from the mitochondria to the cytoplasm can activate a cascade of proteolytic enzymes termed caspases or cysteine proteases that eventually trigger DNA fragmentation (16). Thus, mitochondria play a key role in determining the fate of neurons following HI. Inflammatory factors like cytokines are released and the brain injury becomes more substantial. If the insult is severe, the injured tissues continue to deteriorate with persistence of the inflammation. The supporting cells

including glia and astrocytes continue to release harmful cytokines, leading to additional neuronal deaths, despite restoration of oxygen and blood supply to the brain (17).

1.1.2. MRS after HI brain injury

Nuclear Magnetic Resonance (NMR) phenomenon underlies both Magnetic Resonance Imaging (MRI) and clinical Magnetic Resonance Spectroscopy (MRS) while MRI demonstrates anatomy and highlights structural abnormalities, and MRS may be used to obtain a non-invasive metabolic information both in health and in disease (18).

MRS is one of the most important tools to study biochemical processes in the preterm and term infant brain. Interpretation of a clinical MR spectrum can provide information about cellular energetics and metabolism, neuronal function, and selected neurotransmitters activity (19).

Atomic nuclei, such as hydrogen (proton, ^{1}H), phosphorus (^{31}P), carbon (^{13}C), fluorine (^{19}F) and nitrogen (^{15}N), can be induced to produce radiofrequency signals in the presence of a strong magnetic field. Under normal conditions such atomic nuclei of spins are randomly aligned but when placed in a static magnetic field (B_0) these nuclei become weakly magnetized along the direction of the field and can be imagined to be acting like tiny bar magnets. An MR signal is generated by applying a second time-dependent magnetic field (B_1), which changes the direction of magnetization. The induced magnetization then relaxes back to the original direction after the B_1 pulse has been removed, producing the MR signal which is known as the free induction decay (FID). The resonance frequency of a nucleus is primarily influenced by its gyromagnetic ratio as well as B_0. For MRS applications, the FID can be resolved into a frequency spectrum by the mathematical function of Fourier transformation. The local magnetic environment of a nucleus and therefore the resonance frequency is subtly influenced by its immediate chemical environment. The relative frequency position can be described by a parameter known as chemical shift, a dimensionless unit accounting for the strength of the static magnetic field and measured in parts per million (ppm) (20).

With ^{31}P NMR technique, metabolites such as high-energy phosphates (phosphocreatine (PCr), adenosine triphosphates (α-, β-, γ-ATP)), inorganic phosphate (P_i), phosphomonoesters (PME) and phosphodiesters (PDE) can be detected in brain tissue both in clinics and in experimental set-ups, as shown on **Fig. 2a**. Decreased ATP levels are the sign of an impaired oxidative phosphorylation, and a ratio of PCr/Pi is a measure of the energy reserve of the tissue. PDE and PME are the phospholipids breakdown products.

Multicomponent peaks contain contribution from phosphoethanolamine (PE) and phosphocholine (PC) when it comes to PME; and glycerophopshoethanolamine (GPE), and glycerophosphocholine (GPC) when it comes to PDE. It is time-consuming to measure absolute concentrations of metabolites, and therefore, metabolite ratios (PCr/Pi, ATP/Pi) are calculated more often to demonstrate energy changes in the brain (21). What is more, using the chemical shift difference between Pi and PCr from the ^{31}P spectrum, an intracellular pH can be calculated using the formula introduced by Petroff *et al.* (22).

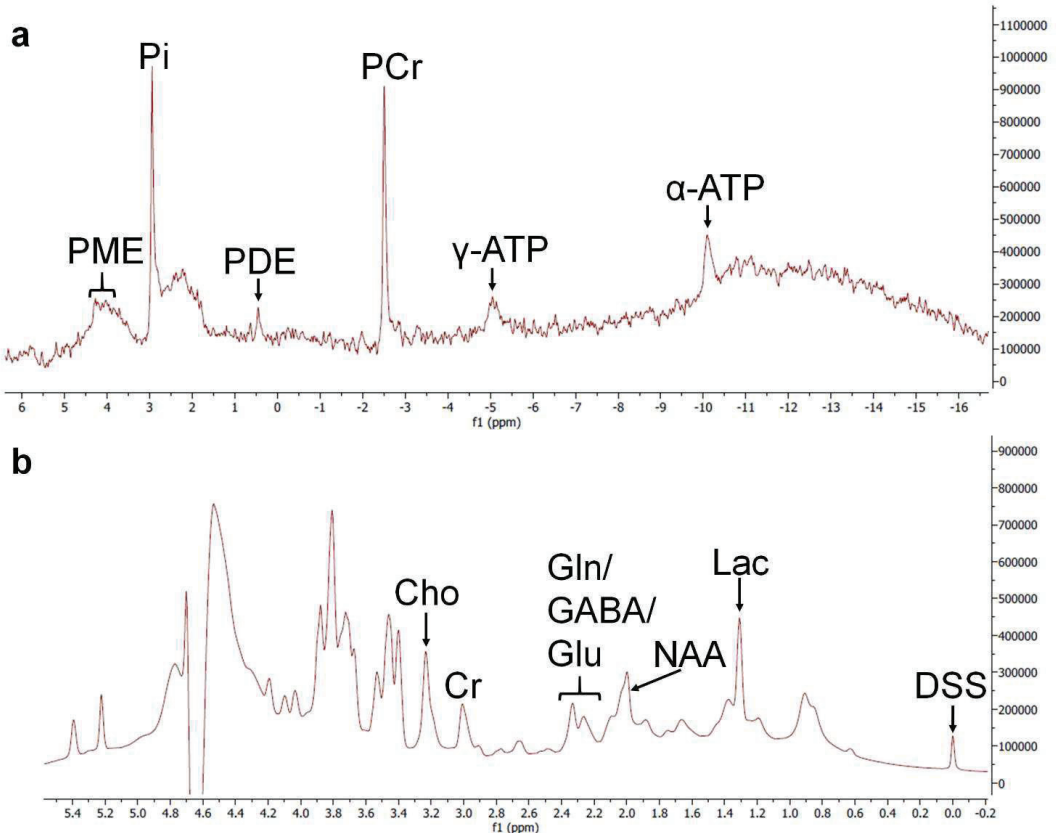

Figure 2. Representative spectra of **a)** ^{31}P and **b)** ^{1}H NMR acquired from rat brain slices perfused with normoxia and aCSF. Metabolite recognition when DSS (internal standard, 3-(Trimethylsilyl)-1-propanesulfonic acid sodium salt) was set at 0 ppm used in ^{1}H NMR, and PCr was set at -2.52 ppm in ^{31}P NMR.

Using ^{1}H NMR, metabolites like choline (Cho), creatine (Cr), *N*-acetylaspartate (NAA), lactate (Lac), glutamate (Glu), glutamine (Gln), and gamma-aminobutyric acid (GABA) peaks among others can be measured (23), as shown on **Fig. 2b**. Given the large amounts of water in the brain, high-quality water suppression is essential for ^{1}H NMR (24). As

with ^{31}P NMR, quantification of absolute concentrations of metabolites is difficult. Therefore, metabolite ratios such as NAA/Cho, NAA/Cr or Lac/NAA are mostly used instead (23).

Table 1. Metabolic response (↑ or ↓) after HI brain injury observed in ^{1}H NMR at specific chemical shift (ppm).

ppm	Metabolite	Abbreviation	Marker of
0.9 – 1.4	↑ Lipids	Lip	Cell membrane degradation
1.3	↑ Lactate	Lac	Hypoxia-ischemia, decreased pyruvate clearance
2.0	↓ N-acetylaspartate	NAA	Neuronal loss, demyelination
2.2 – 2.4	↑ Glutamine/ ↑ γ-amino-butyrate/ ↑ Glutamate	Glu/ GABA/ Gln	Excitotoxicity
3.0	↓ Creatine	Cre	Hypoxia-ischemia, impaired energy metabolism
3.2	↓ Choline	Cho	Neurodegeneration, inflammation
3.5	↑ myo-Inositol	mI	Glial cell marker, increased osmolarity

MRS of term infants with HIE demonstrated that lactate/Cr and *myo*-inositol/Cr may be markedly elevated with PCr/Pi dramatically reduced. The primary effects of the HI brain injury during and right after the insult cannot be observed in clinics. During the first hours after HI insult, MRS is not a routine nor prioritized procedure when a newborn has signs of HIE. However, a secondary energy failure, 8 to 24 h after birth is recorded with a delayed decline in PCr/Pi, and an increase in brain lactate (25,26).

MRS has been an important tool in demonstrating the pattern of energy failure during and after hypoxia–ischemia that has been confirmed in experimental studies showing similar abnormalities as in clinics. In the piglet model (27) during global hypoxia–ischemia and during focal stroke in 7-day old rat pups (28) the primary energy failure was observed where PCr/Pi fell, and pH_i became acidotic. Eventually ATP levels fell, but on resuscitation, metabolites returned to normal within 1 – 2 h. Some 6 – 12 h later, the period of secondary energy failure began where PCr/Pi declined again, and lactate increased. A clear relationship between the severity of HI insult and the magnitude of the secondary changes was observed in cerebral energy metabolism. The more severe the metabolic injury, the worse the histological injury (29). Another piglet study using ^{31}P NMR showed that for an

optimal neuroprotection following perinatal hypoxia-ischemia (HI), therapy should start before secondary energy failure and its irreversible neurotoxic cascade (30).
An adult stroke model has also been studied by MRS. The ^{31}P MRS in patients with stroke mirrored the findings in HI injury of newborns (31). A study on adult patients showed that NAA was significantly reduced, with the loss appearing to occur between 6 and 24 hours after the stroke incident. Creatine and phosphocreatine were also reduced in the infarcted area, whereas no significant change was seen in the choline content (32). In addition, ^{1}H NMR done on adult male rats showed higher lactate level and markedly lower NAA, creatine and choline levels in the injured brain in comparison to the non-ischemic regions (33).
MRS has contributed to the understanding of the pathophysiology of brain injury after HI; illustrating delayed cerebral energy failure, defining a possible 'therapeutic window', as well as showing that there are persisting metabolic changes in the brain months after HI event. What is more, MRS showed the similarities in the metabolic responses after stroke in adults and after HI brain injury in neonates. By combining *in vivo* MRS with *in vitro* and *ex vivo* research, findings may be used to assess the effectiveness of new treatment regimens.

1.1.3. Animal models of HI

Several animal models of HI brain injury have been introduced so far with some of the well-established models being adapted to different species at different ages (34).

The Vannucci model (also known as the Rice-Vannucci model) is one of the most used, well-established rodent model of neonatal HI brain injury and stroke. While initially developed in adult rats (35), the model has been successfully adapted in neonatal rats (36) and neonatal mice (37). Briefly, the experimental set-up comprises unilateral carotid artery ligation, recovery with the dam for approximately 1 h, followed by exposure to 8% oxygen for 1 – 3 h at 37 °C. This model has been very valuable in neonatal HI research through its broad applications and many advantages. One is its popularity, allowing direct comparisons with many other published results, another is that the contralateral hemisphere, exposed to hypoxia in the absence of ischemia that appears normal providing a control hemisphere within the same experimental animal. In addition, thorough behavioral studies support the long-term consequences of this model mimicking neonatal HI (38). The most significant disadvantage of this model is the high variability in size and severity of damage between animals, making comparisons between experiments difficult (39). Additionally, the invasive nature of severing the common carotid artery does not replicate human injury (40). Moreover, a basic difference between experimental *in vivo* models and the reality of HI insult

occurring in clinics is the use of the anesthesia. Apart from the influence on blood pressure, cerebral blood flow and metabolism, anesthetics may have neuroprotective or neurotoxic effects on neonatal brain (41,42), thus modulating some aspects occurring after HI.

When it comes to choosing the optimal species for the HI model, the rodent HI model is the most convenient, cost-effective, and widely used animal model of HI that has already contributed to a better understanding of the pathophysiology of HI brain injury. However, the biggest disadvantage of the HI rodent models is the difference between rodents and humans in the overall complexity of brain organization (43). While correlation between findings in humans and rodents is found, it is important to realize the limitations and translatability of studies in rodents. Rodents are not gyricephalic species and their physiology, cerebral blood flow regulation and white/gray matter ratios are very different from those in humans. Age-dependent regional vulnerability that may stem from uncoordinated maturation of individual cells in the parenchyma and in the vasculature, should also be considered while interpreting the results from HI or focal stroke studies produced in immature rodents of different postnatal ages (44). These limitations have motivated research using large animals. Large animal cerebral ischemia models would be most suitable in translational research considering that the brains are gyrincephalic and that the white/grey matter ratio is more comparable to the human brain. The preterm fetal lamb was found to display cerebral hemodynamics similar to that in the human fetus, both in normal conditions (45) and after HI (46). Moreover, the folding of the surface in the sheep brain cerebrum and the major stages of neurodevelopment are similar to those in humans (47). Despite the abundance of neurophysiological data obtained from studies using fetal sheep, pregnant ewes are large and very expensive (48). Another disadvantage of the fetal sheep model is the lack of opportunity to study motor deficiencies, especially fine motor skill movements that are associated with HI insult (49). Another HI model using a newborn piglet has demonstrated clinical, electrophysiological and neuropathological disturbances similar to those in the asphyxiated term human infant (50). The model is able to mimic comparable changes in brain white matter to a human newborn but high mortality and inconsistency in protocols result in variability in the extent of brain injury and make it difficult to draw firm conclusions (51). A non-human primate model was also developed in baboons at 125 days of gestation is equivalent to 26 weeks of gestation in human and it has shown similarities with human preterm infants in the pattern of white matter injury (52). However, the primate model is associated with the necessity for artificial ventilation and a study by Verney *et al.* (53) show

that ventilatory regimens influence the development of cortical neurons in prematurely delivered baboons that may influence the interpretation and applicability of the results.

Age of the animal used in the HI model is another important feature. Because of the developmental and functional differences between the neonatal and the adult brain, the ability to extrapolate data from adults to the neonatal condition is limited (48). Over the past several years, a model of HI brain damage in the immature rat has been investigated. At this stage of the development, the animal brain is histologically similar to that of a 32- to 34-week gestation human fetus or newborn infant; cerebral cortical neuronal layering is complete, the germinal matrix is involuting, and white matter has undergone little myelination (36). The animal age at the time of HI injury significantly impacts the resulting brain damage. Traditional models of developmental brain injury have utilized rodents at postnatal day from 7 to 10 as being roughly equivalent to a term human infant, based historically on the measurement of post-mortem brain weights during the 1970s made by Dobbing and Sands (54). Nevertheless, this injury model has been also applied to younger P1 and P2 pups, but with very high mortality rates (55), thus widespread use of P7 and older pups with higher survival rates remains accepted and the current standard. It is critical to select the appropriately aged model as the pathology and extent of the resulting neural injury is highly dependent upon the maturational state of the brain (56) and current literature questions the translational value of utilizing standard P7 pups in the Vannucci model regarding a full-term human newborn. The timing of key brain maturation events implicated in HI injuries, including neurogenesis, synaptogenesis, gliogenesis, oligodendrocyte maturation and age-dependent behaviors, occur at various time points in rodent pups before and after P7 (57). Based upon common contributing factors to human full-term neonatal HI injury, such as functional cortical activity, deep grey nuclei vulnerability, and hippocampal vulnerability (58), it is currently estimated that the P10 - P13 rat pups are a more accurate model of human infants at term (59).

Another substantial aspect of HI brain injury model is sex difference found in the pathophysiological mechanisms underlying brain damage evolution and recovery. Clinical findings show that male infants with HI injury manage more poorly than females on cognitive outcomes. Rodent models of neonatal HI support this difference, with results showing that brain injury leads to long-term behavioral deficiency found primarily in male rodents and in female rodents treated with early androgens (60). These results support the idea that sex-specific gonadal hormones may modulate developmental response to injury and link with

overwhelming evidence of developmental androgen effects on typical brain morphology and behavior (61). In neonatal animals, baseline sex differences have been seen with an early hypoxia model (62) as well as an HI model (63) of brain injury; both of which have shown that males exhibit increased brain volume loss, disrupted myelination, and increased behavioral deficits following injury as compared to like-treated females. As with adult injury models, there is also some evidence that the presence of androgens can intensify induced brain damage (64).

Besides *in vivo* animal models of HI brain injury, oxygen-glucose deprivation (OGD) used *in vitro* or *ex vivo* on cells or brain slices is also in use showing similarities with the *in vivo* models of HI brain injury. In most OGD models, cell, or tissue cultures, such as primary neurons or brain tissue slices are usually first incubated or perfused under physiological conditions in an aCSF rich in glucose, and normoxia. Then, conditions are changed to a glucose-free medium under a deoxygenated atmosphere resulting in an oxygen-glucose deprivation (65). Using brain slices in this model has several advantages used *ex vivo*. It is a precisely controlled and reproducible set-up preserving the three-dimensional neuronal network and therefore is closer to an animal model than cell culture; it reduces the number of animals needed when compared to *in vivo*; and the effects of compounds and drugs can be investigated without concern about their ability to pass through the blood-brain barrier (66).

However, as an *ex vivo* and *in vitro,* OGD model shares many disadvantages. It lacks the influence of factors such as blood perfusion, cerebrovascular autoregulation, intracranial pressure etc., which are involved in the pathophysiology of HI brain injury. Moreover, OGD models may have limitations for the study of calcium ions after HI insult given the multiple homeostatic processes involved in the maintenance of intracellular calcium. Importantly, brain slices are only suitable for examining the short-term effect of drugs on various injuries because the slices cannot survive long after intense or prolonged injury. It is also important to remember that the results obtained from brain slices are only an approximation of what occurs in the animal brain. Considering the cell reprogramming that could occur in an artificial environment with environmental pressures that differ from those *in vivo*, potential epigenetic changes in protein expression should make researchers evaluate their results more carefully. *In vivo* animal models are still ultimately necessary to evaluate the anatomic and functional outcomes of a therapeutic strategy (67).

It is very fortunate that a great variety of models are available for the study of neonatal HI brain injury. Furthermore, a development of new models and adaptation of already established models is seen. However, an accurate selection process must be applied to the choice of the appropriate animal model for testing possible treatments for neonatal HI. There is no animal model that completely reflects the complexity of the human condition but usage of several HI-related age-specific models in rodents, and in larger species, enables the improved understanding of brain pathology and development of novel therapies for the immature brain.

1.1.4. Treatment of HIE

Therapeutic hypothermia is the standard treatment for HIE with the goal to intervene during the latent period and minimize the damage from the secondary energy failure (68). There are two approaches of hypothermia available in clinics: selective head cooling (at 34.5 °C) and total body cooling (at 33.5 °C). During therapeutic hypothermia treatment cerebral metabolic rate decreases by about 6 - 7% for every 1 °C drop in the body temperature, which is consequently reducing the oxygen demand, decreasing loss of high-energy organic phosphates and preventing development of metabolic acidosis in the tissue (69).

Therapeutic hypothermia initiated within 6 h after birth for moderate or severe HIE reduced the composite outcome of death or disability at 18 months of age in multiple randomized clinical trials and improved the outcomes at 6 to 7 years of age (70). However, initiating hypothermia before 6 h after birth can be difficult if infants are born in distant communities, if encephalopathy is recognized after this time or when the time of HI insult is unknown. There is uncertainty in effectiveness of hypothermia started 6 – 24 h after birth (71); therefore, new and more effective neuroprotective strategies are urgently required.

The complex pathophysiology of HIE enables multiple treatment targets at different processes involved in the brain injury (72). Results from animal studies reveal many of them as a great promise for translation to clinical use against HI, among others (73):

- xenon (74),
- Innate defense regulator peptide-1018 (IDR-1018) (75),
- Tat-NEMO-binding domain (TAT-NBD) (76),
- memantine (77),
- topiramate (78),
- erythropoietin (79),
- allopurinol (80),
- 2-Iminobiotin (81),
- magnesium sulfate (82),
- melatonin (83).

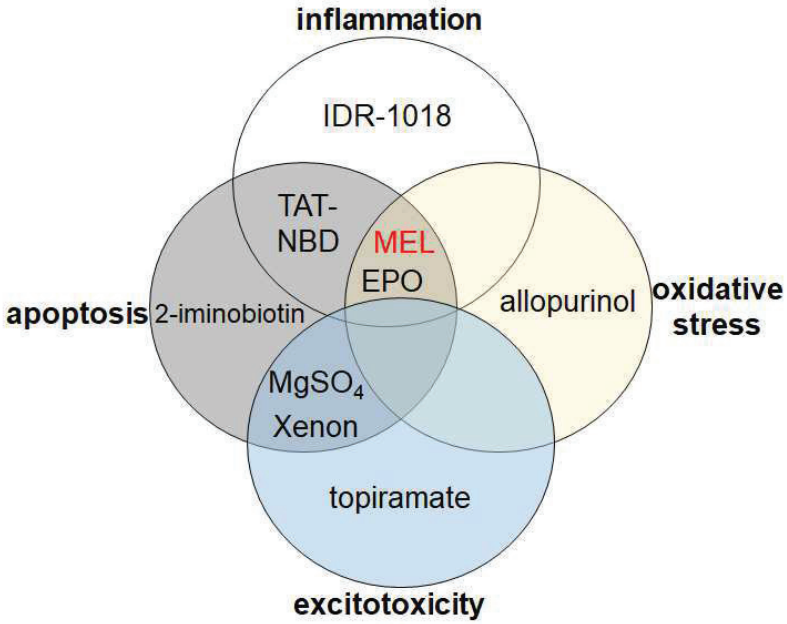

Figure 3. Emerging therapies working against inflammation, apoptosis, excitotoxicity, and oxidative stress. *MEL: melatonin, EPO: erythropoietin, TAT-NBD: tat-NEMO-binding domain peptides, IDR-1018: innate defense regulator peptide-1018, $MgSO_4$: magnesium sulfate.

Melatonin was brought to our attention mostly because of its wide scope working mechanism shown on **Fig. 3** (anti-inflammatory, anti-oxidative, and anti-apoptotic agent), its low toxicity (84) and its use in clinics in oral administration gaining a potential to be used in neonates with HIE.

1.2. Melatonin

Melatonin (N-acetyl-5-methoxytryptamine) is an endogenously produced indole amide secreted mostly in the brain by the pineal gland but it is also locally found in lymphocytes, bone marrow, thymus, gastrointestinal tract, skin, and retina (85). The synthesis and release of melatonin are determined by the environmental light/dark cycle, suggesting melatonin involvement in circadian rhythm. Almost 80% of this hormone is synthesized at night, with serum concentrations between 80 and 120 pg/mL when during the day, serum concentrations are lower, from 10 to 20 pg/mL (86). Once melatonin is produced and released in the bloodstream, it binds to albumin in 60 – 70% while the rest is found in free state able to cross the blood brain barrier and placenta (87). Melatonin is metabolized primarily in the liver and secondarily in kidneys to 6-hydroxymelatonin (6-OHM), which is urinary eliminated as a sulfate or glucuronide conjugate (88). In addition, about 5% of melatonin is eliminated as a free drug via kidneys (89) and the rest of melatonin is eliminated in the central nervous system to N-Acetylserotnin (NAS), 5-methoxytyptamine (5-MT), and N1-Acetyl-5-methoxykynuramine (AMK) via N1-Acetyl-N2-formyl-5-methoxykynuramine (AFMK), among others (**Fig. 4**).

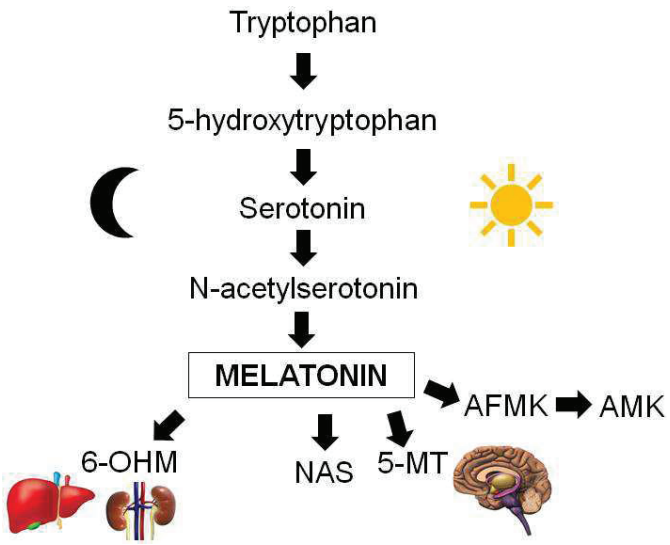

Figure 4. Synthesis and main metabolites of melatonin.

Melatonin plays a role in several physiological functions, including regulation of sleep, body temperature, reproduction and neuroimmunomodulation of both cellular and humoral immunity (90). This hormone and its metabolites are highly effective direct free radical scavengers, with the ability to remove singlet oxygen, superoxide anion radical, hydroperoxide, hydroxyl radical and the lipid peroxide radical (91). It also acts as an indirect antioxidant by increasing the efficiency of mitochondrial electron transport and by activating the most important antioxidant enzymes including superoxide dismutase, catalase, and glutathione peroxidase (92).

The protective functions of melatonin against oxidative mitochondrial damage, inflammatory reaction, and cell death in the white matter have been studied for years in various animal models. Study on rats by Lin *et al.* (93) confirmed that melatonin reduces intracerebral cellular inflammatory response and protects neurons against ischemic injury by reducing the oxidative stress, lipid peroxidation, and radical oxygen species generation. In the study by Yawno *et al.* (94) in a preterm fetal sheep, an increase of oligodendrocyte cells within the periventricular white matter, improved myelin density within the subcortical white matter and improved neuronal survival within the cortex were found after administration of melatonin.

Robertson *et al.* (95) demonstrated in the piglet study that combination of melatonin and hypothermia treatment after HI is more effective than any of these forms of the treatment alone. Melatonin-augmented hypothermia significantly reduced lactate/NAA and lactate/total creatine ratios in the deep grey matter. Signorini *et al.* (96) investigated the possible effect of melatonin treatment in a model of HIE in 7-day old rats. Study showed that after HI in melatonin-treated animals the levels of free iron, F2-isoprostanes, and F4-neuroprostanes were significantly lower than in HI rats without the melatonin treatment. However, to achieve clinical translation from the results of the studies mentioned above, questions regarding melatonin therapeutic window, optimal dosing and the route of administration have to be answered.

Melatonin doses differ in the *in vivo* studies, with one study finding that a dose as small as 1.25 mg/kg of melatonin is showing neuroprotection and reduces the neurological deficit induced by traumatic brain injury in mice (97), and another study finding 20 mg/kg of the drug strongly reduces inflammation and promotes subsequent myelination in the white matter after neonatal stroke (98). Moreover, some of the regimens were studied and found negative effects of the drug after injury. A dose of 150 mg/kg of melatonin significantly increased brain edema and elevated oxidative stress when compared with the vehicle-

treated group (99). Some of the experimental melatonin dosage designs are listed in the **Tab. 2** showing the wide range of the dosage regimens having a therapeutic effect on HI brain injury using different administration types as bolus, continuous, and repeated parenteral injections of melatonin.

Table 2. *In vivo* studies on HI brain injury using different dosage regimens of melatonin. *DMSO: dimethyl sulfoxide, EtOH: ethanol

Melatonin total dose	Solvent used	Animal model	Results
3 mg/kg (IV bolus + infusion for 2 h)	1% EtOH	fetal sheep	Melatonin provides neuroprotection in the late-gestation fetal sheep brain in response to umbilical cord occlusion (100)
5 – 45 mg/kg (single or multiple doses, IP)	5% DMSO	P7 rat	Melatonin protects from the long-term consequences of a neonatal hypoxic-ischemic brain injury (83)
20 - 40 mg/kg (single or double doses, IP)	5% DMSO	P7 rat	Melatonin promotes myelination by decreasing white matter inflammation after neonatal stroke (98)
60 mg/kg (IV infusion of 5 mg/kg/h over 6 h started at 10 min after resuscitation and repeated at 24 h)	2.5% EtOH	P1 piglet	Melatonin augments hypothermic neuroprotection in a perinatal asphyxia model (95)
60 mg in 24 h (IV)	5% EtOH	newborn lambs	Systemic melatonin administration prevents neuropathology in response to perinatal asphyxia (101)

To date, only melatonin formulations for oral administration are clinically available and are used for treating a variety of circadian rhythm disorders, including jetlag and insomnia. However, clinically melatonin has variable oral absorption and high first-pass hepatic metabolism (102), making an oral route of melatonin administration less preferable. Moreover, apart from oral administration is challenging in neonates since HI injury can also affect the gut which can further reduce melatonin's absorption and bioavailability (103).

Melatonin is non-toxic, and highly safe drug. The lethal dose 50 (LD_{50}) for intraperitoneal injection of melatonin was determined in rats (1168 mg/kg) and mice (1131 mg/kg), but could not be achieved after oral administration of melatonin (tested up to 3200 mg/kg in rats) nor after subcutaneous injection (tested up to 1600 mg/kg in rats and mice) (104). There is an evidence in dose escalation experiments of the remarkable lack of toxicity of melatonin in humans up to 100 mg (105). Therefore, melatonin holds a promise in management of infants with HIE.

The therapeutic window for melatonin in the neonatal HI brain injury is unknown but in case of therapeutic hypothermia used in clinics, the goal is to start the hypothermia treatment as soon as possible after the HI insult, at least within 6 h after birth. In neonatal HI this period is stated between the primary and secondary energy failure and represents a latent phase. Based on previous studies in our group, it is conceivable that the therapeutic window of melatonin treatment is longer than 1 hour (106). What is more, we concluded that a dosage higher than 10 mg/kg with multiple administrations during the first 24 h, and probably prolonged duration of treatment are needed to achieve maximum benefit of melatonin treatment (107). Another pressing matter in using melatonin as a drug is its poor solubility in water and light sensitivity. In animal experiments mentioned above, the poor water solubility is typically circumvented using organic solvents, like dimethyl sulfoxide (DMSO) or ethanol (**Tab. 2**), to make injectable melatonin formulations. However, these solvents have potential toxic effects (108), and our group have previously reported mitochondrial impairment in astrocytes when DMSO was used as melatonin solvent (109). This is a possible confounding factor in animal experiments and poses an obstacle towards clinical translation. Thus, there is a need for an injectable melatonin formulation without toxic recipients to realize optimal and predictable bioavailability and, more importantly, to translate this therapy into clinical use in pediatrics.

1.3. Lipid-based nanoparticles

A variety of nanoparticles (NPs) has been developed and characterized for delivering poorly water-soluble drugs. One of the most studied platforms are lipid-based nanoparticles primary consisting of amphiphiles. Amphiphilic molecules, such as phospholipids in cell membranes, consist of a hydrophilic head and a hydrophobic tail. When self-assembled in aqueous solution, phospholipids generate nanostructures such as liposomes and micelles. Moreover, oil-in-water nanoemulsions can be stabilized with monolayers of lipid mixtures (110). The dualistic character of amphiphiles arranges the hydrophobic tails together, minimizing the contact with water, while the hydrophilic heads that decorate the hydrophobic domains form hydrogen bonds with surrounding water molecules. Three widely used lipidic amphiphiles in lipid-based nanoparticle synthesis are cholesterol, DSPC (1,2-Distearoyl-sn-glycero-3-phosphocholine), and DSPE-PEG_{2000} (1,2-distearoyl-*sn*-glycero-3-phosphoethanolamine-N-[amino(polyethylene glycol)-2000]). Two common lipidic nanoparticles are liposomes and oil-in-water nanoemulsions, shown in **Fig. 5**.

Cholesterol is a hydrophobic molecule and preferentially interacts with the core of the phospholipidic membrane. The addition of cholesterol to the lipid bilayer of liposomes reduces their permeability and increases liposomal *in vivo* and *in vitro* stability, because the presence of cholesterol induces a dense packing of phospholipids and inhibits their transfer to for example high-density lipoprotein (HDL) and low-density lipoprotein (LDL) in the circulation. Further, cholesterol can be used to anchor other molecules to the liposomes, such as polyethylene glycol (PEG) (111). The use of phosphatidylcholine (DSPC) with saturated fatty acyl chains and materials that stretch the transition temperature beyond 37 °C offer even greater stabilization (112). For prolongation of the *in vivo* NP circulation time, a milestone is the inclusion of PEG (e.g. PEG2000) in NP composition (113). Similarly, the PEGylation of the liposomal carrier proved to extend the blood-circulation time while delaying the uptake by the reticuloendothelial system (RES). Compared with free doxorubicin, pegylated liposomal doxorubicin has been reported to result in fourfold to 16-fold enhancement of drug levels in malignancies in mice (114).

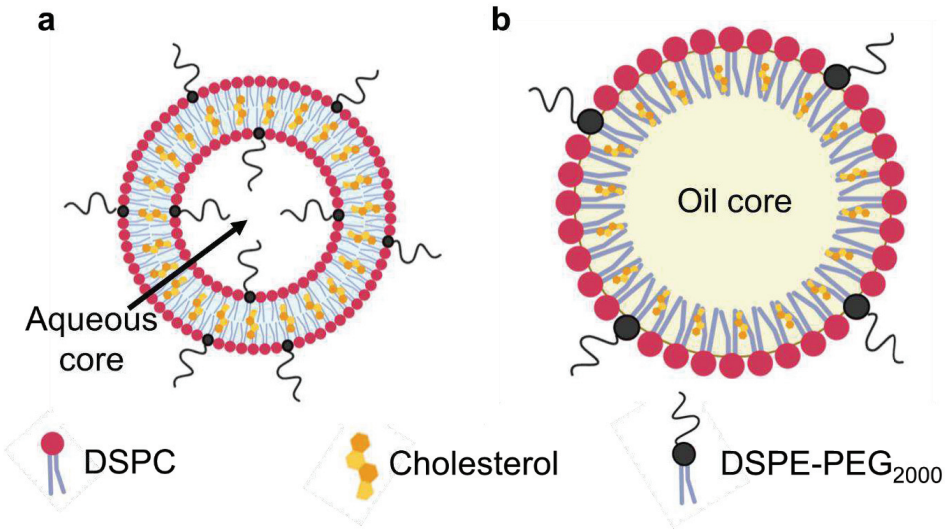

Figure 5. Schematic representation of **a)** liposome with aqueous core and **b)** oil-in-water nanoemulsion with oil core both constructed of DSPC, cholesterol and DSPE-PEG_{2000} components.

Oil-in-water nanoemulsions (NE) are systems mainly composed of two parts: the oil core and the emulsifying agents on the surface. The oil phase can consist of for example triglycerides, diglycerides, monoglycerides, and free fatty acids. The viscosity, density, phase behavior, and interfacial tension of the oil phase components influences the formation, stability, and functional properties of nanoemulsions (115). However, the long-chain triacylglycerides (i.e. soybean oil) are preferred for nanoemulsion formulation due to their low cost, low water solubility, availability, functional, and nutritional attributes (116). Nanoemulsions offer enhanced solubilization capacity for poorly water-soluble drugs, that can lead to a higher bioavailability of the developed therapeutic nanoformulation (117). There are few commercial products which are based on nanoemulsion technology, i.e. an estradiol topical nanoemulsion developed by Novavax called Estrasorb® that is recommended for the reduction of vasomotor symptoms in menopausal women. It is composed of soybean oil, water, polysorbate 80 and water proving that poorly water soluble molecules like estradiol can be successfully formulated and used in clinics (118).

Liposomes are spherical vesicles with particle size ranging from 30 nm to several micrometers consisting of one or more phospholipid bilayers surrounding aqueous unit. Among several drug delivery systems, several liposomal formulations are in clinical

use (119). Depending on the nature of the drug, liposomes can solubilize and transport hydrophilic or lipophilic drug within their phospholipid bilayers and in aqueous core (120).

Lipid-based nanoparticles have gained prominence commercially as drug carriers (121) because of their biocompatibility, biodegradability and low toxicity. In addition, their ability to trap both hydrophilic and lipophilic drugs like melatonin makes them a promising platform for melatonin delivery and neonatal HI brain injury treatment.

1.4. Drug therapy

1.4.1. Administration routes and regimens

The aim of drug therapy is to treat patients by bringing drug's plasma concentration within its therapeutic window. In order to reach it the dosage regimen of drug administration needs to be selected depending on the drug used, the condition to be treated, patient's characteristics (age, gender, physiological status, among others) and how rapidly a steady state (C_{ss}) must be achieved. Steady state refers to the situation where the overall intake of a drug is in equilibrium with its elimination. In practice, the time to reach steady state is four to five half-lives of the drug if it is given at regular intervals; no matter the number of doses, the dose size, or the dosing interval (122).

The aim of a dosage regimen is to achieve the maximum benefit of a drug with its minimum side effects and the decisions defining it are about (123):

- route of administration,
- drug formulation,
- unit dose,
- frequency,
- loading dose,
- length of treatment.

A key factor determining the administration route is whether the drug is being administered for local, systemic, or parenteral effect. The parenteral routes include intravenous (IV), intramuscular (IM), subcutaneous (SC), and intraperitoneal (IP) administration, among others. Knowledge of advantages and disadvantages of different administration routes is important in order to choose the optimal route by which a drug can be given (124).

Each route has advantages and disadvantages (**Tab. 3**) that should be considered depending on the final effect to be achieved, and ultimately the route selected will markedly affect the pharmacokinetics of the substance. In addition, it is important to remember that in laboratory animals, many of the commonly used methods of drug delivery require restraint, sedation, or general anesthesia. The use of such manipulations should be taken under consideration when selecting the administration route so that they are less invasive to the animals (125).

Table 3. Advantages and disadvantages of using IV, IP and PO administration routes (126,127).

Intravenous route (IV)	Intraperitoneal route (IP)	Oral route (PO)
Advantages		
Drugs bypass first-pass metabolism. Bioavailability is 100%.	Relatively rapid absorption.	The simplest, and most convenient for repeated and prolonged use.
Fast onset of drug's action.	Used in smaller laboratory animals when IV is difficult.	Clinically applicable.
Irritating solutions can be administrated.	Large volume of a drug can be injected.	Pain-free.
Amount of a drug can be controlled with high accuracy.	Suitable for repeated administrations.	No sterile precautions are needed.
Disadvantages		
Strict aseptic conditions are required.	Need for sterility.	Delayed onset of action because of the slow absorption.
Injected drug can't be withdrawn.	Risk of damaging intraperitoneal structures (i.e. bowel).	Drugs are metabolized via the first-pass effect resulting in drastically reduced bioavailability.
Introduction of air may produce embolism and be fatal.	Not suitable for irritating compounds because causes chemical peritonitis.	It is not suitable for highly irritant drugs and patients with severe vomiting.
Not suitable for large volume administration.		Requires patient's cooperation.

The intravenous route of delivery is the most efficient method of delivering substances to animals because it circumvents the need for solute absorption. With this method, substances are administered directly into blood vessels (125). Whereas intraperitoneal administration is an injection of substances into the peritoneal cavity; a common technique in small laboratory animals for which intravenous access is challenging but rarely used in larger mammals and humans. It can be used to safely administer large volumes of fluid. Absorption of drug delivered IP is typically much slower than in case of intravenous injection. Although intraperitoneal delivery is considered a parenteral route of administration, the pharmacokinetics of drugs administered IP are more similar to oral administration, because the primary route of absorption is into the mesenteric vessels, which leads into the hepatic portal vein and pass through the liver (128). Therefore, drugs administered IP may go through hepatic metabolism before reaching the blood circulation.

To initiate drug therapy a dosage regimen is administered either by a bolus injection (single dose), continuous infusion or in intervals of time and dose (repeated administration) (129). An IV bolus injection guarantee the rapid achievement of very high peak drug concentrations, as may be required for some drugs. With an IV bolus administration the amount of drug delivery is precisely controlled. After entering the blood circulation, the drug is distributed throughout the body. Once the drug has reached the equilibrium in the plasma and tissues, the decline of plasma drug concentration is driven by elimination of the drug from the body (**Fig. 6**) (130).

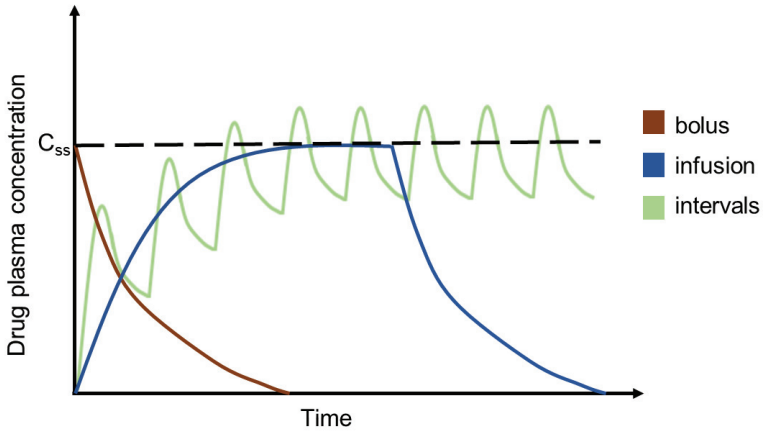

Figure 6. Effect of different IV drug administration types; bolus injection vs infusion vs intervals (repeated administration) on plasma drug concentration-time profile (130).

Another type of drug administration is the infusion regimen used to ensure a constant exposure to the drug over a prolonged time. The drug infusion rate must be adapted to the patient's clearance to have the concentration of a drug in plasma reach its therapeutic target. When a drug is infused IV at a constant rate, a plateau concentration is reached progressively. The amount of drug in the body rises, but as the drug concentration increases, so does the rate of drug elimination. Thus, the rate of elimination will keep increasing until it matches the rate of drug infusion. The amount of drug in the body is then constant and have reached a steady state. When stopping an IV infusion, the decline in plasma drug concentration follows an exponential curve, as seen after an IV bolus injection of the drug (**Fig. 6)** (131).

The most common approach of drug therapy is the repeated administration regimen. In repeated administration, accumulation occurs when the drug is administered before the previous dose is eliminated. The amount of a drug in the body will then progressively rise. In the most common case of first-order kinetics, the rate of drug elimination will increase proportionally. When the rate of drug elimination compensates the rate of drug administration, the average drug concentration reaches its steady state. At steady state, the amount of drug lost in each interval equals the amount of drug gained. Therefore, the plasma concentration fluctuates between doses similarly from one dosing interval to another (130).

1.4.2. Pharmacokinetic processes and parameters

The aim of pharmacokinetics (PK) is to study the relationship between a dosage regimen and the drug plasma concentration-time profile. These studies are usually carried out in healthy individuals to investigate and estimate the interactions between the drug and the body in the general population, and the data obtained provide information about the appropriate drug therapy design (132). The mechanisms that determine the plasma concentration-time profile are commonly referred to ADME scheme:

- Absorption (process of substance entering the blood circulation),
- Distribution (dispersion of substances throughout the fluids and tissues of the body),
- Metabolism (irreversible transformation of drug compounds into metabolites),
- Excretion (removal of the substances from the body) (133).

ADME involve monitoring of drug concentrations in blood and tissues over a period of time and are characterized by pharmacokinetic parameters; C_{max} (maximum plasma concentration of a drug), $T_{1/2}$ (half-life, time required for the drug concentration to fall to 50% of its original value), AUC (area under the curve, exposure of a drug concentration in blood plasma as a function of time), and T_{max} (time at which the C_{max} is observed), among others (**Fig. 7)** (134).

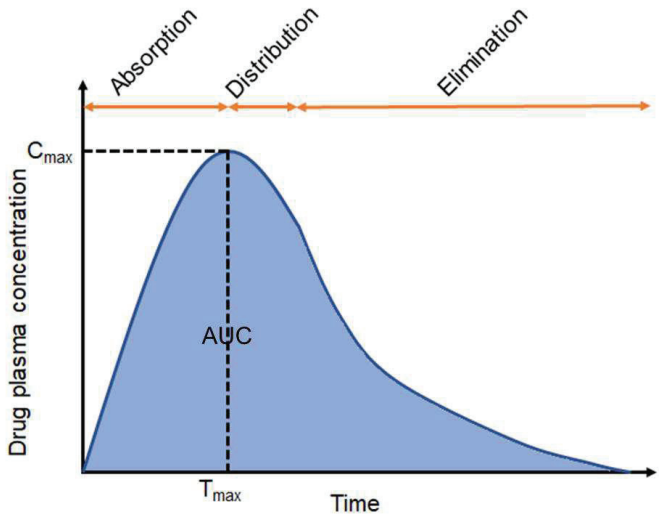

Figure 7. Drug plasma concentration-time profile in the phases of absorption, distribution and elimination following oral administration of a drug.

Knowing PK parameters obtained from the PK studies is essential to decide on the appropriate drug dosing regimen and an optimal pharmaceutical therapy (135).

1.4.3. Pharmacokinetics of melatonin

Currently, melatonin pharmacokinetics has been documented in adults (136), while further investigation in neonates is still needed to optimize the dosage and the frequency of administration. In adult animals and humans, intravenously administrated melatonin half-life ($T_{1/2}$) ranges from 18 - 35 min (137) to 28 - 60 min (136), respectively. Short melatonin $T_{1/2}$ indicates that melatonin should be administered at short intervals to obtain and maintain blood concentrations similar to those effective in experimental animals. Recently, Merchant *et al.* studied the pharmacokinetic profile after infusion of 0.1 mg/kg/h melatonin for two

hours in preterm infants, aiming to obtain blood concentrations of the drug comparable to those observed physiologically in the adults. They reported a higher $T_{1/2}$ in infants compared to adults (138). However, since most animal and human data indicate that the neuroprotective action of melatonin occurs at doses ranging from 5 to 15 mg/kg, doses higher than those are needed to replace the physiological values, and it is important to investigate the pharmacokinetics of melatonin in human newborns at similar doses. It is important to mention that compared to adults, neonates at birth have lower plasma concentrations of albumin (139). Only unbound drug travels across membranes, exerts biological effect, and is eliminated from the body, thus efficacy and toxicity of a drug can be achieved with lower total plasma concentrations in neonates in comparison to adults (140). In addition, neonates have higher circulating bilirubin and free fatty acids, which can displace drugs from albumin binding sites (141). It is possible then that the same dose of melatonin in adults and neonates may result in an increased plasma concentration of unbound melatonin in neonates. Moreover, it should be considered that metabolism and elimination functions are immature in neonates. Newborns have a limited capacity for hepatic biotransformation; cytochrome P450 enzyme-mediated metabolism improves with postnatal age, and approaches adult levels only after the first year of life (142). In particular, conjugation reactions in newborns are inefficient, and result in a reduced ability to eliminate both exogenous and endogenous compounds like melatonin (143).

1.4.4. Pharmacokinetics of lipid-based nanoparticles

When a therapeutic agent is loaded into lipid-based nanoparticles, it adopts the carrier's pharmacokinetics that depend on the physicochemical characteristics of the lipid vehicle, including lipid composition, size, membrane lipid packing, steric stabilization, surface charge, as well as dose, and route of administration (144). In general, the PK profile of the nanoformulation would result in increased drug C_{max}, $T_{1/2}$, AUC, and reduced clearance compared to the free drug (145).

However, it is important to be aware that PK parameters of designed nanoparticle drug formulations in adults will be different in pediatrics. An optimal size of nanoparticles is dictated by the mononuclear phagocyte system (MPS) (146). Particles smaller than 5.5 nm in diameter are filtered through the kidney while vascular fenestrations in the liver are 50-100 nm (147,148). There is no current evidence showing that these fenestration sizes vary between adult and children. However, size-based

accumulation occurs in other organs such as the lung, which is particularly important in the pediatric population due to smaller airway caliber and lower ventilation rate of children (149).

Upon nanoparticle absorption into the blood circulation, a variety of plasma proteins attach to a particle surface, which allows for recognition, internalization, and clearance by macrophages. Smaller nanoparticles (80 nm) have lower protein adsorption (6%) compared to larger sized nanoparticles due to the smaller surface area, doubling the circulation time compared to the larger particles (150). In general, protein adsorption occurs to a much lesser extent in children as it is well known that total plasma protein level is lower in neonates and young infants (45-73 g/L) when compared to adults (65-85 g/L) (151).

Another feature that has an influence on nanoparticle PK and protein binding is nanoparticle surface charge. In general, negatively charged particles exhibit strong phagocytic uptake through the MPS and positively charged particles induce serum protein binding. Thus, neutrally charged nanoparticles demonstrate the lowest MPS clearance and the longest circulation times (152). In the pediatric population, this effect may be slightly less significant as MPS clearance mechanisms are immature and serum protein levels are low (153).

Lastly, nanoparticle composition can also affect serum protein binding. PEG is a relatively inert hydrophilic polymer that provides steric hindrance and charge shielding, preventing protein interaction and binding, and ultimately increasing nanoparticle circulation time (146). For example, it is a major excipient in factor VIII and factor IX therapies for pediatric hemophilia indicating that children can tolerate it. What is more, Stidl *et al*. (154) estimated the total PEG exposure of the pediatric population to be substantial (over 26 g/year) over the past several decades with no evidence of adverse effects. Lipidic content can also affect clearance and circulation time, where an increased lipid dose leads to prolonged half-life of the nanoformulation (155). In one dose-exposure study of a liposomal antifungal formulation of amphotericin B, adults and children (1-17 years old) responded similarly to increased lipid doses (156). This suggests that lipid content trends are preserved between pediatric and adult populations once the MPS system approaches mature function around 1 year of age (153).

While the preclinical evaluation of nanoformulations in pediatric aged animals requires more investigation, a variety of nanoparticle formulations have been tested clinically in the pediatric population when liposomes are the most widely studied nanotechnology-based formulations in pediatrics.

2. Aims

The overall aim of this project was to develop a melatonin formulation without organic solvents, and to investigate its neuroprotective effect on hypoxic-ischemic brain injury.

More specifically, aims were:

1. To synthesize a non-toxic melatonin nanoformulation suitable for melatonin delivery via parenteral administration, and to characterize it *in vitro* and *in vivo* in plasma and brain.
2. To investigate the neuroprotective effect of melatonin nanoformulation *in vivo* using neonatal HI brain injury Vannucci model compared to previous melatonin formulation using organic solvents.
3. To develop and optimize a more controllable and reproducible HI model to investigate melatonin neuroprotective properties.

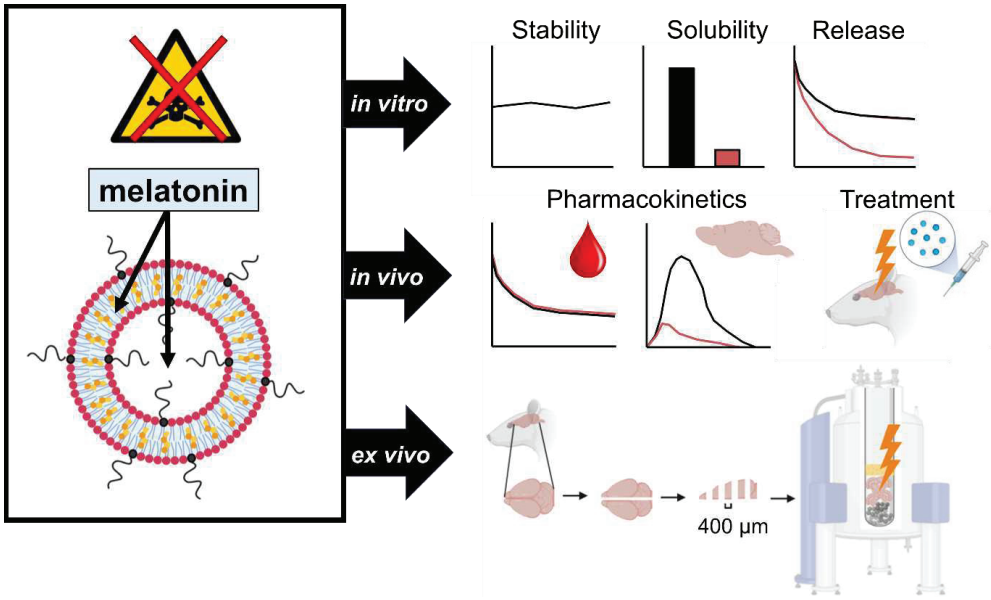

Figure 8. Graphical summary of the aims of the thesis.

3. Materials and methods

3.1. Melatonin-loaded nanoparticles selection and synthesis

In this thesis, lipid-based nanoparticles were used to solubilize melatonin and improve its bioavailability. Four different melatonin-loaded nanoformulations were prepared: melatonin-loaded liposomes (MEL-LP) and three melatonin-loaded nanoemulsions (MEL-NE).

Initially, to identify most suitable oils for the development of MEL-NE, solubility of melatonin in seven oils (C4, C6, C8, C18, MCT, SB, and oleic acid) was determined. Three oils were selected to synthesize MEL-NE: C6, MCT and soybean (SB) oil based on criteria: the length of the fatty acid chain in the oil (NE of short-chain triglycerides are typically less stable under *in vivo* conditions); melatonin solubility in the oil and its FDA-approval (**Fig. 9**).
Melatonin-loaded liposomes, and three nanoemulsions with C6, MCT, and SB oil were synthesized using a generic lipidic composition with DSPC/Cholesterol/DSPE-PEG_{2000} on a 62:33:5 molar ratio, respectively. In case of nanoemulsions, 60 mg of oil was also added, and the whole mix was dissolved in chloroform. The well-established solvent evaporation method was used (157) and the obtained crude nanoparticles were downsized in an iced water-bath using a sonication tip.

In **Paper II** (HI treatment) only the melatonin-loaded liposomes were used in comparison with the conventionally used melatonin dissolved in 5% DMSO/95% PBS, as shown on **Fig. 9.**

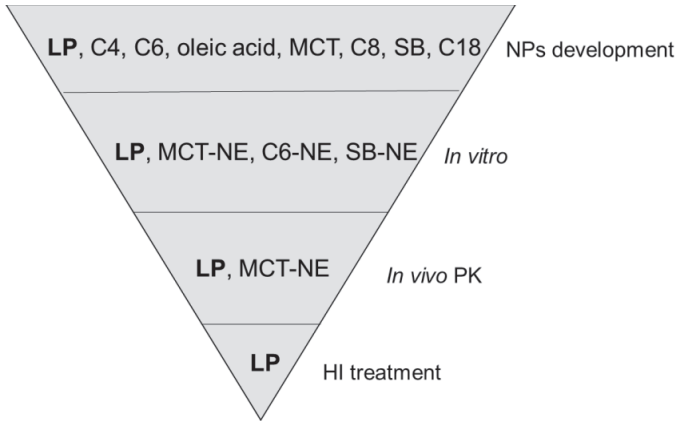

Figure 9. Nanoparticle selection for the *in vitro, in vivo* PK and the HI treatment study.

3.2. Melatonin-loaded nanoformulation characterization

3.2.1. Concentration

An absorption spectroscopy is a commonly used, relatively easy and fast method to determine drug concentration based on the compounds light absorbance that increases linearly with increasing molecule concentration, as predicted by the Beer-Lambert Law (158). Knowing the maximum absorbance of melatonin (159), this method was used to determine drug concentration in seven different oils in order to select the most appropriate oil core for melatonin-loaded nanoemulsion synthesis. Th same method was used to measure the melatonin concentration in all melatonin-loaded formulations (liposomes, and C6-, MCT-, SB-nanoemulsions) in **Paper I** and in liposomal melatonin in **Paper II**. After preparing melatonin-nanoformulations, aliquots were diluted 15 x in isopropanol and vortexed resulting in nanoparticle disassociation. To determine melatonin concentration, the absorption readout on 100 µL of this sample was compared to a melatonin standard curve in isopropanol with the same amount of lipids/oil in the sample (8 points, 0 – 0.4 mg/mL melatonin, $R_2 = 0.99$).

3.2.2. Nanoparticle size and distribution

Dynamic light scattering (DLS) is a well-established and accurate technique that provides information on the mean particle size as well as on the particle size distribution. This method is based on the Brownian motion of dispersed particles. When particles are dispersed in a liquid they move randomly in all directions (160). Such motion of macromolecules depends on their size, temperature, and solvent viscosity (161). When the movement of particles over a time range is monitored, information on the size of macromolecules can be obtained, as large particles diffuse slowly, compared to small particles which move faster (162).

Nanoparticle dispersions are often polydisperse; there may be particles with a distribution of sizes and shapes rather than particles of a single size and shape (163). Polydispersity Index (PDI) is a representation of the distribution of size populations within a given sample. PDI ranges from 0.0 (uniform sample with respect of particle size) to 1.0 (highly polydisperse sample with multiple particle size populations). In drug delivery applications using lipid-based nanoparticles, a PDI of 0.3 and below is acceptable and indicates a homogenous population of phospholipid vesicles (164).

DLS method was used to determine the size (hydrodynamic diameter) and size distribution (dispersity) of liposomal melatonin and three melatonin-NE: C6, MCT, SB (**Paper I** and **II**).

3.2.3. Release study *in vitro*

In vitro release study is commonly used method to predict the *in vivo* behavior of the drug-loaded nanoparticle. Generally, *in vitro* release studies are performed at physiological temperature and in biological fluids. Drug release from nanoformulation can be assessed using sample and separate (SS), continuous flow (CF), or dialysis membrane (DM) method.

The dialysis is the most versatile and popular method, where the physical separation of the nanoformulation is achieved by using a dialysis membrane which allows simple sampling at fixed time intervals. The nanoparticles in a specific release media are located into a dialysis bag or a floating dialysis tube with a membrane of an appropriate molecular weight cut-off (MWCO) (165). A bag/tube is then sealed and placed in a larger container with release media (i.e. PBS), and slowly stirred to minimize unstirred water layer effects (**Fig. 10**). Then, drug released from the nanoparticles diffuses through the dialysis membrane to the outer compartment.

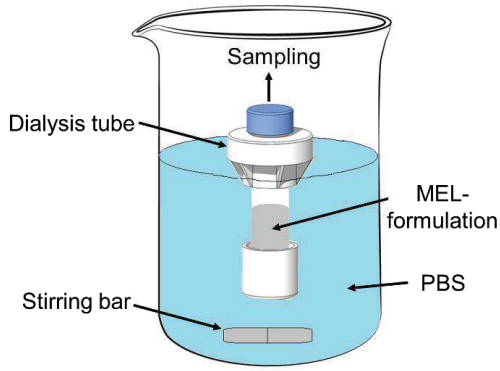

Figure 10. Dialysis floating tube filled with melatonin-nanoformulation placed in PBS, stirred at 150 rpm, protected from light.

In **Paper I**, melatonin formulation sample was placed in the dialysis tube with 100 kDa MWCO membrane. Knowing melatonin molecular weight (232 Daltons), the size of the selected membrane was appropriate allowing the drug to diffuse easily from one medium to another. The floating dialysis tube was placed in 1 L of PBS, at to 37 ˚C, gently stirred, and protected from light. Since melatonin release to the outer medium would not be measurable due to the too low drug concentration in 1 L of PBS, we measured the melatonin from the

dialysis tube at fixed intervals from MEL-LP, C6-NE, MCT-NE, SB-NE as well as from the conventionally used formulation: drug dissolved in organic solvent. Usually, in the *in vivo* studies of melatonin in HI models, melatonin dissolved in 5% of DMSO or 10% of EtOH is used. However, using DMSO was not recommended by a producent of the dialysis tube. The risk of damaging the membrane by DMSO was high, at even small amounts of DMSO as 5%. Instead, 10% of ethanol was used and no damage to the membrane was noticed.

3.3. Animals and HI brain injury models

In all studies involving animals, Sprague-Dawley rats (*Rattus norvegicus*) obtained from Elevage Janvier (Le Genest Saint Isle, Laval, France) were used. All animal experiments were performed according to the European Union and Norwegian regulations and guidelines for animal experimentation, and were approved by the Norwegian authority on animal welfware (Mattilsynet, FOTS 10105). Rats were housed in a controlled light/dark cycle (12 h/12 h), temperature at 21 – 22 ˚C, humidity at 50 – 55%, with environmental enrichment, food, and water *ad libitum*.

For the pharmacokinetic studies (**Paper I**) adult female rats were used, while for the treatment study (**Paper II**) 7-day old rat pups of both sexes were used. In the last study (**Paper III**), brain slices used for the bioreactor were taken from young adult rats.

Table 4. Number of animals used in each study divided into experimental groups.

Paper I		**Paper II**		**Paper III**	
Group	**N**	**Group**	**N**	**Group**	**N**
DMSO	5	Sham	33	Control	6
LP	8	75 min HI	32	OGD-30	5
MCT-NE	8	90 min HI	12	OGD-60	6
				OGD-120	5

In **Paper II**, we have used the *in vivo* Vannucci model to study the treatment effect of the liposomal melatonin after HI brain injury. Seven-day old rat pups (P7) were randomly assigned to HI groups (moderate: 75 min or severe: 90 min) and Sham. Hypoxia-ischemia was induced in rats at P7 using a modified Rice-Vannucci procedure (166). Under isoflurane anaesthesia, the right common carotid artery was identified and thermocauterized. The skin was sutured, and animals returned to dam for a recovery period of 2 h before introducing the hypoxia (8% O_2 in N_2, 37 °C) (**Fig. 11**). For SHAM animals, the common carotid artery

was identified but not cauterized. Three IP injections of either DMSO-melatonin (5% DMSO), liposomal melatonin (3 mg/mL) or PBS were carried out immediately after, 6 and 24 h after HI insult (3 x 30 mg/kg melatonin each) with SHAM animals receiving no treatment. *In vivo* MRI and ^{1}H MRS was done at P8 and P14.

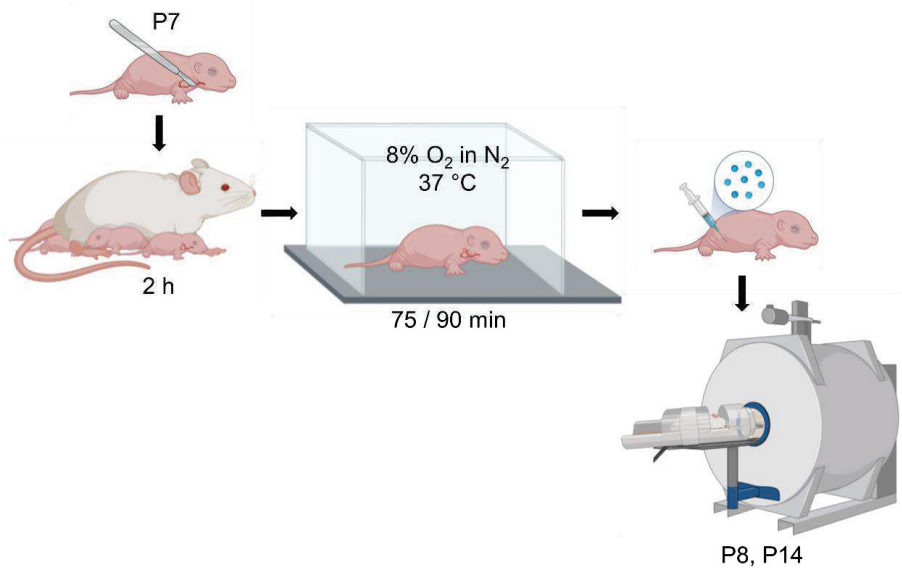

Figure 11. Study design in the HI group using P7 rats.

The second model of HI brain injury, an NMR-compatible perfusion system with OGD with three HI severity levels: mild, moderate, and severe was used on rat brain slices *ex vivo* in **Paper III**.

On the day of the bioreactor study, an animal was anaesthetized with 3 - 4% isoflurane. When a negative pedal pain reflex was obtained, the animal was decapitated using a guillotine. The whole brain was extracted from the skull and brain slices were prepared according to the modified method in protocol by Opitz-Araya X. and Barria A. (167). The brain was cut into two hemispheres; one hemisphere was placed on the dissecting table, midline facing down, and the cerebellum was mounted to the cutting surface using glue. Then, the cerebrum was cut into 400 µm thick slices. Intact brain slices (n = 20) from the cerebrum area were selected and loaded into a 10 mm NMR tube containing 0.6 g of glass beads (Ø = 1 mm) and a sponge filter was placed above the tissue to keep slices in the NMR active region, as shown on **Fig. 12**.

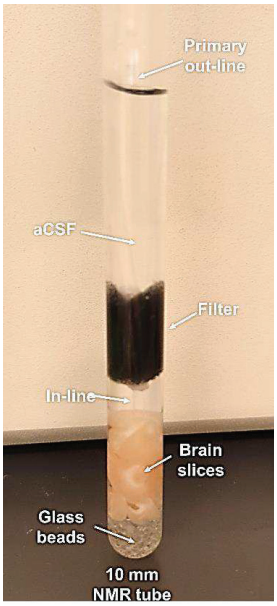

Figure 12. Brain slices loaded into 10 mm NMR tube filled with glass beads, and filter mounted above supplied with aCSF from the in-line.

3.4. Pharmacokinetic profile of melatonin-loaded nanoparticles

In **Paper I**, we compared the pharmacokinetic parameters of melatonin in three different formulations (10 mg/kg BW): liposomes, MCT-nanoemulsions and in 5% DMSO formulation to determine the plasma and brain concentrations of a drug in adult rats. Ultra-high-performance liquid chromatography tandem mass spectrometry (UHPLC-MS/MS) method has been developed. Method validation for analysis of melatonin and its three metabolites (AFMK, AMK, 6-OH) was conducted to confirm the precision and accuracy of drug determination before the animal studies.

3.4.1. In plasma

Blood samples were collected into heparinized tubes from the saphenous or femoral vein at 5 min pre-dose and 5, 10, 20, 30, 60, 120, 240 min post-dose. The first five samples were collected under isoflurane anesthesia and the final three were collected from awake animals. After collection, samples were centrifuged, and supernatant plasma was transferred into new tubes and stored at -20 ˚C prior the UHPLC-MS/MS analysis. Each sample was thawed and mixed with acetonitrile, vortexed, and then centrifuged at 4000 g for 10 min to precipitate proteins. Supernatant was collected to new tubes and dried in a SpeedVac concentrator. All

samples were stored at -20 °C prior to the analysis, then diluted in Milli-Q® water before injection into a UHPLC–MS/MS system. Concentrations of melatonin and breakdown products were determined in the range from 3.125 to 500 nM, and all standards and samples were spiked with 25 nM of melatonin-d_4 as internal standard.

3.4.2. Brain microdialysis

Microdialysis method enables collecting samples of molecules with small molecular weight, i.e. melatonin. It is a widely used technique in neuroscience to quantify the neurotransmitters, hormones, peptides in the extracellular fluid (ECF) in brain from a freely moving and conscious animal (168). With this technique, sampling can be performed continuously, and high-resolution concentration profiles of drugs and its metabolites can be obtained from the animals without the use of anaesthetic agents. What is more, microdialysis provides protein-free samples where enzymatic degradation is eliminated and protein precipitation procedures for analysis are not needed. In addition, it is made without the loss of fluid that is critical when sampling blood from rodents (169).

In our study, we have used an internal standard approach to determine *in vivo* recovery for the dialysate sample during the experiment. In our case, we have chosen melatonin-d_4 due to its matching characteristics of the measured melatonin. Prior to the *in vivo* PK studies, the recoveries of both melatonin and melatonin-d_4 were measured *in vitro*, and the ratio between them was determined. With the assumption that the obtained ratio *in vitro* would remain the same *in vivo*, it was used to calculate the *in vivo* recovery of the drug as a function of time (168).

We have used an aCSF that matches the CSF in rodents as much as possible, and we have performed pilot studies of the surgery. In addition, we have used a guided cannula that facilitate easy insertion into brain tissue when performing a microdialysis probe insertion. An *in vitro* experiment with melatonin was performed proving that the drug does not stick to the tubes or probe material used in the microdialysis study. To minimalize the effect of tissue trauma after the surgery with the implantation of the guised cannula in the striatum, PK experiments were performed after minimum 24 hours from the end of the surgery. UHPLC-MS/MS method was chosen to analyze the microdialysis samples with an estimate of LOQ equal 0.65 nM of melatonin.

3.5. Magnetic resonance

In **Paper I**, melatonin-loaded liposomes and melatonin-MCT-nanoemulsions were characterized by ^{1}H NMR to indicate the lack of organic solvents in the formulations after nanoparticle synthesis process. Samples with 10% D_2O added were analyzed using a 600 MHz Bruker Avance III NMR spectrometer dedicated for biofluids (5 mm BBI probe). Sample of melatonin-MCT-NE with remaining chloroform was used as a control where a chemical shift of chloroform was recognized at 7.70 ppm.

In **Paper II,** *in vivo* MRI and ^{1}H NMR were performed on a small animal 7T magnet (Bruker BioSpec 70/20, Bruker BioSpin, Ettlingen, Germany) using an 86 mm volume resonator for RF transmission and a phased array mouse head surface coil for reception. During scanning, animals were fixed to a water- and air-heated thermoregulated bed using plastic screws and styrofoam, anaesthetized with isoflurane (4% induction, 1.5 - 3% maintenance). For more details about sequences used during scanning go to **Paper II**.

In **Paper III**, NMR experiments were performed using a 600 MHz Bruker Avance III NMR spectrometer, 10 mm BBO probe. Viability of rat brain slices was assessed by ^{31}P NMR (ns = 600, t = 15 min 17 s or ns = 1200, t = 30 min 22 s; RG = 203). The dynamic changes in metabolites under normoxic and hypoxic conditions were monitored using ^{1}H NMR (ns = 32, t = 2 min 22 s, RG = 114). A 1D NOESY (noesygppr1d) pulse sequence was applied with pre-saturation (50 Hz) of water signal during relaxation delay (1 s) and mixing time (10 ms). The stacked ^{1}H NMR spectra were recorded as a pseudo-2D NMR experiment, starting a new ^{1}H experiment every 120 s. The acquisition parameters were identical to the 1D NOESY experiment, except the spectral width was increased to 20 ppm. Distance between DSS and water signal was determined from a zg experiment with similar parameters to the 1D NOESY. Media samples were analyzed using a 600 MHz Bruker Avance III NMR spectrometer dedicated for biofluids (5 mm BBI probe). An 1D NOESY (noesygppr1d) pulse sequence was applied with presaturation (25 Hz) of water signal during relaxation delay (4 s) and mixing time (10 ms).

3.6. NMR-compatible perfusion system: bioreactor

To keep the tissue viable during the experiments, an NMR-compatible perfusion system suppling the brain slices with aCSF at 37 ˚C continuously bubbled with oxygen was built.

Brain slices loaded into NMR tube were supplied with 95%/5% O_2/CO_2 pre-bubbled normal-aCSF containing glucose (more details about the aCSF content in section **2.3.** in **Paper III**). The bioreactor medium was dumped for the first 10 minutes to remove remaining slicing-aCSF medium used during tissue slicing and then the perfusing medium was re-circulated until the introduction of the OGD period. A reservoir of normal-aCSF and reservoir of OGD-aCSF without glucose were placed in a water bath (40 ˚C) outside the NMR spectrometer. The medium was delivered to the NMR tube loaded with brain slices via medical grade extension tubes pumped in a closed circuit with a peristaltic pump while continuously bubbled with either 95%/5% O_2/CO_2 carbogen mixture or 95%/5% N_2/CO_2 gas. The bioreactor in-line and out-line were placed inside a water-heating line (60 ˚C) between the pump and NMR-spectrometer bore, as shown on **Fig. 13**. At the beginning of each bioreactor experiment, the temperature of the probe in the spectrometer bore was adjusted based on the temperature of the perfused aCSF sample to reach 37 ± 1 ˚C. More details about the OGD study design and temperature measurement in **Paper III**.

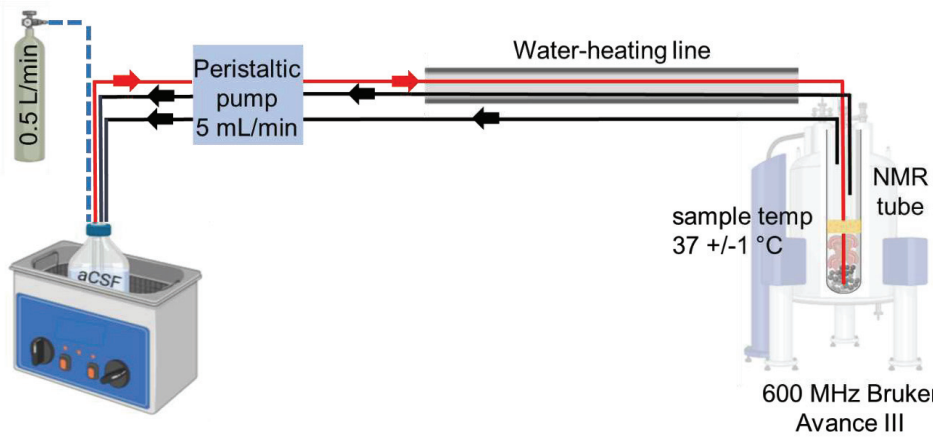

Figure 13. Illustration of the bioreactor set-up with NMR sample containing brain slices supplied with oxygenated aCSF placed in the NMR-spectrometer bore. Bioreactor tubing consisted of in-line tubing (red) to deliver normal-aCSF to the brain slices located in the NMR tube inside the spectrometer bore; primary out-line tubing (black) to return the normal-aCSF from the brain slices back to the normal-aCSF reservoir and a secondary out-line (black) placed in case of malfunction of the primary out-line.

3.7. Histology and immunohistochemistry

In **Paper II** after the treatment study, the evaluation of tissue morphology in the brain tissue was assessed using HES (haematoxylin, eosine, saffron) and Nissl staining, and the

neuronal loss in the brain was measured immunohistochemically using GFAP and CD68 ED1 antibodies.

Conventionally stained sections (HES and Nissl), CD68 and GFAP sections were scored semi-quantitatively at x 20 in the same eight ipsilateral areas. Scores were summed for each staining method for each animal and compared between groups.

In **Paper III**, morphological changes in the brain tissue before and after the bioreactor study was studied using HES (hematoxylin, erythrosine, saffron) staining. Brain slices were collected after the bioreactor experiments and were immersion-fixed in formalin (4% formalin). The brain hemisphere that was not used in bioreactor experiments was also immersion-fixed in formalin for comparison. Samples were paraffin-embedded, sectioned and stained histologically. Stained sections were observed under an optical microscope (x 40) and the results were consulted with a neuropathologist.

3.8. Statistics

Statistical analysis in **Paper I** and **II** was performed using R (version 3.5.2). In **Paper I**, melatonin PK parameters were assessed using a non-compartment analysis for each animal. In **Paper II** group difference was tested using ANOVA after assumptions of normality and homogeneity of variance (Levene's test) were applied. Group means were compared *post hoc* using Tukey's Honest Significance Difference method. Variables not normally distributed were compared using a Kruskal-Wallis Rank sum test and the effect size was estimated as eta squared according to Tomczak and Tomczak (170). Post hoc group mean comparisons were performed using Dunn's method with Holm adjustment for multiple comparisons. Some variables were corrected for weight change. This was accomplished using an ANCOVA model with weight change used as a covariate.

Spectra from **Paper III** were analyzed and processed in MestreNova (MestreLab Research, Santiago de Compostela, Spain) using phase correction, multipoint baseline correction, and sum method. ^{1}H NMR peaks of interest were integrated with respect to the DSS-peak in case of both media and tissue samples. For ^{31}P NMR, peaks of interest were integrated with respect to Pi-peak. Signal intensity of each metabolite was plotted against time using Excel (Microsoft).

4. Summary of papers

Paper I

In vitro and *in vivo* evaluation of organic solvent-free injectable melatonin nanoformulations

Alicja Molska, Axel Karl Gottfrid Nyman, Alexandros Marios Sofias, Kåre Andre Kristiansen, Sjoerd Hak, Marius Widerøe

The aim of this study was to develop and characterize an injectable and non-toxic melatonin nanoformulation with improved melatonin bioavailability using lipid-based recipients.

We synthesized an injectable system by solubilizing melatonin in liposomes (MEL-LP) and nanoemulsions (MEL-NE). We characterized the nanoformulations: their size and size dispersity, melatonin concentration, and melatonin *in vitro* relase from the MEL-nanoformulations using dialysis method in comparison to the conventional melatonin formulation in 10% ethanol. The absence of organic solvents in our nanoformulations was confirmed by ^{1}H NMR. The pharmacokinetic parameteres of melatonin-nanoformulations were studied on adult female rats in blood and brain using brain microdialysis and was compared to the PK parameters of the melatonin dissolved in 5% DMSO.

Nanoparticle characterization confirmed physicochemical stability over a week and an improvement of melatonin solubility with respect to melatonin solubilized in water. *In vitro* release kinetics showed a prolonged release of melatonin solubilized in nanoparticles ($T_{1/2}$ of melatonin-LP: 81 min vs $T_{1/2}$ of melatonin-NE: 50 min, and $T_{1/2}$ of melatonin-EtOH: 26 min). No organic solvents were visible in NMR spectra of melatonin nanoformulations. The pharmacokinetic parameters confirmed similar melatonin levels detected in blood and higher bioavailability in brain after intravenous administration (10 mg/kg) of melatonin nanoformulations in comparison to the free-melatonin in 5% DMSO.

In conclusion, we have developed an organic solvent-free injectable melatonin-nanoformulation by using FDA-approved ingredients that proved similar or improved PK parameters *in vivo* in comparison to the conventional melatonin formulation. In combination with the complete elimination of organic solvents, our melatonin formulation is applicable not only in neonates with HI brain injury, but also in a variety of other pathological conditions.

Paper II

Effects of liposomal melatonin on HI in the neonatal rat

Axel Karl Gottfrid Nyman, Alicja Molska, Alexandros Marios Sofias, Hester Rijkje Berger, Sjoerd Hak, Marius Widerøe.

The aim of this study was to investigate the neuroprotective effect of high dose melatonin nanoformulation in neonatal rats with hypoxic-ischemic brain injury.

The main challenge regarding melatonin used as a therapeutic agent in the acute phase of hypoxic ischemic encephalopathy is melatonin poor solubility in water. Current efforts to mitigate this have included parenteral administration using organic solvents such as DMSO or ethanol. However, the use of organic solvents carries the risk of solvent toxicity, either directly or through modulating the effect of melatonin.

We have attempted to overcome these obstacles by solubilizing melatonin in liposomes. We investigated the neuroprotective effect of high dose melatonin (3 x 30 mg/kg administrated directly after, 6 h and 24 h after the HI insult) in neonatal rats with HI using MRI and MRS techniques.

The results of this study indicate that liposomal melatonin is moderately neuroprotective after HI and avoids the neurometabolic side effects of dissolving melatonin in DMSO, making it a promising formulation for clinical translation. However, a total dose of 90 mg melatonin/kg (both liposomal and in DMSO) over 24 h after the HI insult may mask the neuroprotective effect by inducing a reduction of weight gain the first day after HI insult, resulting in a more severe brain injury. When weight gain is statistically corrected for, liposomal melatonin is superior to melatonin dissolved in DMSO and no treatment. The results of this study indicate that further studies on liposomal melatonin dosage optimization and a second, more controllable HI model are required.

Paper III

Perfusion system for studying dynamic metabolomics in rat brain slices exposed to oxygen-glucose deprivation (OGD) using ^{1}H and ^{31}P NMR

Alicja Molska, Deborah Katherine Hill, Trygve Andreassen, Marius Widerøe.

The aim of this study was to establish a controlled and reproducible model to study metabolic changes during oxygen-glucose deprivation (OGD) in rat brain slices using an NMR-compatible perfusion system.

In vivo animal studies of HI brain injury are often hampered by a high variability in injury severity depending on the initial extent of injury induced by the surgery (171), strain of the animal (172), and weight variation, making the results hard to compare and reproduce (166). *In vitro* and *ex vivo* models may offer many advantages over *in vivo* techniques in the study of the mechanisms involved in brain ischemia: an immediate and direct access to the extracellular compartment due to the lack of a blood–brain barrier and direct control over environmental factors.

In this study, rat brains were cut in 400 µm thick slices and perfused with aCSF in an NMR tube inside an NMR spectrometer. Four experimental conditions were tested: (I) continuous perfusion with aCSF with glucose and normoxia, (II) 30, (III) 60, or (IV) 120 min of oxygen-glucose deprivation (OGD) followed by reperfusion of aCSF with glucose and normoxia. The energetic state of perfused brain slices was measured using ^{31}P NMR and metabolite changes of lactate/NAA were measured using ^{1}H NMR. Media samples were collected every 30 minutes and analysed using ^{1}H NMR.

NMR data clearly distinguished three severity groups (mild, moderate, and severe) after 30, 60, and 120 min of OGD, respectively, compared with Control. ^{31}P NMR spectra obtained from Controls showed that PCr/Pi levels were stable over 5 h of bioreactor experiment. Control ^{1}H NMR spectra showed that Lac/NAA levels were stable with a tendency to gradually increase due to the re-circulation of the aCSF in the perfusion system.

In conclusion, we have successfully developed an NMR-compatible bioreactor system that allowed reproducible characterization of three different severity levels of OGD in rat brain tissue. The ^{31}P and ^{1}H NMR results give satisfactory quality of the spectral information about

changes of metabolites in brain tissue in bioreactor. Future studies to characterize the impact of therapeutic agents on OGD response can now be investigated using this bioreactor system and HI model.

5. Discussion

5.1. A novel melatonin nanoformulation

The overall aim of this thesis was to develop a melatonin formulation without organic solvents and to study its effect on hypoxic-ischemic brain injury.

To overcome melatonin's poor water solubility and the possible toxic effects of organic solvents used in conventional melatonin formulations for parenteral use, lipid-based nanoparticles loaded with melatonin were synthetized using established protocols resulting in formulations with good performance *in vivo* (157,173).

Compounds encapsulated inside nanoparticles have been shown to have an enhanced biodistribution and prolonged half-life compared to the free compound (176). We have succesfully solubilized melatonin in liposomes and nanoemulsions without organic solvents remaining in the final formulation, and we have observed an improved *in vitro* melatonin release from the nanoparticles to the outer compartment in comparison to the free drug released from a dialysis tube. *In vitro* half-life values in the dialysis study were the highest in liposomal melatonin, and the lowest in EtOH-melatonin. Surprisingly, blood results from the pharmacokinetic study *in vivo* performed on healthy adult rats did not show an improvement of melatonin $T_{1/2}$ from nanoparticles. Instead, half-lives of melatonin from liposomes, MCT-NE and DMSO-melatonin were similar in plasma. Since we have dealt with completely different samples and different melatonin concentrations in the *in vitro* and *in vivo* experiments, we have used different methods for measuring drug concentration. In the case of measuring melatonin concentration in the *in vitro* release experiment, absorption spectroscopy was used because it is fast, simple, and accurate. For the *in vivo* study, a more sensitive method (UHPLC-MS/MS) was required to measure melatonin concentration in plasma and brain due to the expected low concentration of the drug. Details about these methods are included in section **3.2.3.** and **3.4.** of the manuscript**,** concluding that both methods are precise (R^2 = 0.99), and suitable for measuring melatonin. *In vivo* results were validated using internal standards, calibration curves, and blank samples. To minimize variability in the *in vivo* results, all samples were handled according to the same protocol and experiments were performed by the same person. A comparison of the three melatonin-formulations *in vivo* showed relatively small differences compared with the results observed *in vitro*.

It is not uncommon for formulations to exhibit excellent drug retention properties *in vitro*, but to display almost complete drug release in a shorter time after systemic administration to animals (174). The aim of performing an *in vitro* release test is to investigate and establish product behavior during various stages of drug product development and is commonly used to predict the *in vivo* behavior (165). There are clear differences between the *in vitro* and *in vivo* experiments, with *in vivo* being more complex in the case of nanoparticle kinetics; nanoparticles can accumulate in organs and drugs can bind to proteins that may have an influence on the drug PK measured in blood (175). Therefore, drawing direct comparisons between the *in vitro* and the *in vivo* studies may not be appropriate. In the case of our results, measured pharmacokinetic parameters from the *in vivo* study are likely to be more relevant for clinical translation, where it is important to ensure that drug candidates have appropriate PK properties and can be evaluated in preclinical pharmacology and safety studies.

The main aim of the PK study was to compare the conventional melatonin formulation using DMSO to the recently developed melatonin-nanoformulations. Compounds encapsulated inside nanoparticles are usually used as drug carriers and their main advantage over the free drug is an enhanced drug biodistribution and prolonged half-life of encapsulated compound compared to the free compound (176). As mentioned above, we did not observe a prolonged half-life of melatonin encapsulated in nanoparticles in our *in vivo* study in blood however, the aim of using lipid-based nanoparticles in our study was not primarily as a drug carrier but as a non-toxic solubilizer. What is more, because of melatonin's non-toxic characteristic, we decided to keep the free melatonin fraction (maximum 20% of the final formulation), which is solubilized in the surroundings of the nanoparticles, rather than removing it by filtration as it is done with involvement of toxic drugs. A possible consequence of injecting a melatonin nanoformulation that includes both nanoparticle-loaded melatonin and free-melatonin is that the measured PK will be a combination of the two fractions. This could mask the true PK profiles of the melatonin nanoformulation and the DMSO-melatonin because the free melatonin has a faster release rate and shorter half-life. Melatonin concentration was not measured on the day of injections but the day before. Then, the melatonin solubilization efficiency for all melatonin-nanoparticles was between 80 and 90% with MCT-nanoemulsion having slightly higher melatonin solubilization efficiency than liposomal melatonin.

Interestingly, melatonin concentrations measured in adult rat brains were higher for nanoformulations than for the DMSO-melatonin indicating that melatonin-NPs are reaching

tissues in higher levels. The pharmacokinetic parameters of melatonin-loaded formulations in brain show no relation to their blood profile, indicating a possible liposomal melatonin uptake into the brain tissue. However, in order to fully understand the biodistribution of lipid-based nanoparticles loaded with melatonin, further research is required. There are some uncertainties about the DMSO data in the brain PK study due to the small sample size (n = 2) in this group but we are still quite confident about the overall result.

To conclude, we successfully formulated melatonin-NPs without organic solvents, which reach the brain and blood in higher or similar concentrations as for DMSO-melatonin. Therefore, for brain treatment purposes, lipid-based nanoparticles are more favorable as melatonin solubility agents than DMSO.

Another important consideration of the first study is that it is not possible to directly translate pharmacokinetic characteristics from adults to neonates; metabolism in neonates is not yet fully mature, and therefore the formulations with melatonin may be metabolized differently (138). Compared with adults and older children, melatonin half-life and clearance in infants are prolonged and the volume of distribution is decreased (177). These observations could be related to several factors; melatonin is extremely lipophilic and the lower body fat content in infants (10%) compared with adults and children (20 - 25% and 15 - 20%, respectively) would affect the volume of distribution and may contribute to higher than expected melatonin concentrations in blood (177). Ideally, we should have used neonatal rats in our PK study, however, *in vivo* brain microdialysis and blood samples collected at the various time-points from neonatatal rats is more challenging than from adults and requires sacrifacing more animals. Although, there are differences between the PK of drugs in adults and neonates, the results from our pharmacokinetic study in blood and microdialysis study in brain performed on adult rats gave us a valuable insight into the *in vivo* behaviour of nanoparticle melatonin formulations when compared to the conventional melatonin form. Therefore, the data obtained from our study could be used to guide treatment study of melatonin in neonates.

5.2. Influence of administration route on drug pharmacokinetics

Nanoparticles can be administrated through different routes including intravenous, intraperitoneal, and oral administration, where the intravenous route results in the highest drug bioavailability (100%). In the pharmacokinetic study, melatonin-formulations were administrated intravenously to the adult rats. However, IV is an inconvenient route to use in neonatal rats due to the small vessels of the animal. Melatonin administrated orally has poor

bioavailability (102), especially when administrated to patients after HI brain injury where the gut can be affected by the injury, reducing the melatonin absorption even further (103). To avoid these problems (summarized in section **1.4.1. Tab. 3**), we used intraperitoneal injection for the treatment study on 7-day old rats.

For the majority of cases, the bioavailability of a pharmacological agent after IV administration is closer to IP rather than IM, SC, or PO. Usually, the rate of absorption after IP administration is one-half to one-fourth as rapid as after IV administration (127). Following rapid absorption from the peritoneal cavity, a compound may face one of the following two pathways to reach systemic circulation: 1) it is absorbed through the visceral peritoneum, and is drained into portal circulation, or 2) the compound gets into the systemic circulation directly bypassing liver when it is absorbed through parietal peritoneum and lymphatics. Notably, small molecular weight compounds, like melatonin, are primarily absorbed through the first pathway, because the surface area of membranes transporting substances into the portal circulation is much larger than in the case of macromolecules (128). Therefore, it is important to recognize and acknowledge the possible differences of the pharmacokinetic parameters from our first paper after IV administration of melatonin loaded in nanoparticles in the adult rats when compared to the kinetics of liposomal melatonin after IP injections in neonates. Thus, the bioavailability of melatonin loaded in the nanoparticles might be lower after IP administration when compared to the IV administration.

In a study by Rip et al. (178), where PEG-liposomes were injected into rats using either IP or IV administration route, it was observed that after single IP administration of nanoparticles, liposomes entered the blood stream more slowly than after IV and remained significantly below the levels of IV administration during the first 4 h. However, after that time, the blood levels of liposomes injected via IP route remained as high as after IV injections for at least 24 h. Moreover, tissue levels of PEG-liposomes after IV or IP administration were not statistically different except for the levels in the spinal cord ($p < 0.05$), where IV administration resulted in higher tissue uptake. The highest nanoparticle concentrations were found in the spleen, followed by liver, lungs, and kidneys. In addition, levels from intact liposomes were detectable in brain homogenates. Based on this study, choosing IP administration for our pegylated-liposomes loaded with melatonin might prolong the duration of a drug in circulation, while after IV, the entire dose of the nanoparticles with melatonin would be taken up to the circulation within minutes after injection. However, to solve these uncertainties further studies are required. In addition, our second study included multiple IP injections of melatonin formulations instead of a single injection, as in the study

mentioned above, presumably resulting in a more stable steady-state of melatonin. Since liposomal melatonin half-life in blood was proven to be short in our first study (around 20 min in all melatonin formulations), using multiple IP administration might not only slow the melatonin uptake in blood but might also increase the half-life of the drug in blood. However, we did not measure PK parameters of IP multiple injections of liposomal melatonin, and we are not certain if in the case of HI brain injury treatment, a longer steady state and slower uptake in blood after IP is more advantageous than high Cmax and faster uptake in blood after IV.

5.3. Dose of melatonin required for neuroprotective effects after HI

Earlier *in vivo* studies on HI brain injury suggest that melatonin protection is dose-dependent, time critical, and influenced by the excipient (179). Melatonin total dose that has been used in animal models of HIE ranges from 3 to 60 mg/kg showing a treatment effect after HI brain injury (180), as shown in section **1.2. Tab. 2.** Previous melatonin treatment studies in our group using the Vannucci model with 7-day old rats revealed that melatonin administration of 10 mg/kg (single dose) (109) and 20 mg/kg (106) (2 x 10 mg/kg injected directly after and 6 h after the insult) both using 5% DMSO as solvent, was not capable of protecting the neuronal mitochondria after HI brain injury. Several factors could explain the lack of neuroprotective melatonin effect; single dose of 10 mg/kg was too low, too long delay between the multiple melatonin doses possibly being unable to reach the drug's steady state or/and because any beneficial effects of the drug might have been masked by modulatory effects of DMSO on cerebral metabolism. What is more, our PK study with melatonin nanoformulations revealed that after IV administration of 10 mg/kg melatonin loaded in liposomes, the drug can reach the brain in the concentration of around 125 nM. However, a study by Uchida *et al*. (181) showed that to observe an antioxidant effect of melatonin on brain slices after ischemic stress by perfusing them with glucose-free aCSF under hypoxia, melatonin concentration of 10 μM and more is required. Based on this, we used 30 mg/kg liposomal melatonin administered multiple times in our treatment study (directly after, 6 h and 24 h after the HI insult) resulting in a total dose of 90 mg melatonin/kg. This dose regimen was based on the optimal volume for IP injections used in 7-day old rats (182) as well as the maximum drug concentration that could be achieved by solubilizing melatonin in our lipid-based nanoparticles (3 mg melatonin/mL formulation). Moreover, melatonin is a highly safe drug with a remarkable lack of toxicity in humans even up to 100 mg (105), and

high doses of melatonin used *in vivo* before have not shown side effects, as mentioned in section **1.2**.

5.3.1. High dose melatonin influence on weight

With higher melatonin dosage in the treatment study, we expected a more significant neuroprotective effect of melatonin after the HI insult. However, we did not observe this in our treatment study using a total melatonin dose of 90 mg/kg over 24 h after the HI injury. Surprisingly, such high dose of the drug resulted in reduction of weight gain and weight loss in melatonin-treated animals in comparison to the non-treated animals. Since the effect on weight change was seen both in DMSO-melatonin, and liposomal melatonin, it is likely to be related to the drug rather than liposomes. In order to confirm no reduction of weight gain caused by liposomes only, a fourth group, only the vehicle (LP), should be included in a treatment study in the future.

An explanation for the weight loss in the treated group can be because melatonin acts as a sedative in high doses (101), and this might have led to reduced feeding. If the effect of reduced weight gain in our treatment study is due to sedative properties of melatonin, the issue would have less relevance clinically since nasogastric tube-feeding is possible in sedated human neonates. However, the reduction of weight gain on the first day after HI insult resulted in a more severe brain injury in our study and might mask the neuroprotective effect of melatonin.

5.3.2. Neuroprotective effect of liposomal melatonin after statistical correction of data for weight change

When results of our treatment study were statistically corrected for weight change, moderate neuroprotective effects of liposomal melatonin after HI brain injury were observed, superior to the conventional melatonin formulation in organic solvent. This is in line with the results from Paper I, showing higher melatonin brain concentration from lipid-based nanoparticles than from DMSO-formulation. Animals treated with melatonin in liposomes showed significantly lower hyperintense brain volume, measured on MR images, than animals treated with PBS seven days after HI insult, indicating less inflammation and necrosis, which confirmed melatonin's anti-inflammatory properties after ischemia injury in brain (183). Nevertheless, large variability in outcomes seen within all treatment groups in this study made small differences in results hard to detect. This is a well-known disadvantage of using the Vannucci model (39). The variable parameters of environment used in the Vannucci

model includes hypoxia duration and oxygen rates, anaesthetic use but also the cellular and anatomical differences between rodent strains, and age of the animal during ischemia, among others. These parameters correlate with wide variation in the resulting size and severity of infarct volume in rodents, having an influence on the study results. What is more, researchers within the same laboratory may exhibit variability between their results as investigators with more experience may have more skilled surgical techniques or faster surgery times (58). Yet the Vannucci model with P7 rat pups is a well-characterized, cost-efficient model that has been previously used and optimized in our group.

5.4. An alternative and more controllable model for HI in brain injury studies

During the work on this thesis, we recognized a need for an alternative model of HI injury from the Vannucci model. The model should be more reproducible with significantly less variability and more control over the environment to measure the effect of melatonin on energy metabolism and mitochondrial function after the brain injury.

To this end, we successfully developed and optimized an *ex vivo* oxygen-glucose deprivation (OGD) model using rat brain slices combined with NMR to measure metabolite changes in tissue in real-time. We used a precisely controlled model and achieved reproducible results using brain slices. We decided to use brain slices instead of cell cultures since tissue is preserving the three-dimensional neuronal structure providing function and metabolism closer to *in vivo* than in the case of cells. We were interested in measuring metabolite changes before, during and after OGD. Thus, we developed an NMR-compatible bioreactor and measured metabolites changes using ^{1}H and ^{31}P NMR. Experiments were performed during normoxia in the presence of glucose in the artificial CSF mimicking the physiological brain condition and in hypoxia with a lack of glucose in the aCSF to imitate HI brain injury. Instead of placing brain slices in a chamber outside the NMR spectrometer, and removing the slices for NMR analysis, as it was done by Liu *et al.* (184), we built a bioreactor with an NMR tube containing brain slices loaded in the NMR spectrometer during the whole experiment allowing for continuous measurements and less disturbances to the sample.

5.4.1. NMR-compatible bioreactor optimization

In order to acquire high resolution NMR signals, while keeping the brain tissue viable, the NMR-compatible bioreactor needed to be optimized. Optimization included designing an NMR-compatible perfusion system that would allow for continuous flow of buffer to the

sample, control of buffer temperature and oxygenation, control of sample position within the NMR magnet, while maintaining a stable, homogeneous magnetic field across the sample volume to allow for high resolution NMR acquisition. We measured a significant reduction of the buffer temperature in the in-line from the heat bath entering the NMR-tube. To prevent that and to keep the temperature stable in the NMR-tube, we first tried insulating the in-line and primary out-line using a foam insulating pipe filled with cotton wrapped around the lines. However, the loss of the temperature was still present. The next approach was to run the in-line and primary out-line through a 60 °C water-filled heating line. This approach, in combination with the temperature adjustment method within the spectrometer bore (section **2.4.**, **Paper III**), resulted in a stable temperature of 37 °C (+/- 1 °C) that was controlled during the whole experiment.

Additionally, the optimization process before the main experiments included studying the optimum amount of tissue in the active region, the ideal amount and size of glass beads on the bottom of the NMR tube to prevent the sample from falling out of the NMR active region, and an optimal length of the glass tip at the end of the in-line, among others. Twenty brain slices from one hemisphere of an adult rat brain were the optimal amount of tissue. This provided adequate tissue for a good NMR signal, did not result in 'over packing' of the NMR active volume which would lead to restriction of buffer flow, but also was densely packed enough to prevent excessive movement of the slices, where tissue movement would result in a reduction in the NMR signal quality due to poor shimming. Next, we investigated the various options to plug the bottom part of the NMR tube to ensure that the sample did not fall out of the active region. We found that it was more convenient to use glass beads instead of an agarose gel plug (1.5% in PBS) as used by others (185). Using glass beads is a faster and more reproducible approach when preparing the NMR-tube for all experiments in comparison to the agarose gel plug. Next, to prevent suction of the floating slices into the out-lines, a filter above the tissue and below the out-lines has to be mounted. We have experienced a better performance of a synthetic sponge filter placed above the tissue when compared to the cotton ball as used by Harris *et al.* (186). While using a cotton ball, we experienced higher risk of tissue moving up over time resulting in shimming problems and less signal from the brain slices in comparison to the synthetic sponge filter. In addition, we found it easier to use the exact same size of the sponge filter in every experiment than in the case of using cotton. Moreover, to avoid the possible differences in shimming when changing the conditions from physiological to OGD, the same amount of salts and D_2O was added to the normoxia-aCSF and hypoxia-aCSF. To prevent the osmolarity differences in

these buffers possibly interfering the shimming, instead of glucose, the same amount of sucrose was added to the OGD-aCSF. To conclude, each experiment was performed with care to details mentioned above to achieve conditions as similar as possible resulting in very reproducible data.

5.4.2. Age of animals used in the bioreactor study

As a first step in optimization and development of the bioreactor study, we chose to use brains from young adult rats since only one bioreactor experiment with one brain from the animal can be performed per day. Using adults is timesaving, and more economical than using neonates. What is more, since the variability of rat brain in adults is smaller than in neonates (187), it is acceptable to include and compare brains from adult rats over a wider age range, resulting in fewer animals being sacrificed when compared to using only 7-day old rats. Studies using the OGD model both on neonatal (184) and adult brain slices (188) showed a similar response of high-energy molecules (ATP, PCr) after the OGD period suggesting that the energy metabolism response is similar in adult and neonatal brain. What is more, ^{31}P MRS of patients with stroke showed the same findings in HI injury of newborns (31). In addition, knowing that the neonatal brain is more resistant to hypoxia (189), differences caused by OGD in the adult brain might be more significant in comparison to the neonatal brain. Adult and neonatal rats are similar in a large scale having the same brain organization structures, however, there might be subtle changes in the metabolite levels after OGD, but we will probably not be able to measure them using NMR due to its limited sensitivity. Thus, the main conclusion of the OGD study and the distinct pattern depending on the length of the OGD would presumably be similar using brains either from the adults or neonates. However, since our study is about the treatment for a neonatal HI brain injury, after initial bioreactor experiments done by us, using only 7-day old rats in melatonin treatment study with bioreactor would be a next step followed by a set-up optimization study using neonates.

5.4.3. Lactate change measurement

The results from our bioreactor study using brain tissue from the young adult rats showed a very significant difference in metabolic response depending on the length of the OGD period and a very high reproducibility of our experiments. Brain metabolism recovered best after the shortest OGD period (30 min) and had the worst metabolic recovery after the longest OGD period (120 min). The decrease of ATP and PCr levels measured after the OGD period

in our bioreactor study is also observed clinically after an HI insult (190), but instead of a significant increase of lactate after the OGD that is seen in infant children, an opposite effect was noticed by us. In the pathophysiology of HI brain injury, the accumulation of lactate in brain tissue is observed clinically due to the switch from aerobic to anaerobic respiration after the lack of oxygen. However, following the brain injury, lactate levels in the blood in the whole body and cerebrospinal fluid increase as well (191). To achieve OGD in the tissue a change from the oxygenated, and rich in glucose aCSF to the one without oxygen and glucose is required using a continuous buffer flow which is a deviation from the real situation *in vivo*. Therefore, the continuous aCSF flow and an absence of the increased lactate in the aCSF in the bioreactor system presumably caused the lack of the accumulation of lactate levels in our OGD experiments. To better mimic the clinical setting when using bioreactor, a system where the flow is stopped could be a solution. However, this could result in variable oxygen levels in the sample due to the gas exchanged with the air surrounding the bioreactor since the bioreactor is not an air-tight system. Another solution would be to add a known amount of lactate to the aCSF but a proper amount of added lactate would require further studies. What is more, since in our bioreactor set-up, lactate production during hypoxia is closely related to the glucose availability in the buffer, a solution here could be a slower decrease of glucose in the aCSF during the OGD period. A proposed change could make the model closer to the real situation, especially since the levels of oxygen and glucose clinically do not decrease so suddenly and simultaneously in the brain after HI as it takes place in the OGD model *ex vivo* but this adjustment requires future studies as well.

An OGD model with a bioreactor set-up is a very good model to measure the changes of the high-energy metabolites from the brain slices using ^{31}P NMR. However, the results of the lactate changes during normoxia/hypoxia conditions should be interpreted cautiously by ^{1}H NMR in the context of bioreactor flow rate, buffer change and its re-circulation. Even though we tried to correct the measured lactate levels in the re-circulated buffer by collecting buffer samples over time (see bioreactor paper section **2.7.**, **3.3.** and **Discussion**), it is important to notice that the results from our study show the opposite behavior of lactate after OGD when compared to the clinical HI brain injury. However, the pattern of lactate changes was highly reproducible and dependent on the length of OGD, which can be used to observe the effect of environmental change or applied treatment on the brain tissue.

5.4.4. Duration of the bioreactor experiment

In our bioreactor set-up we measured the changes in the brain tissue during the OGD period and up to 3 to 4 hours after the end of the OGD period whereas clinically, the changes in brain after HI brain injury are usually measured soonest during the secondary energy failure phase with neuronal damage that occurs 6 to 48 hours after the initial insult (192). It would be interesting to measure metabolic changes in the brain tissue in the bioreactor during the secondary energy failure where the changes caused by hypoxia-ischemia are more prominent. However, we are uncertain if continuing our bioreactor experiments up until the secondary energy failure is feasible owing to tissue degradation in the bioreactor from the constant perfusion. This occurrence was confirmed with HES staining, where we observed a wash-out effect of the extracellular matrix in the brain tissue after 5 – 6 h in the bioreactor when compared to the slices before the bioreactor, as mentioned in the bioreactor paper (section **3.4.**). Even though both ^{1}H and ^{31}P NMR spectra showed stable metabolites in the control groups during the whole bioreactor experiment, longer duration bioreactor experiments might come with a risk of even more tissue slice damage. A solution to this issue can be a reduction of the buffer flow rate to slow down the wash-out effect but this remains to be tested in the future.

The next steps of the bioreactor study using NMR and the OGD model are to measure real-time metabolic responses for pre-treatment and early treatment effects of melatonin on HI brain injury. Melatonin's antioxidative effect on mitochondrial metabolism might be observed by measuring ATP, PCr or lactate levels from the brain slices in three different severity levels of OGD. Since PCr/Pi levels in OGD-60 group (moderate severity) were seen to slightly increase back after reperfusion and dropped again in the following hours, a possible effect of melatonin may cause high-energy metabolites to fully recover to its primary levels. In the mildest severity level, the effect of metabolites coming back to its pre-OGD levels might be seen faster after melatonin treatment. However, when it comes to the most severe group, the length of the OGD might be too long to notice any improvement of melatonin since 120 min lack of glucose and oxygen in the brain slices presumably causes non-recoverable damage in the tissue. Furthermore, an extra feature of using the bioreactor set-up is having control over temperature, providing the possibility of studies involving melatonin treatment combined with hypothermia, which might have an additional positive effect on metabolite levels after OGD. Last, both Vannucci *in vivo* and OGD *ex vivo* models do not completely reflect the complexity of the HI brain injury in humans. Results from studies using the

Vannucci *in vivo* model and the OGD *ex vivo* model could potentially provide a more complete understanding of the melatonin treatment effect on HI brain injury.

6. Conclusions and future perspective

The main achievement of this thesis is that by using liposomes it is feasible to develop a non-toxic parenteral formulation with melatonin indicating a moderate neuroprotective effect in a neonatal HI model. Liposomal melatonin may be a promising melatonin formulation for clinical use. However, complementary preclinical studies are required.

Presented work contribute to improving the melatonin therapy as a potential treatment after neonatal HI brain injury. However, our main concern from the treatment experiments on neonatal rats is the high melatonin dosage (90 mg/kg of melatonin total dose over 24 h after the HI insult) that might mask the neuroprotective effect of the drug by inducing a reduction of weight gain as well as melatonin's possible sedative effect. The results of this study indicate that further experiments need to take the melatonin dosage optimization into consideration. Perhaps a future treatment study using liposomal melatonin with a dose between 10 to 30 mg/kg in multiple administrations within the 24 h after the HI insult should be used, and an HI model that allows more control over drug dosing and offer higher reproducibility would be favorable.

Since high variability of brain damage was seen when Vannucci model was used, a second, more controllable HI model was successfully developed and optimized to study the real-time metabolic changes of brain tissue using MRS techniques. An NMR-compatible bioreactor system allowed reproducible metabolic characterization of three different severity levels of OGD in rat brain slices, mimicking HI brain injury. Future studies to characterize the impact of therapeutic agents as melatonin and melatonin-augmented hypothermia on metabolic response used during the OGD and before the start of the secondary energy failure can now be investigated using this bioreactor system with OGD model.

7. References

1. O'Brien JR, Usher RH, Maughan GB. Causes of birth asphyxia and trauma. Can Med Assoc J. 1966 May;94(21):1077–85.
2. WHO | Causes of child mortality. WHO. 2018;
3. Volpe JJ. P b i : f p n. 2001;64:56–64.
4. Glass HC, Ferriero DM. Treatment of hypoxic-ischemic encephalopathy in newborns. Curr Treat Options Neurol. 2007;9(6):414–23.
5. Graham EM, Ruis KA, Hartman AL, Northington FJ, Fox HE. A systematic review of the role of intrapartum hypoxia-ischemia in the causation of neonatal encephalopathy. Am J Obstet Gynecol. 2008;199(6):587–95.
6. Robertson CM, Perlman M. Follow-up of the term infant after hypoxic-ischemic encephalopathy. Paediatr Child Health. 2006 May;11(5):278–82.
7. Sarnat HB, Sarnat MS. Neonatal Encephalopathy Following Fetal Distress: A Clinical and Electroencephalographic Study. Arch Neurol. 1976 Oct;33(10):696–705.
8. Favié LMA, Cox AR, van den Hoogen A, Nijboer CHA, Peeters-Scholte CMPCD, van Bel F, et al. Nitric Oxide Synthase Inhibition as a Neuroprotective Strategy Following Hypoxic–Ischemic Encephalopathy: Evidence From Animal Studies. Front Neurol. 2018;9:258.
9. Biology P. Principles of Biology. 2013;
10. Zauner A, Daugherty WP, Bullock MR, Warner DS. Brain Oxygenation and Energy Metabolism: Part I—Biological Function and Pathophysiology. Neurosurgery. 2002 Aug;51(2):289–302.
11. Oxidative phosphorylation | Biology (article) | Khan Academy [Internet]. [cited 2021 Feb 1]. Available from: https://www.khanacademy.org/science/ap-biology/cellular-energetics/cellular-respiration-ap/a/oxidative-phosphorylation-etc
12. Melkonian EA, Schury MP. Biochemistry, Anaerobic Glycolysis [Internet]. StatPearls. StatPearls Publishing; 2019 [cited 2021 Feb 1]. Available from: http://www.ncbi.nlm.nih.gov/pubmed/31536301
13. Neurology of the Newborn - 5th Edition [Internet]. [cited 2021 Feb 1]. Available from: https://www.elsevier.com/books/neurology-of-the-newborn/volpe/978-1-4160-3995-2
14. McLean C, Ferriero D. Mechanisms of hypoxic-ischemic injury in the term infant [Internet]. Vol. 28, Seminars in Perinatology. Semin Perinatol; 2004 [cited 2021 Feb 1]. p. 425–32. Available from: https://pubmed.ncbi.nlm.nih.gov/15693399/
15. Vannucci SJ. Hypoxia-ischemia in the immature brain. J Exp Biol. 2004;207(18):3149–54.
16. Grow J, Barks JDE. Pathogenesis of hypoxic-ischemic cerebral injury in the term infant: current concepts. Clin Perinatol. 2002;29(4):585—602, v.
17. Esterlita M, Uy V. Pathophysiology. :1–7.
18. GRIFFITHS J. Nuclear Magnetic Resonance and its Applications to Living Systems. Biochem Soc Trans. 1982 Oct;10(5):433.

19. van der Graaf M. In vivo magnetic resonance spectroscopy: basic methodology and clinical applications. Eur Biophys J. 2009/08/13. 2010 Mar;39(4):527–40.

20. Panigrahy A, Borzage M, Blüml S. Basic principles and concepts underlying recent advances in magnetic resonance imaging of the developing brain. Semin Perinatol. 2010 Feb;34(1):3–19.

21. de Vries LS, Groenendaal F. Patterns of neonatal hypoxic-ischaemic brain injury. Neuroradiology. 2010 Jun;52(6):555–66.

22. Petroff OA, Prichard JW, Behar KL, Alger JR, den Hollander JA, Shulman RG. Cerebral intracellular pH by 31P nuclear magnetic resonance spectroscopy. Neurology. 1985 Jun;35(6):781–8.

23. Groenendaal F, Veenhoven RH, van der Grond J, Jansen GH, Witkamp TD, de Vries LS. Cerebral lactate and N-acetyl-aspartate/choline ratios in asphyxiated full-term neonates demonstrated in vivo using proton magnetic resonance spectroscopy. Pediatr Res. 1994 Feb;35(2):148–51.

24. Wilson M, Andronesi O, Barker PB, Bartha R, Bizzi A, Bolan PJ, et al. Methodological consensus on clinical proton MRS of the brain: Review and recommendations. Magn Reson Med. 2019/03/28. 2019 Aug;82(2):527–50.

25. Azzopardi D, Wyatt JS, Hamilton PA, Cady EB, Delpy DT, Hope PL, et al. Phosphorus metabolites and intracellular pH in the brains of normal and small for gestational age infants investigated by magnetic resonance spectroscopy. Pediatr Res. 1989;25(5):440–4.

26. Hanrahan JD, Cox IJ, Azzopardi D, Cowan FM, Sargentoni J, Bell JD, et al. Relation between proton magnetic resonance spectroscopy within 18 hours of birth asphyxia and neurodevelopment at 1 year of age. Dev Med Child Neurol. 1999 Feb;41(2):S0012162299000171.

27. Lorek A, Takei Y, Cady EB, Wyatt JS, Penrice J, Edwards AD, et al. Delayed ("Secondary") Cerebral Energy Failure after Acute Hypoxia-Ischemia in the Newborn Piglet: Continuous 48-Hour Studies by Phosphorus Magnetic Resonance Spectroscopy. Pediatr Res. 1994 Dec;36(6):699–706.

28. Yager JY, Brucklacher RM, Vannucci RC. Cerebral energy metabolism during hypoxia-ischemia and early recovery in immature rats. Am J Physiol. 1992 Mar;262(3 Pt 2):H672-7.

29. Blumberg RM, Cady EB, Wigglesworth JS, McKenzie JE, Edwards AD. Relation between delayed impairment of cerebral energy metabolism and infarction following transient focal hypoxia-ischaemia in the developing brain. Exp Brain Res. 1997;113(1):130–7.

30. Iwata O, Iwata S, Thornton JS, De Vita E, Bainbridge A, Herbert L, et al. "Therapeutic time window" duration decreases with increasing severity of cerebral hypoxia–ischaemia under normothermia and delayed hypothermia in newborn piglets. Brain Res. 2007;1154:173–80.

31. Ross B, Bluml S. Magnetic resonance spectroscopy of the human brain. Anat Rec. 2001 Apr;265(2):54–84.

32. Gideon P, Henriksen O, Sperling B, Christiansen P, Olsen TS, Jørgensen HS, et al. Early time course of N-acetylaspartate, creatine and phosphocreatine, and

compounds containing choline in the brain after acute stroke. A proton magnetic resonance spectroscopy study. Stroke. 1992 Nov;23(11):1566–72.

33. Peres M, Bourgeois D, Roussel S, Lefur Y, Devoulon P, Remy C, et al. Two-dimensional 1H spectroscopic imaging for evaluating the local metabolic response to focal ischemia in the conscious rat. NMR Biomed. 1992 Jan;5(1):11–9.

34. Millar LJ, Shi L, Hoerder-Suabedissen A, Molnár Z. Neonatal Hypoxia Ischaemia: Mechanisms, Models, and Therapeutic Challenges. Front Cell Neurosci. 2017 May;11:78.

35. LEVINE S. Anoxic-ischemic encephalopathy in rats. Am J Pathol. 1960 Jan;36(1):1–17.

36. Vannucci RC, Vannucci SJ. A model of perinatal hypoxic-ischemic brain damage. Ann N Y Acad Sci. 1997;835:234—249.

37. Albertsson A-M, Bi D, Duan L, Zhang X, Leavenworth JW, Qiao L, et al. The immune response after hypoxia-ischemia in a mouse model of preterm brain injury. J Neuroinflammation. 2014;11(1):153.

38. Lubics A, Reglodi D, Tamás A, Kiss P, Szalai M, Szalontay L, et al. Neurological reflexes and early motor behavior in rats subjected to neonatal hypoxic-ischemic injury. Behav Brain Res. 2005 Feb;157(1):157–65.

39. Vannucci RC, Vannucci SJ. Perinatal Hypoxic-Ischemic Brain Damage: Evolution of an Animal Model. Dev Neurosci. 2005;27(2–4):81–6.

40. Hill A. Current concepts of hypoxic-ischemic cerebral injury in the term newborn. Pediatr Neurol. 1991;7(5):317–25.

41. Fan W, Zhu X, Wu L, Wu Z, Li D. Propofol : an anesthetic possessing neuroprotective effects. 2015;1520–9.

42. Chiao S, Zuo Z. A double-edged sword: volatile anesthetic effects on the neonatal brain. Brain Sci. 2014 Apr;4(2):273–94.

43. Rumajogee P, Bregman T, Miller SP, Yager JY, Fehlings MG. Rodent Hypoxia-Ischemia Models for Cerebral Palsy Research: A Systematic Review. Front Neurol. 2016 Apr;7:57.

44. Mallard C, Vexler ZS. Modeling Ischemia in the Immature Brain: How Translational Are Animal Models? Stroke. 2015/08/13. 2015 Oct;46(10):3006–11.

45. Papile L-A, Rudolph AM, Heymann MA. Autoregulation of Cerebral Blood Flow in the Preterm Fetal Lamb. Pediatr Res. 1985;19(2):159–61.

46. Mallard EC, Gunn AJ, Williams CE, Johnston BM, Gluckman PD. Transient umbilical cord occlusion causes hippocampal damage in the fetal sheep. Am J Obstet Gynecol. 1992;167(5):1423–30.

47. Bernhard CG, Kolmodin GM, Meyerson BA. On the Prenatal Development of Function and Structure in the Somesthetic Cortex of the Sheep. In: Bernhard CG, Schadé JPBT-P in BR, editors. Developmental Neurology. Elsevier; 1967. p. 60–77.

48. Northington FJ. Brief update on animal models of hypoxic-ischemic encephalopathy and neonatal stroke. ILAR J. 2006;47(1):32–8.

49. Back SA, Riddle A, Dean J, Hohimer AR. The instrumented fetal sheep as a model of cerebral white matter injury in the premature infant. Neurotherapeutics. 2012 Apr;9(2):359–70.

50. Thoresen M, Haaland K, Løberg EM, Whitelaw A, Apricena F, Hankø E, et al. A Piglet Survival Model of Posthypoxic Encephalopathy. Pediatr Res. 1996;40(5):738–48.

51. Kyng KJ, Skajaa T, Kerrn-Jespersen S, Andreassen CS, Bennedsgaard K, Henriksen TB. A Piglet Model of Neonatal Hypoxic-Ischemic Encephalopathy. J Vis Exp. 2015 May;(99):e52454–e52454.

52. Griffith JL, Shimony JS, Cousins SA, Rees SE, McCurnin DC, Inder TE, et al. MR imaging correlates of white-matter pathology in a preterm baboon model. Pediatr Res. 2011/12/21. 2012 Feb;71(2):185–91.

53. Verney C, Rees S, Biran V, Thompson M, Inder T, Gressens P. Neuronal damage in the preterm baboon: impact of the mode of ventilatory support. J Neuropathol Exp Neurol. 2010 May;69(5):473–82.

54. Dobbing J, Sands J. Comparative aspects of the brain growth spurt. Early Hum Dev. 1979;3(1):79–83.

55. Brochu M-E, Girard S, Lavoie K, Sébire G. Developmental regulation of the neuroinflammatory responses to LPS and/or hypoxia-ischemia between preterm and term neonates: An experimental study. J Neuroinflammation. 2011;8(1):55.

56. Patel SD, Pierce L, Ciardiello AJ, Vannucci SJ. Neonatal encephalopathy: pre-clinical studies in neuroprotection. Biochem Soc Trans. 2014 Mar;42(2):564–8.

57. Semple BD, Blomgren K, Gimlin K, Ferriero DM, Noble-Haeusslein LJ. Brain development in rodents and humans: Identifying benchmarks of maturation and vulnerability to injury across species. Prog Neurobiol. 2013;106–107:1–16.

58. Hamdy N, Eide S, Sun H-S, Feng Z-P. Animal models for neonatal brain injury induced by hypoxic ischemic conditions in rodents. Exp Neurol. 2020;334:113457.

59. Romijn HJ, Hofman MA, Gramsbergen A. At what age is the developing cerebral cortex of the rat comparable to that of the full-term newborn human baby? Early Hum Dev. 1991;26(1):61–7.

60. Hill CA, Threlkeld SW, Fitch RH. Early testosterone modulated sex differences in behavioral outcome following neonatal hypoxia ischemia in rats. Int J Dev Neurosci Off J Int Soc Dev Neurosci. 2011 Jun;29(4):381–8.

61. Hines M. Early androgen influences on human neural and behavioural development. Early Hum Dev. 2008;84(12):805–7.

62. Mayoral SR, Omar G, Penn AA. Sex Differences in a Hypoxia Model of Preterm Brain Damage. Pediatr Res. 2009;66(3):248–53.

63. Hill CA, Alexander ML, McCullough LD, Fitch RH. Inhibition of X-Linked Inhibitor of Apoptosis with Embelin Differentially Affects Male versus Female Behavioral Outcome following Neonatal Hypoxia-Ischemia in Rats. Dev Neurosci. 2011;33(6):494–504.

64. Nuñez JL, McCarthy MM. Androgens predispose males to GABAA-mediated excitotoxicity in the developing hippocampus. Exp Neurol. 2008;210(2):699–708.

65. Tasca CI, Dal-Cim T, Cimarosti H. In vitro oxygen-glucose deprivation to study ischemic cell death. Methods Mol Biol. 2015;1254:197–210.

66. Daviaud N, Garbayo E, Schiller PC, Perez-Pinzon M, Montero-Menei CN. Organotypic cultures as tools for optimizing central nervous system cell therapies. Exp Neurol. 2013;248:429–40.

67. Li Q, Han X, Wang J. Organotypic Hippocampal Slices as Models for Stroke and Traumatic Brain Injury. Mol Neurobiol. 2016 Aug;53(6):4226—4237.

68. Gillam-Krakauer M, Gowen Jr CW. Birth Asphyxia. In Treasure Island (FL); 2020.

69. Erecinska M, Thoresen M, Silver IA. Effects of Hypothermia on Energy Metabolism in Mammalian Central Nervous System. J Cereb Blood Flow Metab. 2003 May;23(5):513–30.

70. Shankaran S, Pappas A, McDonald SA, Vohr BR, Hintz SR, Yolton K, et al. Childhood outcomes after hypothermia for neonatal encephalopathy. N Engl J Med. 2012 May;366(22):2085–92.

71. Laptook AR, Shankaran S, Tyson JE, Munoz B, Bell EF, Goldberg RN, et al. Effect of Therapeutic Hypothermia Initiated After 6 Hours of Age on Death or Disability Among Newborns With Hypoxic-Ischemic Encephalopathy: A Randomized Clinical Trial. JAMA. 2017 Oct;318(16):1550–60.

72. Greco P, Nencini G, Piva I, Scioscia M, Volta CA, Spadaro S, et al. Pathophysiology of hypoxic–ischemic encephalopathy: a review of the past and a view on the future. Acta Neurol Belg. 2020;120(2):277–88.

73. Wu Q, Chen W, Sinha B, Tu Y, Manning S, Thomas N, et al. Neuroprotective agents for neonatal hypoxic–ischemic brain injury. Drug Discov Today. 2015;20(11):1372–81.

74. Ma D, Hossain M, Pettet GKJ, Luo Y, Lim T, Akimov S, et al. Xenon Preconditioning Reduces Brain Damage from Neonatal Asphyxia in Rats. J Cereb Blood Flow Metab. 2005 Jul;26(2):199–208.

75. Bolouri H, Sävman K, Wang W, Thomas A, Maurer N, Dullaghan E, et al. Innate defense regulator peptide 1018 protects against perinatal brain injury. Ann Neurol. 2014 Mar;75(3):395–410.

76. H. NC, J. HC, Floris G, Frank van B, Annemieke K. Alternate Pathways Preserve Tumor Necrosis Factor-α Production After Nuclear Factor-κB Inhibition in Neonatal Cerebral Hypoxia–Ischemia. Stroke. 2009 Oct;40(10):3362–8.

77. Manning SM, Talos DM, Zhou C, Selip DB, Park H-K, Park C-J, et al. NMDA Receptor Blockade with Memantine Attenuates White Matter Injury in a Rat Model of Periventricular Leukomalacia. J Neurosci. 2008 Jun;28(26):6670 LP – 6678.

78. Noh M-R, Kim SK, Sun W, Park SK, Choi HC, Lim JH, et al. Neuroprotective effect of topiramate on hypoxic ischemic brain injury in neonatal rats. Exp Neurol. 2006;201(2):470–8.

79. Fan X, Heijnen CJ, van der Kooij MA, Groenendaal F, van Bel F. Beneficial Effect of Erythropoietin on Sensorimotor Function and White Matter After Hypoxia-Ischemia in Neonatal Mice. Pediatr Res. 2011;69(1):56–61.

80. Palmer C, Towfighi J, Roberts RL, Heitjan DF. Allopurinol Administered after

Inducing Hypoxia-Ischemia Reduces Brain Injury in 7-Day-Old Rats. Pediatr Res. 1993;33(4):405–11.

81. Tweel ERW van den, van Bel F, Kavelaars A, Peeters-Scholte CM, Haumann J, Nijboer CHA, et al. Long-Term Neuroprotection with 2-Iminobiotin, An Inhibitor of Neuronal and Inducible Nitric Oxide Synthase, after Cerebral Hypoxia-Ischemia in Neonatal Rats. J Cereb Blood Flow Metab. 2005 Jan;25(1):67–74.

82. Türkyilmaz C, Türkyilmaz Z, Atalay Y, Söylemezoglu F, Celasun B. Magnesium pre-treatment reduces neuronal apoptosis in newborn rats in hypoxia–ischemia. Brain Res. 2002;955(1):133–7.

83. Carloni S, Perrone S, Buonocore G, Longini M, Proietti F, Balduini W. Melatonin protects from the long-term consequences of a neonatal hypoxic-ischemic brain injury in rats. J Pineal Res. 2008;44(2):157–64.

84. Andersen LPH, Gögenur I, Rosenberg J, Reiter RJ. The Safety of Melatonin in Humans [Internet]. Vol. 36, Clinical Drug Investigation. Springer International Publishing; 2016 [cited 2021 Feb 2]. p. 169–75. Available from: https://link.springer.com/article/10.1007/s40261-015-0368-5

85. Chen Y, Tain Y, Sheen J, Huang L. Melatonin utility in neonates and children. J Formos Med Assoc. 2012;111(2):57–66.

86. Karasek M, Winczyk K, Diseases M. Mela tonin in humans 1. 2006;19–39.

87. Pardridge WM, Mietus LJ. Transport of Albumin-bound Melatonin Through the Blood-Brain Barrier. J Neurochem. 1980 Jun;34(6):1761–3.

88. Melatonin _ C13H16N2O2 - PubChem.

89. Tordjman S, Chokron S, Delorme R, Charrier A, Bellissant E, Jaafari N, et al. Melatonin: Pharmacology, Functions and Therapeutic Benefits. Curr Neuropharmacol. 2017 Apr;15(3):434–43.

90. Srinivasan V, Spence DW, Trakht I, Pandi-Perumal SR, Cardinali DP, Maestroni GJ. Immunomodulation by Melatonin: Its Significance for Seasonally Occurring Diseases. Neuroimmunomodulation. 2008;15(2):93–101.

91. Tan D-X, Manchester LC, Terron MP, Flores LJ, Reiter RJ. One molecule, many derivatives: A never-ending interaction of melatonin with reactive oxygen and nitrogen species? J Pineal Res. 2007 Jan;42(1):28–42.

92. Tomás-Zapico C, Coto-Montes A. A proposed mechanism to explain the stimulatory effect of melatonin on antioxidative enzymes. J Pineal Res. 2005 Sep;39(2):99–104.

93. Lin Y, Chen T, Hung C, Tai S, Huang S, Chang C, et al. Melatonin protects brain against ischemia/reperfusion injury by attenuating endoplasmic reticulum stress. Int J Mol Med. 2018 Mar;42(1):182–92.

94. Yawno T, Mahen M, Li J, Fahey MC, Jenkin G, Miller SL. The Beneficial Effects of Melatonin Administration Following Hypoxia-Ischemia in Preterm Fetal Sheep. Front Cell Neurosci. 2017 Sep;11:296.

95. Robertson NJ, Faulkner S, Fleiss B, Bainbridge A, Andorka C, Price D, et al. Melatonin augments hypothermic neuroprotection in a perinatal asphyxia model. Brain. 2013 Jan;136(1):90–105.

96. Signorini C, Ciccoli L, Leoncini S, Carloni S, Perrone S, Comporti M, et al. Free iron, total F_2 -isoprostanes and total F_4 -neuroprostanes in a model of neonatal hypoxic-ischemic encephalopathy: neuroprotective effect of melatonin. J Pineal Res. 2009 Mar;46(2):148–54.

97. Mésenge C, Margaill I, Verrecchia C, Allix M, Boulu RG, Plotkine M. Protective effect of melatonin in a model of traumatic brain injury in mice. J Pineal Res. 1998 Aug;25(1):41–6.

98. Villapol S, Fau S, Renolleau S, Biran V, Charriaut-Marlangue C, Baud O. Melatonin Promotes Myelination by Decreasing White Matter Inflammation After Neonatal Stroke. Pediatr Res. 2011 Jan;69(1):51–5.

99. Lee S, Jadhav V, Ayer RE, Rojas H, Hyong A, Lekic T, et al. Dual effects of melatonin on oxidative stress after surgical brain injury in rats. J Pineal Res. 2009 Jan;46(1):43–8.

100. Miller SL, Yan EB, Castillo-Meléndez M, Jenkin G, Walker DW. Melatonin provides neuroprotection in the late-gestation fetal sheep brain in response to umbilical cord occlusion. Dev Neurosci. 2005;27(2–4):200–10.

101. Aridas JDS, Yawno T, Sutherland AE, Nitsos I, Ditchfield M, Wong FY, et al. Systemic and transdermal melatonin administration prevents neuropathology in response to perinatal asphyxia in newborn lambs. J Pineal Res. 2018;64(4):1–14.

102. DeMuro RL, Nafziger AN, Blask DE, Menhinick AM, Bertino JS. The Absolute Bioavailability of Oral Melatonin. J Clin Pharmacol. 2000 Jul;40(7):781–4.

103. Young CM, Kingma SDK, Neu J. Ischemia-Reperfusion and Neonatal Intestinal Injury. J Pediatr. 2011 Feb;158(2):e25–8.

104. Cardinali DP. Melatonin: Clinical Perspectives in Neurodegeneration. Front Endocrinol (Lausanne). 2019 Jul;10:480.

105. Cardinali DP. High doses of melatonin as a potential therapeutic tool for the neurologic sequels of covid-19 infection. 2020;3(4):311–7.

106. Berger HR, Nyman AKG, Morken TS, Vettukattil R, Brubakk A-M, Widerøe M. Early metabolite changes after melatonin treatment in neonatal rats with hypoxic-ischemic brain injury studied by in-vivo 1H MR spectroscopy. Baud O, editor. PLoS One. 2017 Sep;12(9):e0185202.

107. Berger HR, Nyman AKG, Morken TS, Vettukattil R, Brubakk A-M, Widerøe M. Early metabolite changes after melatonin treatment in neonatal rats with hypoxic-ischemic brain injury studied by in-vivo1H MR spectroscopy. PLoS One. 2017;12(9):e0185202.

108. Marek E, Kraft WK. Ethanol pharmacokinetics in neonates and infants. Curr Ther Res Clin Exp. 2014 Dec;76:90–7.

109. Berger HR, Morken TS, Vettukattil R, Brubakk AM, Sonnewald U, Widerøe M. No improvement of neuronal metabolism in the reperfusion phase with melatonin treatment after hypoxic-ischemic brain injury in the neonatal rat. J Neurochem. 2016;136(2):339–50.

110. Alsbaiee A, Beingessner RL, Fenniri H. 17 - Self-assembled nanomaterials for tissue-engineering applications. In: Webster TJBT-N, editor. Woodhead Publishing

Series in Biomaterials. Woodhead Publishing; 2012. p. 490–533.

111. Hosta-Rigau L, Zhang Y, Teo BM, Postma A, Städler B. Cholesterol - A biological compound as a building block in bionanotechnology. Nanoscale [Internet]. 2013 Jan 7 [cited 2021 Jan 13];5(1):89–109. Available from: www.rsc.org/nanoscale

112. Bitounis D, Fanciullino R, Iliadis A, Ciccolini J, Bolognese A, Segall AI, et al. Optimizing Druggability through Liposomal Formulations: New Approaches to an Old Concept. Int Sch Res Netw ISRN Pharm. 2012;2012:11.

113. Milla P, Dosio F, Cattel L. PEGylation of Proteins and Liposomes: a Powerful and Flexible Strategy to Improve the Drug Delivery. Curr Drug Metab [Internet]. 2012 Jan 1 [cited 2021 Jan 13];13(1):105–19. Available from: http://www.eurekaselect.com/openurl/content.php?genre=article&issn=1389-2002&volume=13&issue=1&spage=105

114. Gabizon A, Shmeeda H, Barenholz Y. Pharmacokinetics of Pegylated Liposomal Doxorubicin Review of Animal and Human Studies. Vol. 42, Clin Pharmacokinet. 2003.

115. Tadros T, Izquierdo P, Esquena J, Solans C. Formation and stability of nano-emulsions. Adv Colloid Interface Sci. 2004 May 20;108–109:303–18.

116. Witthayapanyanon A, Acosta EJ, Harwell JH, Sabatini DA. Formulation of ultralow interfacial tension systems using extended surfactants. J Surfactants Deterg [Internet]. 2006 Dec 1 [cited 2021 Jan 20];9(4):331–9. Available from: http://doi.wiley.com/10.1007/s11743-006-5011-2

117. Patravale V, Dandekar P, Jain R. 1 - Nanoparticulate systems as drug carriers: the need. In: Patravale V, Dandekar P, Jain RBT-NDD, editors. Woodhead Publishing Series in Biomedicine. Woodhead Publishing; 2012. p. 1–28.

118. Simon JA, Group for the ES. Estradiol in micellar nanoparticles: the efficacy and safety of a novel transdermal drug-delivery technology in the management of moderate to severe vasomotor symptoms. Menopause. 2006;13(2).

119. Bobo D, Robinson KJ, Islam J, Thurecht KJ, Corrie SR. Nanoparticle-Based Medicines: A Review of FDA-Approved Materials and Clinical Trials to Date. Pharm Res. 2016;33(10):2373–87.

120. Akbarzadeh A, Rezaei-Sadabady R, Davaran S, Joo SW, Zarghami N, Hanifehpour Y, et al. Liposome: classification, preparation, and applications. Nanoscale Res Lett. 2013 Feb;8(1):102.

121. Hofheinz R-D, Gnad-Vogt SU, Beyer U, Hochhaus A. Liposomal encapsulated anti-cancer drugs. Anticancer Drugs. 2005;16(7).

122. Blode H, Brett M, Bührens KG, Cawello W, Frick A, Gieschke R, et al. Collection of terms, symbols, equations, and explanations of common pharmacokinetic and pharmacodynamic parameters and some statistical functions. 2004;1–23.

123. Birkett DJ. Desiging dose regimens [Internet]. Vol. 19, Australian Prescriber. Australian Government Publishing Service; 1996 [cited 2021 Jan 13]. p. 76–8. Available from: https://www.nps.org.au/australian-prescriber/articles/pharmacokinetics-made-easy-11-designing-dose-regimens

124. Medicines administration 1: understanding routes of administration | Nursing Times

[Internet]. [cited 2021 Jan 13]. Available from: https://www.nursingtimes.net/clinical-archive/medicine-management/medicines-administration-1-understanding-routes-of-administration-24-04-2020/

125. Turner P V, Brabb T, Pekow C, Vasbinder MA. Administration of substances to laboratory animals: routes of administration and factors to consider. J Am Assoc Lab Anim Sci. 2011 Sep;50(5):600–13.

126. Intravenous Route of Drug Administration: Advantages and Disadvantages - Pharmapproach.com [Internet]. [cited 2021 Jan 13]. Available from: https://www.pharmapproach.com/intravenous-route-of-drug-administration-advantages-and-disadvantages/

127. Al Shoyaib A, Rahman Archie S, Karamyan VT. Intraperitoneal Route of Drug Administration: Should it Be Used in Experimental Animal Studies? Available from: https://doi.org/10.1007/s11095-019-2745-x

128. LUKAS G, BRINDLE SD, GREENGARD P. THE ROUTE OF ABSORPTION OF INTRAPERITONEALLY ADMINISTERED COMPOUNDS. J Pharmacol Exp Ther. 1971;178(3).

129. Chambers DJ. Principles of intravenous drug infusion. Anaesth Intensive Care Med. 2019;20(1):61–4.

130. Pharmacokinetics – Online content for student [Internet]. [cited 2021 Jan 13]. Available from: https://sepia2.unil.ch/pharmacology/

131. Ahmed TA. Pharmacokinetics of Drugs Following IV Bolus, IV Infusion, and Oral Administration. In: Basic Pharmacokinetic Concepts and Some Clinical Applications [Internet]. InTech; 2015 [cited 2021 Jan 13]. Available from: http://dx.doi.org/10.5772/61573

132. Products M, Use V, Date C, Party EW. Guideline on conduct of pharmacokinetic studies in target animal species Guideline on the conduct of pharmacokinetic studies in target animal species Table of contents. 2017;44(November):1–13.

133. Dhanapal R, Ratna JV. Innovative Drug Discovery. 2012;2(2):89–97.

134. Giorgi G. A short introduction to pharmacokinetics. 2002;33–44.

135. Backes WL. Pharmacokinetics. In: Enna SJ, Bylund DBBTTCPR, editors. New York: Elsevier; 2007. p. 1.

136. Harpsøe NG, Andersen LPH, Gögenur I, Rosenberg J. Clinical pharmacokinetics of melatonin: a systematic review. Eur J Clin Pharmacol. 2015;71(8):901–9.

137. Yeleswaram K, McLaughlin LG, Knipe JO, Schabdach D. Pharmacokinetics and oral bioavailability of exogenous melatonin in preclinical animal models and clinical implications. J Pineal Res. 1997 Jan;22(1):45–51.

138. Merchant NM, Azzopardi D V., Hawwa AF, Mcelnay JC, Middleton B, Arendt J, et al. Pharmacokinetics of melatonin in preterm infants. Br J Clin Pharmacol. 2013;76(5):725–33.

139. Ehrnebo M, Agurell S, Jalling B, Boréus LO. Age differences in drug binding by plasma proteins: Studies on human foetuses, neonates and adults. Eur J Clin Pharmacol. 1971;3(4):189–93.

140. Ku LC, Smith PB. Dosing in neonates: special considerations in physiology and trial design. Pediatr Res. 2014/09/30. 2015 Jan;77(1–1):2–9.

141. Kearns GL, Abdel-Rahman SM, Alander SW, Blowey DL, Leeder JS, Kauffman RE. Developmental Pharmacology — Drug Disposition, Action, and Therapy in Infants and Children. N Engl J Med. 2003 Sep;349(12):1157–67.

142. Tateishi T, Nakura H, Asoh M, Watanabe M, Tanaka M, Kumai T, et al. A COMPARISON OF HEPATIC CYTOCHROME P450 PROTEIN EXPRESSION BETWEEN INFANCY AND POSTINFANCY. Life Sci. 1997;61(26):2567–74.

143. McCarver DG, Hines RN. The Ontogeny of Human Drug-Metabolizing Enzymes: Phase II Conjugation Enzymes and Regulatory Mechanisms. J Pharmacol Exp Ther. 2002 Feb;300(2):361 LP – 366.

144. Bozzuto G, Molinari A. CEOR-52063-c-quality--cost-and-quality-of-life-pharmacoeconomic-analysi. Int J Nanomedicine Dovepress [Internet]. 2015;10:975–99. Available from: http://dx.doi.org/10.2147/IJN.S68861

145. Yellepeddi VK, Joseph A, Nance E. Pharmacokinetics of nanotechnology-based formulations in pediatric populations [Internet]. Vols. 151–152, Advanced Drug Delivery Reviews. Elsevier B.V.; 2019 [cited 2021 Jan 13]. p. 44–55. Available from: https://doi.org/10.1016/j.addr.2019.08.008

146. Alexis F, Pridgen E, Molnar LK, Farokhzad OC. Factors affecting the clearance and biodistribution of polymeric nanoparticles. In: Molecular Pharmaceutics [Internet]. American Chemical Society; 2008 [cited 2021 Feb 2]. p. 505–15. Available from: /pmc/articles/PMC2663893/?report=abstract

147. Soo Choi H, Liu W, Misra P, Tanaka E, Zimmer JP, Itty Ipe B, et al. Renal clearance of quantum dots. Nat Biotechnol [Internet]. 2007 Oct [cited 2021 Feb 2];25(10):1165–70. Available from: /pmc/articles/PMC2702539/?report=abstract

148. Ernsting MJ, Murakami M, Roy A, Li SD. Factors controlling the pharmacokinetics, biodistribution and intratumoral penetration of nanoparticles [Internet]. Vol. 172, Journal of Controlled Release. NIH Public Access; 2013 [cited 2021 Feb 2]. p. 782–94. Available from: /pmc/articles/PMC3891171/?report=abstract

149. Sly PD, Schüepp K. Nanoparticles and Children's Lungs: Is there a need for caution? Vol. 13, Paediatric Respiratory Reviews. W.B. Saunders; 2012. p. 71–2.

150. Fang C, Shi B, Pei YY, Hong MH, Wu J, Chen HZ. In vivo tumor targeting of tumor necrosis factor-α-loaded stealth nanoparticles: Effect of MePEG molecular weight and particle size. Eur J Pharm Sci. 2006 Jan 1;27(1):27–36.

151. Ignjatovic V, Lai C, Summerhayes R, Mathesius U, Tawfilis S, Perugini MA, et al. Age-related differences in plasma proteins: How plasma proteins change from neonates to adults. PLoS One [Internet]. 2011 [cited 2021 Feb 2];6(2). Available from: /pmc/articles/PMC3041803/?report=abstract

152. Gustafson HH, Holt-Casper D, Grainger DW, Ghandehari H. Nanoparticle uptake: The phagocyte problem [Internet]. Vol. 10, Nano Today. Elsevier B.V.; 2015 [cited 2021 Feb 2]. p. 487–510. Available from: /pmc/articles/PMC4666556/?report=abstract

153. Simon AK, Hollander GA, McMichael A. Evolution of the immune system in humans from infancy to old age [Internet]. Vol. 282, Proceedings of the Royal Society B:

Biological Sciences. Royal Society of London; 2015 [cited 2021 Feb 2]. Available from: /pmc/articles/PMC4707740/?report=abstract

154. Stidl R, Denne M, Goldstine J, Kadish B, Korakas KI, Turecek PL. Polyethylene glycol exposure with antihemophilic factor (Recombinant), PEGylated (rurioctocog alfa pegol) and other therapies indicated for the pediatric population: History and safety. Pharmaceuticals [Internet]. 2018 Sep 1 [cited 2021 Feb 2];11(3). Available from: /pmc/articles/PMC6160981/?report=abstract

155. Allen TM, Hansen C. Pharmacokinetics of stealth versus conventional liposomes: effect of dose. BBA - Biomembr. 1991 Sep 30;1068(2):133–41.

156. Seibel NL, Shad AT, Bekersky I, Groll AH, Gonzalez C, Wood L V., et al. Safety, tolerability, and pharmacokinetics of liposomal amphotericin b in immunocompromised pediatric patients. Antimicrob Agents Chemother [Internet]. 2017 Feb 1 [cited 2021 Feb 2];61(2). Available from: /pmc/articles/PMC5278758/?report=abstract

157. Hak S, Helgesen E, Hektoen HH, Huuse EM, Jarzyna PA, Mulder WJM, et al. The Effect of Nanoparticle Polyethylene Glycol Surface Density on Ligand-Directed Tumor Targeting Studied *in Vivo* by Dual Modality Imaging. ACS Nano. 2012 Jun;6(6):5648–58.

158. Dyamenahalli K, Famili A, Shandas R. Characterization of shape-memory polymers for biomedical applications. Shape Memory Polymers for Biomedical Applications. Elsevier Ltd.; 2015. 35–63 p.

159. Yeligar VC, Rajmane MA, Chougule KB, Chougule VK, Patil SS. Development and Validation of UV Spectrophotometric Method for Simultaneous Estimation of Melatonin and Quercetin in Liposome Formulation.

160. Babick F. Chapter 3.2.1 - Dynamic light scattering (DLS). In: Hodoroaba V-D, Unger WES, Shard AGBT-C of N, editors. Micro and Nano Technologies. Elsevier; 2020. p. 137–72.

161. Harding SE, Jumel K. Light Scattering. Curr Protoc Protein Sci. 1998 Feb;11(1):7.8.1-7.8.14.

162. Stetefeld J, McKenna SA, Patel TR. Dynamic light scattering: a practical guide and applications in biomedical sciences. Biophys Rev. 2016;8(4):409–27.

163. De Maat MPM, Verschuur M. Fibrinogen heterogeneity: Inherited and noninherited. Curr Opin Hematol. 2005;12(5):377–83.

164. Mozafari MR, Nanoscience A, Initiative N, Danaei M, Gene D, Karmania P, et al. Impact of particle size and polydispersity index on the clinical applications of lipidic nanocarrier systems Impact of particle size and polydispersity index on the clinical applications of lipidic nanocarrier systems Australasian Nanoscience and Nanotech. 2018;(May).

165. D'Souza S. A Review of *In Vitro* Drug Release Test Methods for Nano-Sized Dosage Forms. Adv Pharm. 2014;2014:1–12.

166. Rice JE, Vannucci RC, Brierley JB. The influence of immaturity on hypoxic-ischemic brain damage in the rat. Ann Neurol. 1981 Feb;9(2):131–41.

167. Opitz-Araya X, Barria A. Organotypic hippocampal slice cultures. J Vis Exp. 2011

Feb;(48).

168. Chefer VI, Thompson AC, Zapata A, Shippenberg TS. Overview of brain microdialysis. Curr Protoc Neurosci. 2009 Apr;Chapter 7:Unit7.1.

169. Hammarlund-Udenaes M. Microdialysis as an Important Technique in Systems Pharmacology—a Historical and Methodological Review. AAPS J. 2017;19(5):1294–303.

170. Tomczak M, Tomczak E. The need to report effect size estimates revisited. An overview of some recommended measures of effect size. Trends Sport Sci. 2014;1(21):19–25.

171. Hagberg H, Bona E, Gilland E, Puka-Sundvall M. Hypoxia-ischaemia model in the 7-day-old rat: possibilities and shortcomings. Acta Paediatr Suppl. 1997 Jul;422:85–8.

172. Sheldon RA, Sedik C, Ferriero DM. Strain-related brain injury in neonatal mice subjected to hypoxia – ischemia. 1998;

173. Sofias AM, Andreassen T, Hak S. Nanoparticle Ligand-Decoration Procedures Affect in Vivo Interactions with Immune Cells. Mol Pharm. 2018 Dec;15(12):5754–61.

174. Shabbits JA, Chiu GNC, Mayer LD. Development of an in vitro drug release assay that accurately predicts in vivo drug retention for liposome-based delivery systems. J Control Release. 2002;84(3):161–70.

175. Aggarwal P, Hall JB, McLeland CB, Dobrovolskaia MA, McNeil SE. Nanoparticle interaction with plasma proteins as it relates to particle biodistribution, biocompatibility and therapeutic efficacy. Adv Drug Deliv Rev. 2009;61(6):428–37.

176. Gabizon A, Catane R, Uziely B, Kaufman B, Safra T, Cohen R, et al. Prolonged Circulation Time and Enhanced Accumulation in Malignant Exudates of Doxorubicin Encapsulated in Polyethylene-glycol Coated Liposomes. Cancer Res. 1994 Feb;54(4):987 LP – 992.

177. Smits A, Allegaert K. Perinatal pharmacology: Applications for neonatal neurology. Eur J Paediatr Neurol. 2011;15(6):478–86.

178. Rip J, Chen L, Hartman R, Van Den Heuvel A, Reijerkerk A, Van Kregten J, et al. Glutathione PEGylated liposomes: Pharmacokinetics and delivery of cargo across the blood-brain barrier in rats. J Drug Target [Internet]. 2014 [cited 2021 Apr 7];22(5):460–7. Available from: /pmc/articles/PMC4651142/

179. Robertson NJ, Lingam I, Meehan C, Martinello KA, Avdic-Belltheus A, Stein L, et al. High-Dose Melatonin and Ethanol Excipient Combined with Therapeutic Hypothermia in a Newborn Piglet Asphyxia Model. Sci Rep [Internet]. 2020 Dec 1 [cited 2021 Jan 20];10(1):1–13. Available from: https://www.nature.com/articles/s41598-020-60858-x

180. Cardinali DP. An Assessment of Melatonin's Therapeutic Value in the Hypoxic-Ischemic Encephalopathy of the Newborn. Front Synaptic Neurosci. 2019;11:34.

181. Uchida K, Samejima M, Okabe A, Fukuda A. Neuroprotective effects of melatonin against anoxia/aglycemia stress, as assessed by synaptic potentials and superoxide production in rat hippocampal slices. J Pineal Res. 2004 Nov;37(4):215–22.

182. Group RL. Recommended Dose Volumes for Common Laboratory Animals IQ 3Rs Leadership Group - Contract Research Organization Working Group Recommended

Dose Volumes for Common Laboratory Animals IQ 3Rs Leadership Group - Contract Research Organization Working Group.

183. Esposito E, Cuzzocrea S. Antiinflammatory activity of melatonin in central nervous system. Curr Neuropharmacol. 2010 Sep;8(3):228–42.

184. Liu J, Litt L, Segal MR, Kelly MJS, Yoshihara HAI, James TL. Outcome-related metabolomic patterns from H / 31 P NMR after mild hypothermia treatments of oxygen – glucose deprivation in a neonatal brain slice model of asphyxia. 2011;547–59.

185. Qiao KW. A system of methods to investigate brain metabolism of a mouse model using Hyperpolarized °C. 2018.

186. Harris T, Azar A, Sapir G, Gamliel A, Nardi-Schreiber A, Sosna J, et al. Real-time ex-vivo measurement of brain metabolism using hyperpolarized [1-13C]pyruvate. Sci Rep [Internet]. 2018 Dec 1 [cited 2021 Apr 13];8(1):9564. Available from: www.nature.com/scientificreports/

187. Mengler L, Khmelinskii A, Diedenhofen M, Po C, Staring M, Lelieveldt BPF, et al. Brain maturation of the adolescent rat cortex and striatum: Changes in volume and myelination. Neuroimage. 2014 Jan 1;84:35–44.

188. Espanol MT, Litt L, Chang L-H, James TL, Weinstein PR, Chan PH. Adult Rat Brain-Slice Preparation for Nuclear Magnetic Resonance Spectroscopy Studies of Hypoxia. Anesthesiology. 1996 Jan;84(1):201–10.

189. Yager JY, Shuaib A, Thornhill J. The effect of age on susceptibility to brain damage in a model of global hemispheric hypoxia-ischemia. Brain Res Dev Brain Res. 1996 May;93(1–2):143–54.

190. RUTHERFORD, M. MRI of the neonatal brain. Magn Reson imaging brain preterm infants 24 weeks' gestation to term [Internet]. 2002 [cited 2021 Jan 11];25–49. Available from: http://ci.nii.ac.jp/naid/10027490882/en/

191. Cureton EL, Kwan RO, Dozier KC, Sadjadi J, Pal JD, Victorino GP. A Different View of Lactate in Trauma Patients: Protecting the Injured Brain. J Surg Res. 2010 Mar 1;159(1):468–73.

192. Allen KA, Brandon DH. Hypoxic Ischemic Encephalopathy: Pathophysiology and Experimental Treatments. Newborn Infant Nurs Rev. 2011 Sep;11(3):125–33.

193. Lee ACC, Kozuki N, Blencowe H, Vos T, Bahalim A, Darmstadt GL, et al. Intrapartum-related neonatal encephalopathy incidence and impairment at regional and global levels for 2010 with trends from 1990. Pediatr Res. 2013 Dec;74 Suppl 1(S1):50–72.

194. Jacobs SE, Berg M, Hunt R, Tarnow-Mordi WO, Inder TE, Davis PG. Cooling for newborns with hypoxic ischaemic encephalopathy. Cochrane database Syst Rev. 2013 Jan;3(1):CD003311.

195. Stauch B, Johansson LC, McCorvy JD, Patel N, Han GW, Huang X-P, et al. Structural basis of ligand recognition at the human MT1 melatonin receptor. Nature. 2019 May;569(7755):284–8.

196. Johansson LC, Stauch B, McCorvy JD, Han GW, Patel N, Huang X-P, et al. XFEL structures of the human MT2 melatonin receptor reveal the basis of subtype

selectivity. Nature. 2019 May;569(7755):289–92.

197. Tan DX, Manchester LC, Esteban-Zubero E, Zhou Z, Reiter RJ. Melatonin as a potent and inducible endogenous antioxidant: Synthesis and metabolism. Vol. 20, Molecules. 2015.

198. Skaper SD, Floreani M, Ceccon M, Facci L, Giusti P. Excitotoxicity, oxidative stress, and the neuroprotective potential of melatonin. Ann N Y Acad Sci. 1999 Dec;890(1 NEUROPROTECTI):107–18.

199. Sercombe L, Veerati T, Moheimani F, Wu SY, Sood AK, Hua S. Advances and Challenges of Liposome Assisted Drug Delivery. Front Pharmacol. 2015 Jan;6:286.

200. Molska A, Nyman AKG, Sofias AM, Kristiansen KA, Hak S, Widerøe M. In vitro and in vivo evaluation of organic solvent-free injectable melatonin nanoformulations. Eur J Pharm Biopharm. 2020;152.

201. Netto CA, Sanches E, Odorcyk FK, Duran-Carabali LE, Weis SN. Sex-dependent consequences of neonatal brain hypoxia-ischemia in the rat. Vol. 95, Journal of Neuroscience Research. 2017.

202. Provencher SW. Estimation of metabolite concentrations from localized in vivo proton NMR spectra. Magn Reson Med. 1993;30(6):672–9.

203. Provencher SW. LCModel1 & LCMgui User's Manual. 2018.

204. Davidson AC, Hinkley D V. 5. Confidence Intervals. In: Bootstrap Methods and their Applications. 1997. p. 191–255.

205. Davidson AC, Hinkley D V. 4. Tests. In: Bootstrap Methods and their Applications. 1997. p. 136–90.

206. Xu L-X, Lv Y, Li Y-H, Ding X, Wang Y, Han X, et al. Melatonin alleviates brain and peripheral tissue edema in a neonatal rat model of hypoxic-ischemic brain damage: the involvement of edema related proteins. BMC Pediatr. 2017 Dec;17(1):90.

207. Carloni S, Riparini G, Buonocore G, Balduini W. Rapid modulation of the silent information regulator 1 by melatonin after hypoxia-ischemia in the neonatal rat brain. J Pineal Res. 2017;63(3):1–11.

208. Cetinkaya M, Alkan T, Ozyener F, Kafa IM, Kurt MA, Koksal N. Possible neuroprotective effects of magnesium sulfate and melatonin as both pre- and post-treatment in a neonatal hypoxic-ischemic rat model. Neonatology. 2011;99(4):302–10.

209. Ozyener F, Çetinkaya M, Alkan T, Gören B, Kafa IM, Kurt MA, et al. Neuroprotective effects of melatonin administered alone or in combination with topiramate in neonatal hypoxic-ischemic rat model. Restor Neurol Neurosci. 2012;30(5):435–44.

210. Miller SP, Ramaswamy V, Michelson D, Barkovich AJ, Holshouser B, Wycliffe N, et al. Patterns of brain injury in term neonatal encephalopathy. J Pediatr. 2005;146(4):453–60.

211. Ribeiro MFM, Azambuja AS, Fabres RB, da Rosa LA, Sanches EF, de Fraga LS, et al. Effects of progesterone on the neonatal brain following hypoxia-ischemia. Metab Brain Dis. 2018;33(3):813–21.

212. Farias E, Sarmento N, Spindler C, Moysés F, Rodrigues I, Luis M, et al. Effects of

pre- and postnatal protein malnutrition in hypoxic – ischemic rats. Brain Res. 2011;1438:85–92.

213. Oakden E, Chiswick M, Rothwell N, Loddick S. The Influence of Litter Size on Brain Damage Caused by Hypoxic-Ischemic Injury in the Neonatal Rat. 2002;52(5):692–6.

214. Robertson NJ, Tan S, Groenendaal F, van Bel F, Juul SE, Bennet L, et al. Which neuroprotective agents are ready for bench to bedside translation in the newborn infant? J Pediatr. 2012 Apr;160(4):544-552.e4.

215. Helfer G, Barrett P, Morgan PJ. A unifying hypothesis for control of body weight and reproduction in seasonally breeding mammals. J Neuroendocrinol. 2019 Mar;31(3):e12680.

216. Paulose JK, Cassone VM. The melatonin-sensitive circadian clock of the enteric bacterium Enterobacter aerogenes. Gut Microbes. 2016 Sep;7(5):424–7.

217. Bates TE, Strangward M, Keelan J, Davey GP, Munro PM, Clark JB. Inhibition of N-acetylaspartate production: implications for 1H MRS studies in vivo. Neuroreport. 1996 May;7(8):1397–400.

218. Yuan C, Gao J, Guo J, Bai L, Marshall C, Cai Z, et al. Dimethyl Sulfoxide Damages Mitochondrial Integrity and Membrane Potential in Cultured Astrocytes. Buch SJ, editor. PLoS One. 2014 Sep;9(9):e107447.

219. Rae CD. A guide to the metabolic pathways and function of metabolites observed in human brain 1H magnetic resonance spectra. Neurochem Res. 2014;39(1):1–36.

220. Ueda Y, Noor JI, Nagatomo K, Doi T, Ikeda T, Nakajima A, et al. Generation of lipid radicals in the hippocampus of neonatal rats after acute hypoxic-ischemic brain damage. Exp brain Res. 2006 Feb;169(1):117–21.

221. Jong CJ, Azuma J, Schaffer S. Mechanism underlying the antioxidant activity of taurine: prevention of mitochondrial oxidant production. Amino Acids. 2012 Jun;42(6):2223–32.

222. Gasparovic C, Rosenberg GA, Wallace JA, Estrada EY, Roberts K, Pastuszyn A, et al. Magnetic resonance lipid signals in rat brain after experimental stroke correlate with neutral lipid accumulation. Neurosci Lett. 2001;301(2):87–90.

223. Passani L, Elkabes S, Coyle JT. Evidence for the presence of N-acetylaspartylglutamate in cultured oligodendrocytes and LPS activated microglia. Brain Res. 1998 May;794(1):143–5.

224. Brand A, Richter-Landsberg C, Leibfritz D. Multinuclear NMR Studies on the Energy Metabolism of Glial and Neuronal Cells. Dev Neurosci. 1993;15(3–5):289–98.

225. Tkáč I, Öz G, Adriany G, Uğurbil K, Gruetter R. In vivo 1 H NMR spectroscopy of the human brain at high magnetic fields: Metabolite quantification at 4T vs. 7T. Magn Reson Med. 2009 Oct;62(4):868–79.

226. Welin A-K, Svedin P, Lapatto R, Sultan B, Hagberg H, Gressens P, et al. Melatonin Reduces Inflammation and Cell Death in White Matter in the Mid-Gestation Fetal Sheep Following Umbilical Cord Occlusion. Pediatr Res. 2007 Feb;61(2):153–8.

227. Robertson NJ, Faulkner S, Fleiss B, Bainbridge A, Andorka C, Price D, et al. Melatonin augments hypothermic neuroprotection in a perinatal asphyxia model. Brain. 2013 Jan;136(Pt 1):90–105.

228. Volpe JJ. Brain injury in the premature infant - from pathogenesis to prevention. Brain Dev. 1997;19(8):519–34.

229. Cooper DJ. Induced hypothermia for neonatal hypoxic-ischemic encephalopathy: pathophysiology, current treatment, and nursing considerations. Neonatal Netw. 2011;30(1):29—35.

230. Martha Douglas-Escobar, MD; Michael D. Weiss M. Hypoxic-Ischemic Encephalopathy A Review for the Clinician. JAMA Pediatr. 2015;169(4):397–403.

231. Allen KA BD. NIH Public Access. Newborn Infant Nurs Rev. 2011;11(3):125–33.

232. Beilharz EJ, Williams CE, Dragunow M, Sirimanne ES, Gluckman PD. Mechanisms of delayed cell death following hypoxic-ischemic injury in the immature rat: evidence for apoptosis during selective neuronal loss. Mol Brain Res. 1995;29(1):1–14.

233. Vexler ZS, Ferriero DM. Molecular and biochemical mechanisms of perinatal brain injury. 2001;99–108.

234. Hope PL, Cady EB, Chu A, Delpy DT, Gardiner RM, Reynolds EOR. Brain Metabolism and Intracellular pH During Ischaemia and Hypoxia: An In Vivo 31 P and 1 H Nuclear Magnetic Resonance Study in the Lamb. J Neurochem. 1987 Jul;49(1):75–82.

235. Palmer C, Brucklacher RM, Christensen MA, Vannucci RC. Carbohydrate and energy metabolism during the evolution of hypoxic-ischemic brain damage in the immature rat. J Cereb blood flow Metab Off J Int Soc Cereb Blood Flow Metab. 1990 Mar;10(2):227–35.

236. William GD, Palmer C, Roberts RL, Heitjan DF, Smith MB. 31P NMR spectroscopy of perinatal hypoxic-ischemic brain damage: A model to evaluate neuroprotective drugs in immature rats. NMR Biomed. 1992;5(3):145–53.

237. Mrcpi JDH, Sargentoni J, Mu DCRR, Radiographer S, Bell JD, Lecturer S, et al. Relation between proton magnetic resonance spectroscopy within 18 hours of birth asphyxia and neurodevelopment at 1 year of age. 1999;76–82.

238. Cimarosti H, Henley JM. Investigating the mechanisms underlying neuronal death in ischemia using in vitro oxygen-glucose deprivation: potential involvement of protein SUMOylation. Neuroscientist. 2008 Dec;14(6):626–36.

239. Russell W, Burch R. PRILIMINERY AND CONTENTS.pdf. 1959.

240. Sommer CJ. Ischemic stroke: experimental models and reality. Acta Neuropathol. 2017;133(2):245–61.

241. Lin C-H, Nicol CJB, Cheng Y-C, Yen C, Wang Y-S, Chiang M-C. Neuroprotective effects of resveratrol against oxygen glucose deprivation induced mitochondrial dysfunction by activation of AMPK in SH-SY5Y cells with 3D gelatin scaffold. Brain Res. 2020;1726:146492.

242. Loetscher PD, Rossaint J, Rossaint R, Weis J, Fries M, Fahlenkamp A, et al. Argon: Neuroprotection in in vitro models of cerebral ischemia and traumatic brain injury. Crit Care. 2009;13(6):R206.

243. Cho S, Wood A, Bowlby M. Brain Slices as Models for Neurodegenerative Disease and Screening Platforms to Identify Novel Therapeutics. Curr Neuropharmacol. 2007;5(1):19–33.

244. Gmati D, Chen J, Jolicoeur M. Development of a small-scale bioreactor: Application to in vivo NMR measurement. Biotechnol Bioeng. 2005;89(2):138–47.

245. Fernández-López D, Martínez-Orgado J, Casanova I, Bonet B, Leza JC, Lorenzo P, et al. Immature rat brain slices exposed to oxygen–glucose deprivation as an in vitro model of neonatal hypoxic–ischemic encephalopathy. J Neurosci Methods. 2005 Jun;145(1–2):205–12.

246. Findeisen M, Brand T, Berger S. A1H-NMR thermometer suitable for cryoprobes. Magn Reson Chem. 2007 Feb;45(2):175–8.

247. Patiño P, Parada E, Farré-Alins V, Molz S, Cacabelos R, Marco-Contelles J, et al. Melatonin protects against oxygen and glucose deprivation by decreasing extracellular glutamate and Nox-derived ROS in rat hippocampal slices. Neurotoxicology. 2016 Dec;57:61–8.

248. Lange R, Staaland H, Mostad A. The effect of salinity and temperature on solubility of oxygen and respiratory rate in oxygen-dependent marine invertebrates. J Exp Mar Bio Ecol. 1972;9(3):217–29.

249. Cho S, Wood A, Bowlby MR. Brain slices as models for neurodegenerative disease and screening platforms to identify novel therapeutics. Curr Neuropharmacol. 2007 Mar;5(1):19–33.

250. Ting JT, Daigle TL, Chen Q, Feng G. Acute brain slice methods for adult and aging animals: application of targeted patch clamp analysis and optogenetics. Methods Mol Biol. 2014;1183:221–42.

251. Alexander AD. Tolerance j, f. fazekas,. 2020;

252. Smith AL, Garbus H, Rosenkrantz TS, Fitch RH. Sex differences in behavioral outcomes following temperature modulation during induced neonatal hypoxic ischemic injury in rats. Brain Sci. 2015 May;5(2):220–40.

253. Thomaz DT, Rafognatto R, Luisa A, Binder B, Scheffer L, Willms A, et al. Guanosine Neuroprotective Action in Hippocampal Slices Subjected to Oxygen and Glucose Deprivation Restores ATP Levels , Lactate Release and Glutamate Uptake Impairment : Involvement of Nitric Oxide. Neurochem Res. 2020;45(9):2217–29.

254. Magistretti PJ, Allaman I. A Cellular Perspective on Brain Energy Metabolism and Functional Imaging. Neuron. 2015 May 20;86(4):883–901.

255. Liu J, Litt L, Segal MR, Kelly MJS, Yoshihara HAI, James TL. Outcome-Related Metabolomic Patterns from 1H/31P NMR after Mild Hypothermia Treatments of Oxygen—Glucose Deprivation in a Neonatal Brain Slice Model of Asphyxia. J Cereb Blood Flow Metab. 2010 Aug;31(2):547–59.

256. Meyer DA, Torres-altoro MI, Tan Z, Tozzi A, Filippo M Di, Dinapoli V, et al. Ischemic Stroke Injury Is Mediated by Aberrant Cdk5. 2014;34(24):8259–67.

257. Murata A, Agematsu K, Korotcova L, Gallo V, Jonas RA, Ishibashi N. Rodent brain slice model for the study of white matter injury. J Thorac Cardiovasc Surg. 2013;146(6):1526-1533.e1.

258. Juzekaeva E, Gainutdinov A, Mukhtarov M, Khazipov R. Dynamics of the Hypoxia-Induced Tissue Edema in the Rat Barrel Cortex in vitro. Front Cell Neurosci. 2018 Dec;12:502.

259. Wells GAH, Wells M. Neuropil vacuolation in brain: a reproducible histological processing artefact. J Comp Pathol. 1989;101(4):355–62.

260. Rahaman P, Del Bigio MR. Histology of Brain Trauma and Hypoxia-Ischemia. Acad forensic Pathol. 2018/08/31. 2018 Sep;8(3):539–54.

8. Papers

Paper I

European Journal of Pharmaceutics and Biopharmaceutics 152 (2020) 248–256

Contents lists available at ScienceDirect

European Journal of Pharmaceutics and Biopharmaceutics

journal homepage: www.elsevier.com/locate/ejpb

In vitro and *in vivo* evaluation of organic solvent-free injectable melatonin nanoformulations

Alicja Molska[a,1], Axel Karl Gottfrid Nyman[a,1], Alexandros Marios Sofias[a,b], Kåre Andre Kristiansen[c], Sjoerd Hak[a,d,e], Marius Widerøe[a,*]

[a] Department of Circulation and Medical Imaging, Faculty of Medicine and Health Sciences, Norwegian University of Science and Technology (NTNU), Trondheim, Norway
[b] Department of Nanomedicine and Theranostics, Institute for Experimental Molecular Imaging, Faculty of Medicine, RWTH Aachen University, Aachen, Germany
[c] Department of Biotechnology and Food Science, Faculty of Natural Sciences, Norwegian University of Science and Technology (NTNU), Trondheim, Norway
[d] Department of Physics, Faculty of Medicine and Health Sciences, Norwegian University of Science and Technology (NTNU), Trondheim, Norway
[e] Department of Biotechnology and Nanomedicine, SINTEF Industry, Trondheim, Norway

ARTICLE INFO

Keywords:
Nanomedicine
Liposome
Nanoemulsion
Melatonin
Brain microdialysis
Hypoxic-ischemic brain injury

ABSTRACT

Melatonin is a neurohormone with potenial therapeutic effects in many diseases including neonatal hypoxic-ischemic (HI) brain injury. Due to limited solubility in water there is currently no clinically available melatonin formulation for parenteral use. Clinical use of melatonin has thus relied on oral administration, which in many cases is hampered by low and variable bioavailability. In animal treatment studies of neonatal HI, this issue have been circumvented by using parenteral administration of melatonin dissolved in ethanol (EtOH) or dimethyl sulfoxide (DMSO), solvents that are potentially neurotoxic, especially to the newborn brain. Thus, there is an urgent need for a non-toxic injectable melatonin formulation. The aim of this study was to develop such a formulation comprised of melatonin and biocompatible lipid-based nanoparticles with improved melatonin bioavailability. We herein report the development and characterization of an injectable system composed of melatonin and liposomes (LP) or oil-in-water nanoemulsions (NE). Nanoparticle characterization confirmed physicochemical stability over a week and an improvement with respect to melatonin solubilization in water (2.6 mg/mL in our injectable system). Determination of the *in vitro* release kinetics showed a prolonged release when melatonin is solubilized in nanoparticles ($T_{1/2}$: 81 min vs 50 min vs 26 min for melatonin-LP, melatonin-NE, and melatonin-EtOH respectively). The pharmacokinetic (PK) parameters were confirmed *in vivo* in adult rats as similar melatonin levels detected in blood and indicated higher bioavailability in brain after intravenous administration of melatonin nanoformulations (10 mg/kg) in comparison to the free-melatonin administration. In conclusion, we have developed an organic solvent-free injectable formulation for melatonin by utilizing FDA-approved components, as a safe alternative for facilitating the potential of melatonin against variety of pathological conditions.

1. Introduction

Melatonin is a neurohormone secreted primarily from the pineal gland that has multiple physiological roles, including circadian rhythm mediation and oxidative stress regulation [1]. Treatment effects of administered melatonin has been studied in neurodegenerative diseases [2], cancer [3], osteoporosis [4] and ischemia/reperfusion brain injury [5] among others. Our focus is on melatonin as a neuroprotective agent in hypoxic-ischemic (HI) brain injury in neonates [6].

In HI, the current treatment regime with hypothermia is only partially effective with almost 50% of treated newborns suffering adverse outcomes [7]. Animal studies have shown that melatonin administration can provide improved outcome after HI brain insult, where it acts against excitotoxicity, oxidative stress and inflammation [8]. To achieve clinical translation of these results, questions regarding therapeutic window and optimal dosing have to be answered. Another pressing matter is the need for a parenteral formulation of melatonin for clinical use. To date, only melatonin formulations for oral administration are clinically available. Melatonin is poorly soluble in water, light sensitive, and exhibits variable and low bioavailability due to low

* Corresponding author at: Department of Circulation and Medical Imaging, Faculty of Medicine and Health Sciences, NTNU, Medisinsk teknisk forskningssenter (MTFS), Post box 8905, 7491 Trondheim, Norway.
E-mail address: marius.wideroe@ntnu.no (M. Widerøe).
[1] The authors contributed equally to the study.

https://doi.org/10.1016/j.ejpb.2020.05.003
Received 29 November 2019; Received in revised form 29 April 2020; Accepted 4 May 2020
Available online 18 May 2020
0939-6411/ © 2020 Elsevier B.V. All rights reserved.

absorption and high first-pass metabolism [9]. Moreover, apart from oral administration being challenging in neonates, HI injury can also affect the gut, which can further reduce melatonin's absorption and bioavailability [10].

In animal experiments, these issues are typically circumvented using organic solvents, like DMSO or EtOH, to make injectable melatonin formulations. These solvents have potential toxic effects [11], and we have previously reported mitochondrial impairment in astrocytes when DMSO was used as melatonin solvent [6]. This is a possible confounding factor in animal experiments, and poses an obstacle towards clinical translation. Thus, there is a need for an injectable melatonin formulation without toxic recipients to realize optimal and predictable bioavailability and, more importantly, to translate this therapy into clinical use.

To develop an injectable melatonin formulation without toxic solvents, utilizing nanoparticle technology is a promising strategy. Lipid-based nanoparticles, in our case liposomes (LP) [12] and nanoemulsions (NE) [13], are very suitable solubilizers for lipophilic substances like melatonin. These nanoparticles are composed of naturally occurring phospholipids and biocompatible synthetic lipids, and various formulations are clinically approved [14]. In general, production and optimization of these nanoparticles can be performed through well established, robust, and relatively simple procedures [15,16]. In addition to a beneficial safety profile, solubilization in nanoparticles may also improve melatonin bioavailability due to slow release from the long-circulating nanoparticles.

Although melatonin may have potential in many clinical settings, we are studying melatonin's effects on the brain. To assess melatonin concentrations in the brain after intravenous administration, we established an *in vivo* brain microdialysis system. Using this set-up, brain extracellular fluid of freely moving animals can be sampled at a temporal resolution of minutes [17]. Subsequent mass spectrometry allows for highly sensitive and specific melatonin detection (LOD = 0.2 nM, LOQ = 0.65 nM).

We here demonstrate that lipidic melatonin formulations exhibit similar pharmacokinetic (PK) profile in blood compared to melatonin administered in DMSO. However, since they lack potentially toxic organic components, lipidic melatonin formulations are attractive candidates for studying melatonin's effects in *in vivo* settings. Furthermore, by measuring melatonin brain concentrations using the microdialysis set-up, we here show that lipidic melatonin formulations improve melatonin bioavailability in the brain.

2. Materials and methods

2.1. Materials

N-acetyl-5-methoxytryptamine (melatonin), N-[2-(5-methoxy-1H-indol-3-yl)ethyl-1,1,2,2-d4]-acetamid (melatonin-d_4), N1-acetyl-N2-formyl-5-methoxykynuramine (AMFK), N1-acetyl-5-methoxykynuramine (AMK), 3-(N-Acetylaminoethyl)-6-hydroxy-5-methoxyindole (6-OH-melatonin), soybean oil (SB), tributyrin (C4), tricaproin (C6), oleic acid, tricaprylin (C8), triolein (C18), DMSO and EtOH were purchased from Sigma-Aldrich Chemie GmbH, Germany. The modified Ringer solution consisted of NaCl (145 mM), KCl (0.6 mM), $CaCl_2$ (1.2 mM), and $MgCl_2$ (1.0 mM) in PBS pH 7.4 (Sigma-Aldrich Chemie GmbH, Germany). Cholesterol, 1,2-Distearoyl-*sn*-glycero-3-phosphocholine (DSPC), 1,2-distearoyl-*sn*-glycero-3-phosphoethanolamine-*N*-[methoxy (polyethylene glycol)-2000] (DSPE-PEG_{2000}) were purchased from Avanti Polar Lipids (Alabaster, AL, USA). Medium-chain triglycerides (MCT) were purchased from Lipoid GmbH (Ludwigshafen, Germany).

2.2. Nanoparticle synthesis

Nanoparticles were synthesized based on established methods [15]. In brief, 15 μmol of lipids (DSPC/Cholesterol/PEG2000-DSPE on a 62:33:5 M ratio respectively) and 3 mg melatonin were dissolved in 200 μL of chloroform. For NE 60 mg oil (4 mg oil/μmol of lipid) was also added to this mix and dissolved. The mix was dripped into 1 mL isotonic HEPES buffered saline (HBS) of pH 7.4, at 70 °C, under vigorous stirring at 1000 rpm. The solution remained at constant temperature (70 °C) for 6 min to ensure complete evaporation of the organic solvents. The obtained crude nanoparticles were downsized in an iced water bath using a tip-sonicator (Heat Systems Ultrasonics Inc., Model W-225). The sonication was applied proportionally to the total lipid and oil mass of the formulation: 5 min at 50% duty cycle in case of 15 μmol lipids for LP, and 20 min at 50% duty cycle of 15 μmol lipids for NE. Upon preparation, the nanoparticles were stored at room temperature in the dark.

2.3. Melatonin quantification

Melatonin in the prepared nanoformulations was quantified by absorption spectroscopy at 300 nm using a SpectraMax i3x (Molecular Devices, USA). In brief, melatonin-nanoparticle aliquots were diluted 15 times in isopropanol and vortexed for at least 15 s, resulting in nanoparticle disassociation. To determine melatonin concentration, the absorption readout on 100 μL of this sample was compared to a melatonin standard curve in isopropanol with the same amount of lipids/oil in the sample (8 points, 0 – 0.4 mg/mL melatonin concentration).

2.4. Melatonin solubility in oils

In order to select an appropriate oil phase for melatonin-NE, melatonin was added in various oils (C4, C6, C8, C18, MCT, SB, and oleic acid) at a concentration of 4 mg melatonin/g oil. The mixtures were shaken at 700 rpm for 7 days in the dark, and then centrifuged at 4000 g for 15 min. The melatonin concentration in the supernatants was determined as described in paragraph 2.3.

2.5. Size of melatonin nanoformulations

The nanoparticle size (hydrodynamic diameter, nm) and size distribution (dispersity, Đ) were measured using dynamic light scattering (DLS, Zetasizer Nano-ZS, Malvern Instruments). All samples were diluted 1:100 in Milli-Q® water prior to the measurements. The reported values are averages of three individual measurements.

2.6. Determination of melatonin solubility in nanoparticle injectable systems

In order to quantify melatonin contained in the injectable formulation, nanoparticle solutions with a final theoretical concentration of 3 mg melatonin/mL of formulation were prepared. After preparation, the formulations were centrifuged at 4000 g for 2 min to force precipitation of the non-solubilized melatonin, and supernatants were collected and determined as described in paragraph 2.3.

2.7. Stability of melatonin in nanoparticle injectable systems

To determine melatonin stability in four melatonin nanoparticles (LP, C6-NE, MCT-NE, and SB-NE), the presence of three major melatonin breakdown products (AFMK, AMK, 6-OH-melatonin) was determined using UHPLC–MS/MS 7 days after nanoparticle synthesis. During these 7 days, nanoparticles were stored in the dark at room temperature. Before the analysis, 15 μL of sample was mixed with 185 μL of acetonitrile, vortexed, and then centrifuged at 4000 g for 10 min in order to precipitate lipids. Supernatant was collected to new tubes, and dried in a Savant SC250EXP SpeedVac concentrator (Thermo Scientific) for 1 h, at 7 mTorr, 60 °C. All samples were stored at −20 °C prior to the analysis, then diluted in Milli-Q® water before injection into a UHPLC–MS/MS system. Concentrations of melatonin and breakdown products were determined in the range from 3.125 to 500 nM, and all

standards and samples were spiked with 25 nM of melatonin-d_4 as internal standard. UHPLC–MS/MS system consisted of a chromatographic column (Waters ACQUITY UPLC® CSH Fluoro-Phenyl, 100 Å, 100 × 2.1 mm, particle size 1.7 μm), and the column manager was set to 45 °C. Mobile phase A consisted of water with 0.1 (v/v)% formic acid, and mobile phase B was acetonitrile with 0.10 (v/v)% formic acid. Flow rate was set at 0.5 mL/min. Conditions were kept constant at 99.0% A for half a minute, then a linear gradient was programmed from 99.0% A to 1.0% A in 3.5 min, followed by 1.0% A kept for a 0.5 min period, before the gradient was brought back to 99.0% A in 0.10 min. Finally, the column was equilibrated for 0.90 min before starting a new injection. Analysis was performed with an ACQUITY UPLC system coupled to a Xevo TQ-S triple quadrupole mass spectrometer (Waters, Milford, MA, USA) equipped with an electrospray (ESI) source operating in positive mode. Data were acquired and processed using MassLynx software (v4.1) and TargetLynx application manager.

2.8. In vitro melatonin release

Melatonin release from nanoparticles suspensions (n = 3) was determined as following: 1 mL of each nanoformulation was placed in a dialysis tube (Sigma, MWCO 100 kDa) and dialyzed against 1 L PBS at 37 °C, 150 rpm stirring, in dark. 30 μL of samples from the dialysis tube were collected at 7 time-points: 0, 5, 30, 60, 120, 180, 240 min, and centrifuged at 4000 g for 2 min. Then, the supernatant was collected, and melatonin was quantified as described in paragraph 2.3. Since melatonin diluted in 1 L of PBS is undetectable, the quantification of the released amount was calculated indirectly by collecting samples from the dialysis tube. Therefore, before the final calculation of the melatonin concentration the volume loss due to the sampling at various time points was taken into account. As a control we used melatonin dissolved in 10% EtOH in water (also n = 3). For each trial a linear regression line was fitted through the log-transformed concentrations, and the elimination rate constant k_e was defined as the regression coefficient for the intercept. Half-life $T_{1/2}$ of melatonin released from nanoparticles suspensions was calculated as $-\log_{(2)}{}^{*}k_e$. A two-tailed, two-sample equal variance *t* test was used for statistical comparison.

2.9. ^{1}H NMR spectroscopy

^{1}H NMR spectroscopy was used to confirm complete removal of chloroform used in preparing melatonin nanoformulations. Melatonin-LP or melatonin-MCT-NE was transferred to 3 mm NMR tubes and spiked with 10% D_2O used as a lock solvent. NMR spectra were recorded at 300 K on a Bruker Biospin 600 MHz AVANCE III instrument, fitted with a QCI cryoprobe.

2.10. In vivo pharmacokinetics

2.10.1. Animals

Female Sprague Dawley rats (*Rattus norvegicus*) were obtained from Elevage Janvier (Le Genest Saint Isle, Laval, France), aged 12 weeks, and weighing from 200 to 400 g. All animal experiments were performed according to the European Union and Norwegian regulations and guidelines for animal experimentation, and were approved by the Norwegian authority on animal welfware (Mattilsynet). Rats were housed in groups of three in a controlled light/dark cycle (12 h/12 h), with environmental enrichment and food and water *ad libitum*. Animals used in microdialysis experiments were housed individually to avoid damage to the microdialysis guide cannula by other rats. All PK experiments were performed between 08.00 and 16.00o'clock.

2.10.2. Determination of melatonin concentration in plasma

To determine the PK parameters of melatonin in plasma, 1 mL of 3 mg/mL melatonin in LP, MCT-NE, or dissolved in 5% DMSO (95% PBS) as a conventional formulation, was injected in the tail vein of a 300 g rat. The injected volumes were corrected according to the body weight of each rat (272–305 g). Blood samples were collected into heparinized tubes from the saphenous or femoral vein at 5 min pre-dose and 5, 10, 20, 30, 60, 120, 240 min post-dose. The first five samples were collected under isoflurane anaesthesia and the final three were collected from awake animals. Samples were then centrifuged at 1500 g for 10 min at 4 °C, and supernatant plasma was transferred to clean tubes. All samples were stored at −20 °C until the sample preparation for the UHPLC–MS/MS analysis. Each sample was thawed and 15 μL of sample was mixed with 185 μL of acetonitrile, vortexed, and then centrifuged at 4000 g for 10 min in order to precipitate lipids. Supernatant was collected to new tubes, and dried in a Savant SC250EXP SpeedVac concentrator (Thermo Scientific) for 1 h, at 7 mTorr, 60 °C. All samples were stored at −20 °C prior to the analysis, then diluted in Milli-Q® water before injection into a UHPLC–MS/MS system described in paragraph 2.7. Concentrations of melatonin and breakdown products were determined in the range from 3.125 to 500 nM, and all standards and samples were spiked with 25 nM of melatonin-d_4 as internal standard.

2.10.3. In vivo brain microdialysis

Microdialysis, a method illustrated in Fig. 1, was performed to estimate the PK parameters in the brain of melatonin-LP or melatonin-MCT-NE in comparison to melatonin dissolved in 5% DMSO. On day 1, a metal-free microdialysis guide cannula (CMA, Sweden) was surgically implanted in the right striatum [18]. On days 7, 14 and 21, animals underwent microdialysis sampling following tail vein injections with melatonin formulations at a melatonin dose of 10 mg/kg body weight. A microdialysis probe with 3 mm membrane length and a molecular cutoff at 20 kDA was connected to a microdialysis pump using FEP tubing and tubing adapters (CMA, Kista, Sweden), and prepared according to the manufacturer's instructions before insertion into the guide cannula. Using a perfusion speed of 2 μL/min, the probe was perfused with a perfusion solution containing 20 ng/mL of melatonin-d_4 as internal standard for microdialysis calibration in modified Ringer solution. The probes were perfused for 90 min before sample collection to allow equilibration of the periprobe space. A pre-injection sample was collected 10 min before the melatonin administration. All samples were weighed to monitor the flow through the probe. Melatonin was analyzed with a modified method described in paragraph 2.7 where samples were injected directly to the UHPLC–MS/MS system without the precipitation with acetonitrile and evaporation stage. Unfortunately, melatonin-d_4 could not be accurately quantified. Comparison of dialysate concentrations are therefore based on the assumption of similar membrane behavior in each experiment, using each animal as its own control to reduce the risk of systematic error.

2.10.4. Data analysis

R (version 3.5.2) was used for the data statistical analysis. Melatonin PK parameters were assessed using non-compartment analysis for each animal. Constant elimination was assumed after 30 min. A linear regression line was fitted through the log-transformed concentrations, and elimination rate constant k_e was defined as the regression coefficient for the intercept. The elimination half-life, $T_{1/2}$, was calculated as $-\log_{(2)}{}^{*}k_e$. AUC was estimated using the trapezoidal rule for each concentration–time-curve. C_{max} was defined as the maximum observed concentration, and T_{max} as the time at which C_{max} was observed.

3. Results

3.1. Melatonin solubility in oils

In order to identify suitable oils for the development of melatonin-NE, melatonin solubility in seven oils was determined. Triglycerides with the shortest fatty acid chains (C4) were better solvents for

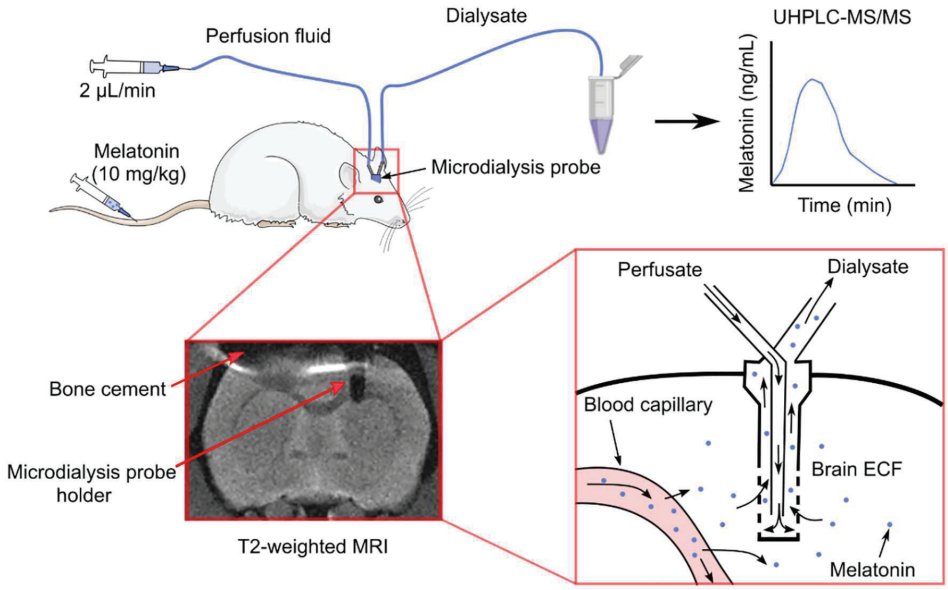

Fig. 1. Cartoon of the microdialysis method.

melatonin, with solubility of approximately 4.5 mg melatonin/g of oil. Triglycerides with the longest fatty acid chains, C18, had the lowest melatonin solubility; 0.23 mg melatonin/g of oil. All other oils displayed a melatonin solubility between those values (Fig. 2a).

3.2. Colloidal stability of melatonin nanoformulations

Even though C4 oil showed the best melatonin solubility capacity, we decided to exclude it from further investigation, as it compromised NE stability. We selected C6, MCT, and SB oils for synthesizing NE since C6 oil showed the second-best melatonin solubility, and MCT and SB oils are already FDA-approved and widely used in drug development using lipid-based nanoparticles. We synthesized three melatonin-NE (C6-NE, MCT-NE, SB-NE), and one melatonin-LP. LP and NE were approximately 120 nm and 200 nm in diameter respectively, with a dispersity between 0.2 and 0.3 and remained stable over a week when stored in the dark at room temperature (Fig. 2b-c).

3.3. Determination of melatonin solubilization enhancement

Melatonin solubilization efficiency was determined as the amount of solubilized melatonin in the final nanoparticle solution over the initial amount of used melatonin (3 mg/mL of formulation). The solubilization efficiency for all four melatonin-nanoparticles was between 80 and 90% with melatonin-MCT-NE having slightly higher melatonin solubilization efficiency than the other three melatonin-nanoformulations (Fig. 2d).

3.4. In vitro release profile of melatonin formulations

The *in vitro* release kinetics showed a prolonged melatonin release from nanoparticles in PBS. Melatonin release was slowest from LP ($T_{1/2}$ = 80.9 ± 3.6 min) followed by the three melatonin-NE which all showed $T_{1/2}$ of approximately 50 min. The use of nanoparticles for increasing melatonin solubility improved also the release profile of the drug, as the $T_{1/2}$ for free-melatonin (dissolved in 10% EtOH in water) in our dialysis set-up was only 26.1 ± 8.4 min. Similarly to the half-life values of the released melatonin and AUC were the highest in melatonin-LP (3523.27 mg*min/mL), and the lowest in melatonin-EtOH (1513.92 mg*min/mL) (Fig. 2e-f).

3.5. Melatonin stability

To study the stability of melatonin in the nanoformulations, we used UHPLC–MS/MS to determine the levels of three major melatonin breakdown products, AFMK, AMK and 6-OH-melatonin. One week after nanoparticle preparation, the amount of breakdown products was < 10%, verifying the ability of all four nanoparticles to maintain melatonin stability. Out of the three major breakdown products, AMK was undetectable, while only low levels of 6-OH melatonin and AFMK were detected (between 3 and 6% of initial melatonin) (Fig. 3).

3.6. ^{1}H NMR spectroscopy for validating organic solvent removal

During nanoparticle synthesis, chloroform was initially used as solubilizer for nanoparticle ingredients and was expected to be evaporated during nanoparticle heating at 70 °C for 6 min. To confirm complete removal of the organic solvent, we performed ^{1}H NMR spectroscopy on melatonin-LP and melatonin-MCT-NE. A control sample of melatonin-MCT-NE with remaining chloroform (insufficient evaporation time; 70 °C for 1 min) was used as control. A chemical shift of chloroform was recognized at 7.70 ppm (indicated with a red arrow in Fig. 4a). Spectra of melatonin-MCT-NE and melatonin-LP prepared using appropriate evaporation time (70 °C for 6 min) confirmed complete removal of chloroform (Fig. 4b-c).

3.7. In vivo pharmacokinetics

Melatonin-LP, melatonin-MCT-NE or melatonin-DMSO were administered intravenously to adult rats in order to evaluate the PK profile of melatonin in blood and brain. The following parameters, i.e., C_{max}, T_{max}, $T_{1/2}$, and AUC, were evaluated in circulation through blood sampling and in brain using a microdialysis set-up. All three melatonin-formulations were found to display a comparable PK behavior in circulation (Fig. 5a-f), while in brain all melatonin-NP injectable formulations showed superiority over the free-melatonin (Fig. 6a-e).

When looking at time above certain critical concentrations

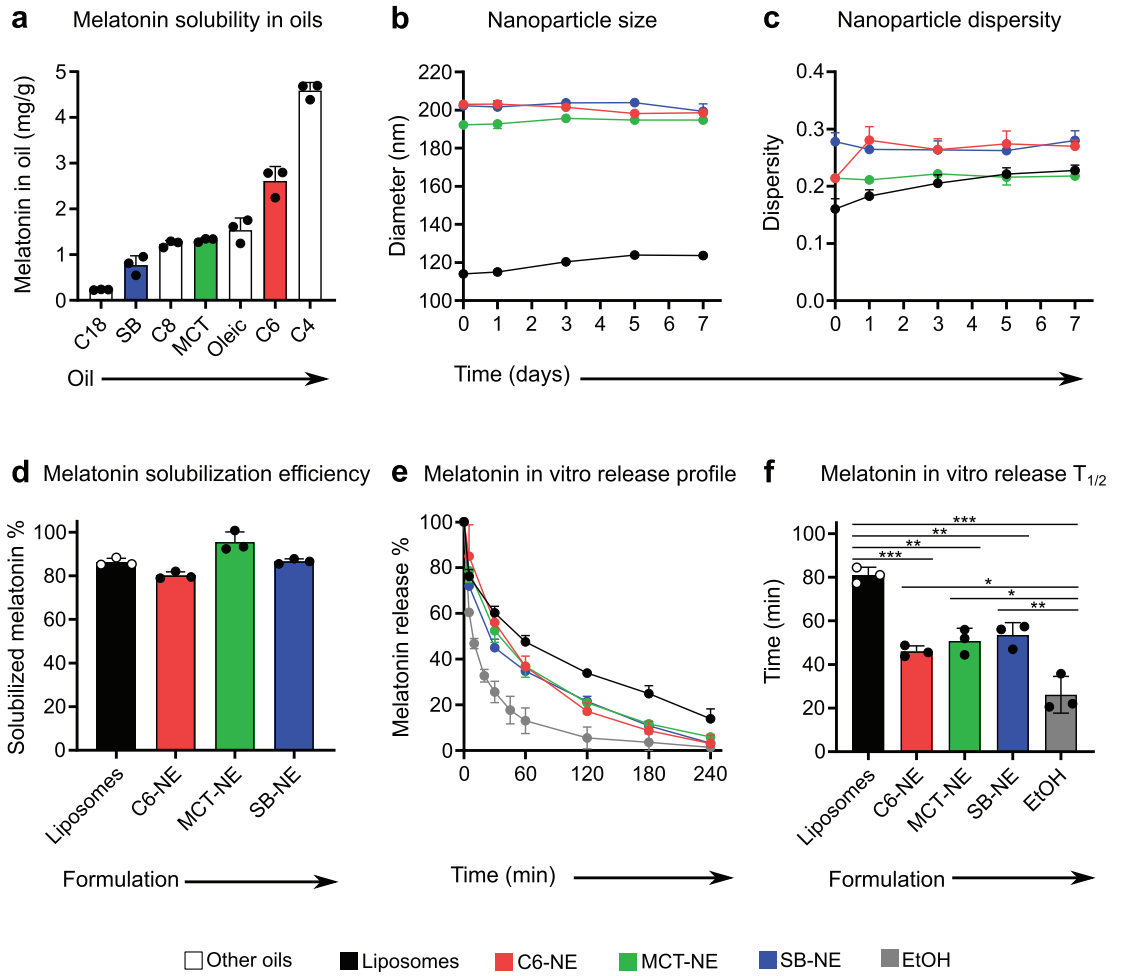

Fig. 2. *In vitro* characterization data. (a) Melatonin solubility in oils. (b) Particle hydrodynamic diameter as z-average of melatonin nanoformulations as a function of time after preparation measured with dynamic light scattering. (c) Size distribution (dispersity, Đ) of melatonin nanoformulations as a function of time measured with dynamic light scattering. (d) Melatonin solubilization efficiency (%) in melatonin nanoformulations. (e) Melatonin release profile in melatonin formulations as a function of time. (f) Release half-life for melatonin formulations. * = $P < 0.05$, ** = $P < 0.01$, *** = $P < 0.001$. All data reported as mean ± SD, n = 3, points represent actual values of experiments.

(Table 1), melatonin-LP had longer time above 1 nM ($P = 0.0028$), 100 nM ($P = 0.021$) and 200 nM ($P = 0.034$) compared to melatonin-DMSO. Melatonin-MCT had longer time above 100 nM ($P = 0.0051$) and 200 nM ($P = 0.034$) compared to melatonin-DMSO.

4. Discussion

We have developed an injectable lipid-based melatonin-nanoformulation using only clinically approved ingredients. We have demonstrated that intravenous administration of melatonin-nanoformulations (LP or MCT-NE) results in similar PK parameters in circulation and improved bioavailability in the brain compared to administration of melatonin dissolved in organic solvents.

We started by identifying an appropriate phospholipid mixture for the lipid-based formulation. Although melatonin loading as well as formulation stability are affected by phospholipid mixture, we prioritized clinical tolerability when making our final choice. To maximize melatonin loading in NE, we determined melatonin solubility in various triglycerides because these oils are the most common oils used in NE for *in vivo* applications. We measured the highest melatonin solubility in triglycerides with the shortest fatty acid chains (C4) while the lowest solubility was observed in triglycerides with the longest fatty acid chains (C18). These findings are consistent with other studies showing that solvent capacity of triglycerides increases with decreasing chain length [19]. However, since NE of short-chain triglycerides are typically less stable under *in vivo* conditions and prone to Oswald ripening, we did not pursue NE preparation with C4 oil [20,21]. For further NE development, we selected three oils: C6, MCT, and soybean oil. C6 was chosen because of the high melatonin solubility, while the last two oils were chosen because they are already FDA-approved, and are widely used in pharmaceutical applications. We assessed colloidal stability of our four melatonin formulations (LP, C6-NE, MCT-NE, and SB-NE) using dynamic light scattering. LP were significantly smaller than NE and all four formulations showed acceptable stability and dispersity

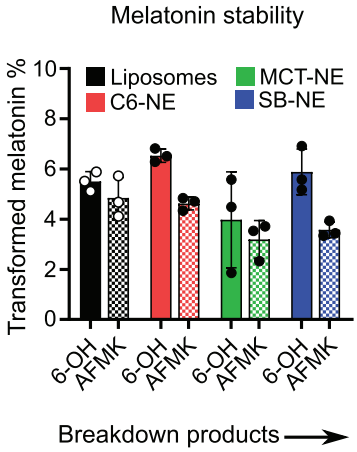

Fig. 3. Levels of melatonin metabolites measured 7 days after preparation of melatonin nanoformulations as a measure for degradation of melatonin over time. Metabolite levels are reported as % of initial total melatonin content (mean ± SD, n = 3, points represent actual values of experiments).

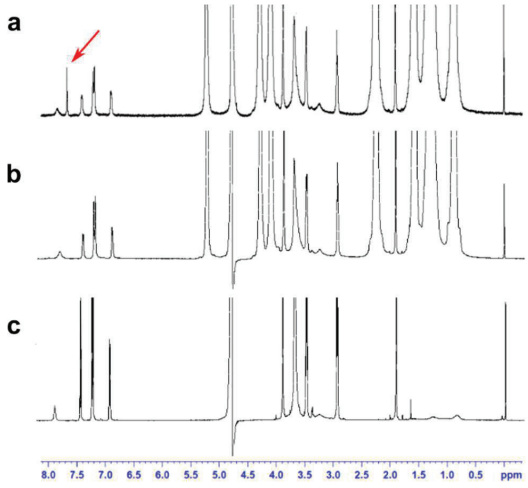

Fig. 4. ^{1}H NMR spectra of melatonin formulations. (a) Melatonin-MCT-NE with $CHCl_3$ signal present (red arrow). (b) Melatonin-MCT-NE without the organic solvent (c) Liposomal melatonin without the organic solvent. Spectra has been cropped to emphasize $CHCl_3$ chemical shift at 7.70 ppm.

below 0.3 over a week. For the melatonin solubilization efficiency we chose a UV spectrophotometric technique that has been found to be precise, accurate and sensitive method for determination of melatonin in liposomal form previously [22]. The melatonin solubilization efficiency at a melatonin starting concentration of 3 mg/mL was high and very similar for all formulations. This resulted in formulations that can readily be applied in *in vivo* studies with respect to the desired dose volumes for intravenous injections (from 10 to 30 mg of melatonin/kg body weight).

Melatonin is a light sensitive molecule that easily undergoes oxidation where melatonin breakdown products are formed. A week after particle preparation, we found only small amounts of AFMK and 6-OH-melatonin in the samples, and we were unable to detect AMK. This situation occurred presumably because AMK is formed from AFMK. We consider such low amounts of melatonin breakdown products acceptable, especially since AFMK and 6-OH-melatonin are, like melatonin, non-toxic and effective free radical scavengers [23]. Moreover, these melatonin metabolites will be readily formed upon melatonin *in vivo* administration [24].

In the *in vitro* release assay, we observed slower melatonin release from a dialysis tube for melatonin-nanoformulations in comparison to free-melatonin dissolved in 10% EtOH. This can be explained by the fact that melatonin diffusion from the oil-core from NE, and from lipid bilayers in case of LP, is hindered by the aqueous medium that acts as a barrier to the melatonin transport due to its poor solubility in water. Interestingly, melatonin release from LP was slower than the release from the NE. Melatonin can be entrapped in the lipid bilayer and in the aqueous core in case of LP while it can be incorporated in the oil-core or the phospholipid coating in case of NE. We assume that melatonin has higher compatibility with the liposomal bilayer than with the oil-core and the phospholipid monolayer in case of the NE. Nevertheless, our findings are in line with other studies comparing the *in vitro* drug release from NE with smaller LP [25].

The final step of the *in vitro* characterization was to assure complete removal of chloroform (used in the particle synthesis) from the formulations. Using ^{1}H NMR spectroscopy, we were unable to detect chloroform, confirming the preparation of a melatonin formulation without any organic solvents present. To summarize the *in vitro* characterization, LP were smaller, had slower drug release and longer half-life of melatonin *in vitro* than NE. Thus, LP were considered the most favorable vehicle for melatonin administration *in vivo* but we also decided to include a second melatonin-nanoformulation; melatonin-NE with an already FDA-approved oil (MCT) since the *in vitro* results indicated that MCT-NE has slightly higher melatonin solubilization efficiency than LP.

In our study, we used adult rats to evaluate PK of melatonin-LP and melatonin-MCT-NE in comparison to melatonin administered dissolved in DMSO. After injecting 1 mL of each formulation containing 3 mg/mL of melatonin, we found all three of them to display a similar PK profile in circulation. Additionally, we found a higher initial melatonin concentration in DMSO-solved melatonin than in our melatonin-nanoformulations. This observation is in line with our *in vitro* study (Fig. 2d) showing that the melatonin solubilization efficiency in our nanoformulations is approximately 80–90%, and therefore, lower than 100% solubilization efficiency that is achieved when melatonin is dissolved in 5% DMSO. Nevertheless, the normalized results show similar PK profiles of melatonin in all three formulations. The issue of lower initial melatonin concentration (depicted as lower C_{max} and AUC values for melatonin-nanoformulations) can be easily corrected by just injecting a higher volume of nanoformulations accordingly. The relatively fast clearance from blood of melatonin solved in nanoformulations is somewhat contrary to what one would expect given the normally long circulation times for lipid nanoparticle systems. Since our nanoformulations are used as “solubilizers” (i.e. improve solubilization of melatonin in aqueous solutions without the need of using organic solvents) and not as “carriers” (i.e. strictly improve the pharmacokinetic properties in circulation), the small amounts of solubilized non-encapsulated melatonin were not removed before injection. This choice is based on the fact that all available solubilized melatonin can only result into an additional therapeutic benefit since the drug is not toxic. Therefore, the extra free-melatonin in circulation could contribute to “masking” differences between the PK profile of the nanoparticle-melatonin and the DMSO-melatonin.

Using a microdialysis system, we performed real-time measurements of melatonin concentrations in the brain of freely moving animals. All animals were injected with a similar dose of melatonin (10 mg of melatonin/kg body weight) of all three formulations. The PK parameters, $T_{1/2}$, C_{max}, T_{max}, AUC in brain were superior for both melatonin-NPs in comparison to the melatonin dissolved in DMSO.

Various studies have shown that conventional LP do not cross the BBB *in vivo* unless the BBB is disrupted or particles are decorated with

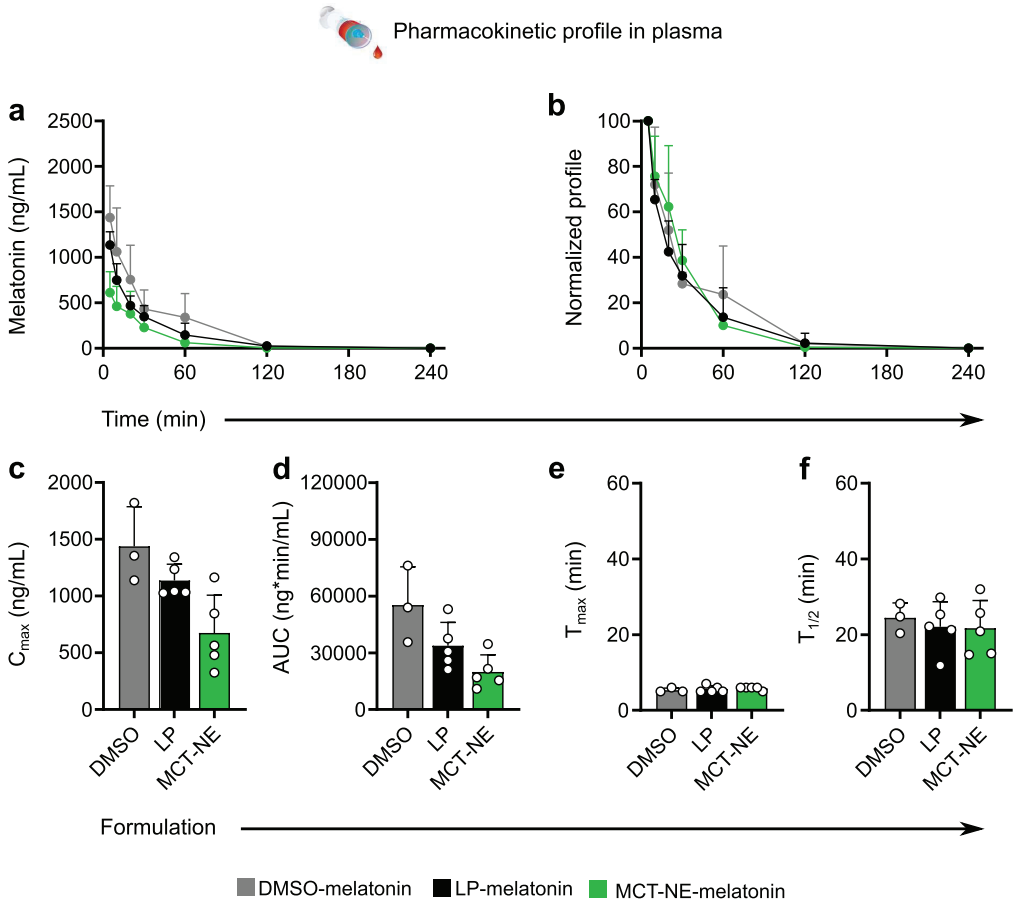

Fig. 5. *In vivo* plasma characterization data. (a) Melatonin concentration in plasma (mean ± SD) after a bolus injection of 1 mL of 3 mg/mL melatonin in DMSO, LP or MCT-NE. (b) Normalized profile of melatonin concentration in plasma (mean ± SD). (c-f) Estimated PK parameters of melatonin in DMSO, LP or MCT-NE (mean ± SD), c: C_{max}, d: AUC, e: T_{max}, f: $T_{1/2}$.

specific ligands [26]. Thus, the increased brain concentrations with melatonin-NPs compared to melatonin dissolved in DMSO were somewhat surprising. However, these results were consistent, and interestingly, the same increased brain concentration relative to plasma concentration has been seen in two previous studies using liposomal formulations of methotrexate and the opioid peptide DAMGO [18,27]. One possible explanation, suggested in these studies, could be a fusion of NPs with the endothelial luminal membrane leading to intracellular melatonin release in brain endothelial cells with subsequent facilitated brain uptake of melatonin over the BBB. However, further studies to investigate the mechanisms for brain uptake are needed to fully understand these results.

The mean C_{max} of melatonin in the brain after injection of melatonin-nanoformulation was almost 500 times higher than physiological melatonin levels in infants brain [28]. In the *in vitro* studies, increased survival and differentiation of neural stem cells has been seen at melatonin concentrations of 1 nM [29], while protection against hypoxia and nutrient deprivation has been reported as dose-dependent up to 200 nM [30]. Protection against oxidative stress seems to require melatonin concentrations of 10 μM and higher [31]. Using liposomes, we were able to increase time above 100 nM from 7.5 min to 83.3 min, and time above 200 nM from 2.5 min to 55 min. This indicates that injection of melatonin nanoparticles (10 mg/kg body weight) results in therapeutic levels of melatonin in the brain. However, the quantity of melatonin collected using microdialysis most often represents a fraction of the actual extracellular concentration, since at most flow rates (> 0.1 μL/min), the rate of analyte removal from the inside of the probe is higher than the rate of analyte replacement to the probe membrane surface [32]. Therefore, the actual brain extracellular fluid (ECF) melatonin concentrations were, most likely, higher than what we have measured. Since we did not succeed in correcting for this effect using deuterated melatonin in the perfusate, the concentrations reported in our study should be interpreted as lower limits rather than true ECF concentrations.

5. Conclusion

In this study we have demonstrated a successful production of an injectable melatonin nanoformulation, which consists solely of clinically approved lipids, is stable over time, improves melatonin solubilization, and prolongs *in vitro* melatonin release in comparison to conventional formulations with organic solvents. Moreover, the *in vivo* results indicate that administration of melatonin lipidic nanoparticles provides higher levels of melatonin in brain, longer time above critical

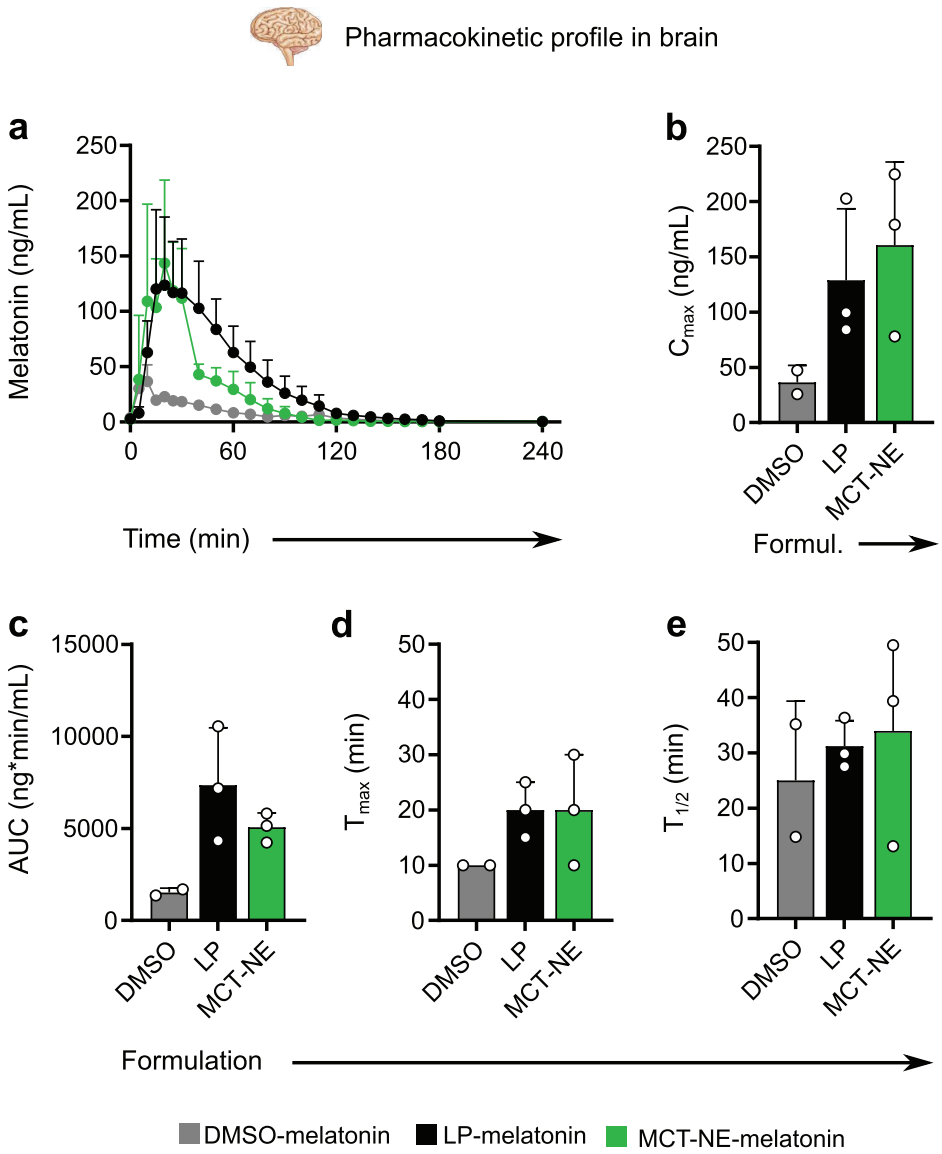

Fig. 6. *In vivo* brain characterization data. (a) Melatonin concentration in brain (mean ± SD) after a bolus injection of 10 mg/kg melatonin in DMSO, LP or MCT-NE. (b-e) Estimated PK parameters of melatonin in DMSO, LP or MCT-NE (mean ± SD), b: C_{max}, c: AUC, d: T_{max}, e: $T_{1/2}$.

Table 1
Average time above certain critical concentrations in the brain extracellular fluid (ECF) for the different formulations. The percentage denotes the fraction of animals in each group that reached the critical concentration.

Concentration		DMSO					MCT-NE					LP				
		Time above (range)					Time above (range)					Time above (range)				
1	nM	*180*	*minutes*	*(180–180)*	*100*	*%*	*203*	*minutes*	*(140–240)*	*100*	*%*	*243*	*minutes*	*(240–250)*	*100*	*%*
10	nM	*125*	*minutes*	*(120–130)*	*100*	*%*	*98,3*	*minutes*	*(85–120)*	*100*	*%*	*148*	*minutes*	*(120–170)*	*100*	*%*
100	nM	*7,5*	*minutes*	*(5–10)*	*100*	*%*	*46,7*	*minutes*	*(40–55)*	*100*	*%*	*83,3*	*minutes*	*(60–100)*	*100*	*%*
200	nM	*2,5*	*minutes*	*(0–5)*	*50*	*%*	*33*	*minutes*	*(25–45)*	*100*	*%*	*55*	*minutes*	*(35–70)*	*100*	*%*
500	nM	*0*	*minutes*		*0*	*%*	*10*	*minutes*	*(0–20)*	*67*	*%*	*8*	*minutes*	*(0–25)*	*33*	*%*
1000	nM	*0*	*minutes*		*0*	*%*	*0*	*minutes*		*0*	*%*	*0*	*minutes*		*0*	*%*

pharmacological concentrations and similar melatonin concentration in circulation compared to melatonin dissolved in DMSO. In combination with the complete elimination of organic solvents, this not only makes our melatonin formulation applicable in neonates with HI brain injury, but also in a variety of other pathological conditions.

Acknowledgements

The authors gratefully thank Catharina de Lange Davies for allowing to use the facilities at the Department of Physics at the Norwegian University of Science and Technology, and Francis Combes from the Department of Nutrition, Genetics and Ethology at Ghent University, Merelbeke, Belgium for technical support during the animal study. We thank Margareta Hammarlund-Udenaes at the Department of Pharmaceutical Biosciences, Uppsala University, for help with establishing the microdialysis method. This work was financially supported by the Norwegian University of Science and Technology, Faculty of Medicine and Health Sciences (AM and AKGN: PhD stipend), the Central Norway Regional Health Authority (Helse Midt-Norge; AMS: PhD stipend; SH: researcher grant) and the Norwegian Research Council. MR and animal studies were performed at the MR Core Facility and Comparative Medicine Core Facility at the Norwegian University of Science and Technology.

Declaration of Competing Interest

The authors declare no competing interests.

References

[1] H.-M. Zhang, Y. Zhang, Melatonin: a well-documented antioxidant with conditional pro-oxidant actions, J. Pineal Res. 57 (2014) 131–146, https://doi.org/10.1111/jpi.12162.
[2] D.P. Cardinali, D.E. Vigo, N. Olivar, M.F. Vidal, L.I. Brusco, Melatonin Therapy in Patients with Alzheimer's Disease, Antioxidants. 3 (2014) 245–277, https://doi.org/10.3390/antiox3020245.
[3] Y. Li, S. Li, Y. Zhou, X. Meng, J.-J. Zhang, D.-P. Xu, H.-B. Li, Y. Li, S. Li, Y. Zhou, X. Meng, J.-J. Zhang, D.-P. Xu, H.-B. Li, Melatonin for the prevention and treatment of cancer, Oncotarget. 8 (2017) 39896–39921 https://doi.org/10.18632/oncotarget.16379.
[4] Y. Han, Y.-M. Kim, H.S. Kim, K.Y. Lee, Melatonin promotes osteoblast differentiation by regulating Osterix protein stability and expression, Sci. Rep. 7 (2017) 5716, https://doi.org/10.1038/s41598-017-06304-x.
[5] M. Cervantes, G. Moral, G. Letechipa-Vallejo, Melatonin and ischemiareperfusion injury of the brain, J. Pineal Res. 45 (2008) 1–7, https://doi.org/10.1111/j.1600-079X.2007.00551.x.
[6] H.R. Berger, T.S. Morken, R. Vettukattil, A.M. Brubakk, U. Sonnewald, M. Widerøe, No improvement of neuronal metabolism in the reperfusion phase with melatonin treatment after hypoxic-ischemic brain injury in the neonatal rat, J. Neurochem. 136 (2016) 339–350, https://doi.org/10.1111/jnc.13420.
[7] A.D. Edwards, P. Brocklehurst, A.J. Gunn, H. Halliday, E. Juszczak, M. Levene, B. Strohm, M. Thoresen, A. Whitelaw, D. Azzopardi, Neurological outcomes at 18 months of age after moderate hypothermia for perinatal hypoxic ischaemic encephalopathy: synthesis and meta-analysis of trial data, BMJ. 340 (2010) c363, , https://doi.org/10.1136/bmj.c363.
[8] T.E. Inder, J.J. Volpe, Mechanisms of perinatal brain injury, Semin. Neonatol. 5 (2000) 3–16, https://doi.org/10.1053/SINY.1999.0112.
[9] R.L. DeMuro, A.N. Nafziger, D.E. Blask, A.M. Menhinick, J.S. Bertino, The Absolute Bioavailability of Oral Melatonin, J. Clin. Pharmacol. 40 (2000) 781–784, https://doi.org/10.1177/00912700022009422.
[10] C.M. Young, S.D.K. Kingma, J. Neu, Ischemia-Reperfusion and Neonatal Intestinal Injury, J. Pediatr. 158 (2011) e25–e28, https://doi.org/10.1016/J.JPEDS.2010.11.009.
[11] E. Marek, W.K. Kraft, Ethanol pharmacokinetics in neonates and infants, Curr. Ther. Res. Clin. Exp. 76 (2014) 90–97, https://doi.org/10.1016/j.curtheres.2014.09.002.
[12] V.P. Torchilin, Recent advances with liposomes as pharmaceutical carriers, Nat. Rev. Drug Discov. 4 (2005) 145–160, https://doi.org/10.1038/nrd1632.
[13] T.G. Mason, J.N. Wilking, K. Meleson, C.B. Chang, S.M. Graves, Nanoemulsions: formation, structure, and physical properties, J. Phys. Condens. Matter. 18 (2006) R635–R666, https://doi.org/10.1088/0953-8984/18/41/R01.
[14] S.B. Lim, A. Banerjee, H. Önyüksel, Improvement of drug safety by the use of lipid-based nanocarriers, J. Control. Release. 163 (2012) 34–45, https://doi.org/10.1016/J.JCONREL.2012.06.002.
[15] A.M. Sofias, T. Andreassen, S. Hak, Nanoparticle Ligand-Decoration Procedures Affect in Vivo Interactions with Immune Cells, Mol. Pharm. 15 (2018) 5754–5761, https://doi.org/10.1021/acs.molpharmaceut.8b00908.
[16] S. Hak, E. Helgesen, H.H. Hektoen, E.M. Huuse, P.A. Jarzyna, W.J.M. Mulder, O. Haraldseth, C. de L. Davies, The Effect of Nanoparticle Polyethylene Glycol Surface Density on Ligand-Directed Tumor Targeting Studied *in Vivo* by Dual Modality Imaging, ACS Nano. 6 (2012) 5648–5658, https://doi.org/10.1021/nn301630n.
[17] M. Hammarlund-Udenaes, The use of microdialysis in CNS drug delivery studies: Pharmacokinetic perspectives and results with analgesics and antiepileptics, Adv. Drug Deliv. Rev. 45 (2000) 283–294, https://doi.org/10.1016/S0169-409X(00)00109-5.
[18] A. Lindqvist, J. Rip, J. Van Kregten, P.J. Gaillard, M. Hammarlund-Udenaes, In vivo Functional Evaluation of Increased Brain Delivery of the Opioid Peptide DAMGO by Glutathione-PEGylated Liposomes, Pharm. Res. 33 (2016) 177–185, https://doi.org/10.1007/s11095-015-1774-3.
[19] Y. Cao, M. Marra, B.D. Anderson, Predictive Relationships for the Effects of Triglyceride Ester Concentration and Water Uptake on Solubility and Partitioning of Small Molecules into Lipid Vehicles, J. Pharm. Sci. 93 (2004) 2768–2779, https://doi.org/10.1002/JPS.20126.
[20] T.J. Wooster, M. Golding, P. Sanguansri, Impact of Oil Type on Nanoemulsion Formation and Ostwald Ripening Stability, Langmuir. 24 (2008) 12758–12765, https://doi.org/10.1021/la801685v.
[21] M. Pathak, Nanoemulsions and Their Stability for Enhancing Functional Properties of Food Ingredients, Nanotechnol. Appl. Food. (2017) 87–106, https://doi.org/10.1016/B978-0-12-811942-6.00005-4.
[22] (PDF) Development and Validation of UV Spectrophotometric Method for Simultaneous Estimation of Melatonin and Quercetin in Liposome Formulation, (n.d.). https://www.researchgate.net/publication/319037941_Development_and_Validation_of_UV_Spectrophotometric_Method_for_Simultaneous_Estimation_of_Melatonin_and_Quercetin_in_Liposome_Formulation (accessed September 27, 2019).
[23] R.J. Reiter, J.C. Mayo, D.-X. Tan, R.M. Sainz, M. Alatorre-Jimenez, L. Qin, Melatonin as an antioxidant: under promises but over delivers, J. Pineal Res. 61 (2016) 253–278, https://doi.org/10.1111/jpi.12360.
[24] S.V. Rozov, E.V. Filatova, A.A. Orlov, A.V. Volkova, A.R.A. Zhloba, E.L. Blashko, N.V. Pozdeyev, N [1] -acetyl-N [2] -formyl-5-methoxykynuramine is a product of melatonin oxidation in rats, J. Pineal Res. 35 (2003) 245–250, https://doi.org/10.1034/j.1600-079X.2003.00081.x.
[25] T. Chen, T. Gong, T. Zhao, Y. Fu, Z. Zhang, T. Gong, A comparison study between lycobetaine-loaded nanoemulsion and liposome using nRGD as therapeutic adjuvant for lung cancer therapy, Eur. J. Pharm. Sci. 111 (2018) 293–302, https://doi.org/10.1016/J.EJPS.2017.09.041.
[26] J. Huwyler, D. Wu, W.M. Pardridge, Brain drug delivery of small molecules using immunoliposomes, Proc. Natl. Acad. Sci. USA 93 (1996) 14164–14169, https://doi.org/10.1073/PNAS.93.24.14164.
[27] Y. Hu, J. Rip, P.J. Gaillard, E.C.M. de Lange, M. Hammarlund-Udenaes, The Impact of Liposomal Formulations on the Release and Brain Delivery of Methotrexate: An In Vivo Microdialysis Study, J. Pharm. Sci. 106 (2017) 2606–2613, https://doi.org/10.1016/j.xphs.2017.03.009.
[28] A. Brzezinski, Melatonin in Humans, N. Engl. J. Med. 336 (1997) 186–195, https://doi.org/10.1056/NEJM199701163360306.
[29] X. Kong, X. Li, Z. Cai, N. Yang, Y. Liu, J. Shu, L. Pan, P. Zuo, Melatonin Regulates the Viability and Differentiation of Rat Midbrain Neural Stem Cells, Cell. Mol. Neurobiol. 28 (2008) 569–579, https://doi.org/10.1007/s10571-007-9212-7.
[30] F. Wang, H. Zhou, Z. Du, X. Chen, F. Zhu, Z. Wang, Y. Zhang, L. Lin, M. Qian, X. Zhang, X. Li, A. Hao, Cytoprotective effect of melatonin against hypoxia/serum deprivation-induced cell death of bone marrow mesenchymal stem cells in vitro, Eur. J. Pharmacol. 748 (2015) 157–165, https://doi.org/10.1016/j.ejphar.2014.09.033.
[31] K. Uchida, M. Samejima, A. Okabe, A. Fukuda, Neuroprotective effects of melatonin against anoxia/aglycemia stress, as assessed by synaptic potentials and superoxide production in rat hippocampal slices, J. Pineal Res. 37 (2004) 215–222, https://doi.org/10.1111/j.1600-079X.2004.00159.x.
[32] T.S. Shippenberg, A.C. Thompson, Overview of microdialysis, Curr. Protoc. Neurosci. Chapter 7 (2001), https://doi.org/10.1002/0471142301.ns0701s00 Unit7.1.

Paper II

This paper is awaiting publication and is not included in NTNU Open

Paper III

This paper is awaiting publication and is not included in NTNU Open

ISBN 978-82-326-5471-0 (printed ver.)
ISBN 978-82-326-6641-6 (electronic ver.)
ISSN 1503-8181 (printed ver.)
ISSN 2703-8084 (online ver.)

NTNU

Norwegian University of
Science and Technology